TECHNICAL SPECIFICATION

ISO/TS 19130-2

First edition
2014-01-15

Geographic information — Imagery sensor models for geopositioning —

Part 2: SAR, InSAR, lidar and sonar

Information géographique — Modèles de capteurs d'images de géopositionnement —

Partie 2: SAR, InSAR, lidar et sonar

Reference number
ISO/TS 19130-2:2014(E)

Contents

Page

Foreword

ISO (the International Organization for Standardization) is a worldwide federation of national standards bodies (ISO member bodies). The work of preparing International Standards is normally carried out through ISO technical committees. Each member body interested in a subject for which a technical committee has been established has the right to be represented on that committee. International organizations, governmental and non-governmental, in liaison with ISO, also take part in the work. ISO collaborates closely with the International Electrotechnical Commission (IEC) on all matters of electrotechnical standardization.

The procedures used to develop this document and those intended for its further maintenance are described in the ISO/IEC Directives, Part 1. In particular the different approval criteria needed for the different types of ISO documents should be noted. This document was drafted in accordance with the editorial rules of the ISO/IEC Directives, Part 2. www.iso.org/directives

Attention is drawn to the possibility that some of the elements of this document may be the subject of patent rights. ISO shall not be held responsible for identifying any or all such patent rights. Details of any patent rights identified during the development of the document will be in the Introduction and/or on the ISO list of patent declarations received. www.iso.org/patents

Any trade name used in this document is information given for the convenience of users and does not constitute an endorsement.

For an explanation on the meaning of ISO specific terms and expressions related to conformity assessment, as well as information about ISO's adherence to the WTO principles in the Technical Barriers to Trade (TBT) see the following URL: Foreword - Supplementary information

The committee responsible for this document is ISO/TC ISO/TC 211, *Geographic information/Geomatics*.

ISO/TS 19130 consists of the following parts, under the general title *Geographic information — Imagery sensor models for geopositioning*:

— *Geographic information — Imagery sensor models for geopositioning*

— *Part 2: Geographic information — Imagery sensor models for geopositioning — Part 2: SAR, InSAR, lidar and sonar*

Introduction

The purpose of this Technical Specification is to specify the geolocation information that an imagery data provider shall supply in order for the user to be able to find the earth location of the data using a detailed physical sensor model for Synthetic Aperture Radar (SAR), Light Detection And Ranging (lidar) and Sound Navigation And Ranging (sonar). The intent is to standardize sensor descriptions and specify the minimum geolocation metadata requirements for data providers and geopositioning imagery systems. Observations in this document are the generic meaning of the word; observations are not in the meaning of ISO 19156 observations.

Vast amounts of data from imaging systems have been collected, processed and distributed by government mapping and remote sensing agencies and by commercial data vendors. In order for this data to be useful in extraction of geographic information, further processing of the data are needed. Geopositioning, which determines the ground coordinates of an object from image coordinates, is a fundamental processing step. Because of the diversity of sensor types and the lack of a common sensor model standard, data from different producers may contain different parametric information, lack parameters required to describe the sensor that produces the data, or lack ancillary information necessary for geopositioning and analysing the data. Often, a separate software package must be developed to deal with data from each individual sensor or data producer. Standard sensor models and geolocation metadata allow agencies or vendors to develop generalized software products that are applicable to data from multiple data producers or from multiple sensors. With such standards, different producers can describe the geolocation information of their data in the same way, thus promoting interoperability of data between application systems and facilitating data exchange.

Part 1 provided a location model and metadata relevant to all sensors. It also included metadata specific to whiskbroom, pushbroom, and frame sensors, and some metadata for Synthetic Aperture Radar (SAR) sensors. In addition, it provided metadata for functional fit geopositioning, whether the function was part of a correspondence model or a true replacement model. It also provided a schema for these metadata elements. Comments on Part 1 stated that metadata needed to be specified for additional sensors. The technology of such sensors has now become sufficiently mature that standardization is now possible. This Technical Specification extends the specification of the set of metadata elements required for geolocation by providing physical sensor models for LIght Detection And Ranging (lidar) and SOund Navigation And Ranging (sonar), and it presents a more detailed set of elements for SAR. This Technical Specification also defines the metadata needed for the aerial triangulation of airborne and spaceborne images. This Technical Specification also provides a schema for all of these metadata elements.

Geographic information — Imagery sensor models for geopositioning —

Part 2:
SAR, InSAR, lidar and sonar

1 Scope

This Technical Specification supports exploitation of remotely sensed images. It specifies the sensor models and metadata for geopositioning images remotely sensed by Synthetic Aperture Radar (SAR), Interferometric Synthetic Aperture Radar (InSAR), LIght Detection And Ranging (lidar), and SOund Navigation And Ranging (sonar) sensors. The specification also defines the metadata needed for the aerial triangulation of airborne and spaceborne images.

This Technical Specification specifies the detailed information that shall be provided for a sensor description of SAR, InSAR, lidar and sonar sensors with the associated physical and geometric information necessary to rigorously construct a Physical Sensor Model. For the case where precise geoposition information is needed, this Technical Specification identifies the mathematical formulae for rigorously constructing Physical Sensor Models that relate two-dimensional image space to three-dimensional ground space and the calculation of the associated propagated error.

This Technical Specification does not specify either how users derive geoposition data or the format or content of the data the users generate.

2 Conformance

This Technical Specification specifies 5 conformance classes. There is one conformance class for each type of sensor. Any set of geopositioning information claiming conformance to this Technical Specification shall satisfy the requirements for at least one conformance class as specified in Table 1. The requirements for each class are shown by the presence of an X in the boxes for all clauses in the application test suite (ATS) required for that class. If the requirement is conditional, the box contains a C. The conditions are defined in the corresponding UML models.

Table 1 — Conformance classes

		Section of this part of ISO 19130							
		A.1.1	A.1.2	A.1.3	A.2	A.3	A.4	A.5	A.6
Conformance Class	SAR	X	C		X				
	InSAR	X	C			X			
	Lidar	X	X	X			X		
	Sonar	X	X	X				X	
	Aerial triangulation	X	C						X

3 Normative references

The following referenced documents are indispensable for the application of this document. For dated references, only the edition cited applies. For undated references, the latest edition of the referenced document (including any amendments) applies.

ISO/TS 19103:2005, *Geographic information — Conceptual schema language*

ISO 19107:2003, *Geographic information — Spatial schema*

ISO 19108:2002, *Geographic information — Temporal schema*

ISO 19111:2007, *Geographic information — Spatial referencing by coordinates*

ISO 19115-1:2014, *Geographic information — Metadata — Part 1: Fundamentals*

ISO 19115-2:2009, *Geographic information — Metadata — Part 2: Extensions for imagery and gridded data*

ISO 19123:2005, *Geographic information — Schema for coverage geometry and functions*

ISO 19157:2013, *Geographic information — Data quality*

ISO/TS 19130:2010, *Geographic information — Imagery sensor models for geopositioning*

4 Terms and definitions

For the purposes of this document, the following terms and definitions apply.

4.1
active sensor
sensor (4.66) that generates the energy that it uses to perform the sensing

4.2
active sonar
type of *active sensor* (4.1) that transmits sound waves into the water and receives the returned waves echoed from objects in the water

4.3
adjustable model parameters
model parameters that can be refined using available additional information, such as ground control points, to improve or enhance modeling corrections

[SOURCE: ISO/TS 19130:2010, 4.2]

4.4
ARP
aperture reference point
3D location of the centre of the synthetic aperture

Note 1 to entry: It is usually expressed in ECEF coordinates in metres.

[SOURCE: ISO/TS 19130:2010, 4.4]

4.5
area recording
instantaneously recording an image in a single *frame* (4.22)

4.6
attitude
orientation of a body, described by the angles between the axes of that body's coordinate system and the axes of an external coordinate system

[SOURCE: ISO 19116:2004, 4.2]

4.7
attribute
named property of an entity

[SOURCE: ISO/IEC 2382-17:1999, 17.02.12]

4.8
azimuth resolution
<SAR> *resolution* (4.60) in the cross-range direction

Note 1 to entry: This is usually measured in terms of the impulse response of the SAR *sensor* (4.66) and processing system. It is a function of the size of the synthetic aperture, or alternatively the dwell time (e.g. larger aperture -> longer dwell time - > better resolution).

[SOURCE: ISO/TS 19130:2010, 4.7]

4.9
beam width
<SAR> useful angular width of the beam of electromagnetic energy

Note 1 to entry: For SAR, beam width is usually measured in radians and is the angular width between two points that have 1/2 of the power (3 dB below) of the centre of the beam. It is a property of the antenna. Power emitted outside of this angle is too little to provide a usable *return* (4.62).

Note 2 to entry: Angle, measured in a horizontal plane, between the directions on either side of the axis at which the *intensity* (4.37) of a beam of energy drops to a specified fraction of the value it has on the axis.

[SOURCE: ISO/TS 19130:2010, 4.8, modified — Notes 1 and 2 have been added.]

4.10
broadside
<SAR> direction orthogonal to the *velocity vector* (4.81) and parallel to the plane tangent to the Earth's ellipsoid at the nadir point of the *ARP* (4.4)

[SOURCE: ISO/TS 19130:2010, 4.9]

4.11
complex image
first-level product produced by processing SAR *Phase History Data* (4.48)

4.12
datum
parameter or set of parameters that define the position of the origin, the scale, and the orientation of a coordinate system

[SOURCE: ISO 19111:2007, 4.14]

4.13
depression angle
vertical angle from the platform horizontal plane to the *slant range direction* (4.56), usually measured at the *ARP* (4.4)

Note 1 to entry: Approximately the complement of the *look angle* (4.42).

4.14
Differential Global Navigational Satellite System
enhancement to Global Positioning System that uses GNSS and DGNSS to broadcast the difference between the positions indicated by the satellite systems and the known fixed positions

4.15
Doppler angle
<SAR> angle between the *velocity vector* (4.81) and the *range vector* (4.58)

[SOURCE: ISO/TS 19130:2010, 4.19]

4.16
Doppler shift
wavelength change resulting from relative motion of source and detector

Note 1 to entry: In the SAR context, it is the frequency shift imposed on a radar signal due to relative motion between the *transmitter* (4.79) and the object being illuminated.

[SOURCE: ISO/TS 19130:2010, 4.20]

4.17
draught
vertical distance, at any section of a vessel from the surface of the water to the bottom of the keel

[SOURCE: IHO Hydrographic Dictionary, S-32, Fifth Edition]

4.18
easting
E
distance in a coordinate system, eastwards (positive) or westwards (negative) from a north-south reference line

[SOURCE: ISO 19111:2007, 4.16]

4.19
field of regard
total angular extent over which the *field of view (FOV)* (4.20) may be positioned

Note 1 to entry: The field of regard is the area that is potentially able to be viewed by a system at an instant in time. It is determined by the system's FOV and the *range* (4.54) of directions in which the system is able to point.

[SOURCE: Adapted from the Manual of Photogrammetry]

4.20
field of view
FOV
instantaneous region seen by a *sensor* (4.66), provided in angular measure

Note 1 to entry: In the airborne case, this would be *swath* (4.75) width for a linear array, ground footprint for an area array, and for a whiskbroom scanner it refers to the swath width.

[SOURCE: Manual of Photogrammetry]

4.21
first return
first reflected signal that is detected by a 3D imaging system, time of flight (TOF) type, for a given sampling position and a given emitted pulse

[SOURCE: Adapted from STM E2544]

4.22
frame
<lidar> data collected by the *receiver* (4.59) as a result of all *returns* (4.62) from a single emitted pulse

Note 1 to entry: A complete 3D data sample of the world produced by a *lidar* (4.40) taken at a certain time, place, and orientation. A single lidar frame is also referred to as a *range* (4.54) image.

[SOURCE: Adapted from NISTIR 7117]

4.23
geiger mode
photon counting mode for *lidar* (4.40) systems, where the detector is biased and becomes sensitive to individual photons

Note 1 to entry: These detectors exist in the form of arrays and are bonded with electronic circuitry. The electronic circuitry produces a measurement corresponding to the time at which the current was generated; resulting in a direct time-of-flight measurement. A lidar that employs this detector technology typically illuminates a large scene with a single pulse. The direct time-of-flight measurements are then combined with platform location/*attitude* (4.6) data along with pointing information to produce a three-dimensional product of the illuminated scene of interest. Additional processing is applied which removes existing noise present in the data to produce a visually exploitable data set.

[SOURCE: Adapted from Albota 2002]

4.24
geodetic coordinate system
coordinate system in which position is specified by geodetic latitude, geodetic longitude and (in the three-dimensional case) ellipsoidal height

[SOURCE: ISO 19111:2007, 4.18]

4.25
geodetic datum
datum (4.12) describing the relationship of a two- or three-dimensional coordinate system to the Earth

Note 1 to entry: In most cases, the geodetic datum includes an ellipsoid description (ISO/TS 19130:2010)

Note 2 to entry: The term and this Technical Specification may be applicable to some other celestial bodies.

[SOURCE: ISO 19111:2007, 4.24, modified — Notes 1 and 2 have been added.]

4.26
geographic coordinates
longitude, latitude and height of a ground or elevated point

Note 1 to entry: Geographic coordinates are related to a coordinate reference system or compound coordinate reference system. Depth equals negative height.

4.27
geographic information
information concerning phenomena implicitly or explicitly associated with a location relative to the Earth

[SOURCE: ISO 19101:2002, 4.16]

4.28
geolocating
geopositioning an object using a Physical *Sensor Model* (4.68) or a True Replacement Model

[SOURCE: ISO/TS 19130:2010, 4.34]

4.29
grazing angle
<SAR> vertical angle from the local surface tangent plane to the *slant range direction* (4.56)

Note 1 to entry: It is usually measured at the GRP and approximately the complement of the *incident angle* (4.35)

[SOURCE: ISO/TS 19130:2010, 4.39, modified — Note 1 to entry has been added.]

4.30
hydrophone
<sonar> component of the sonar system which receives the sound echo and converts it to an electric signal

4.31
heave
oscillatory rise and fall of a ship due to the entire hull being lifted by the force of the sea

[SOURCE: IHO Hydrographic Dictionary S-32, Fifth Edition]

4.32
hydrographic swath
<sonar> strip or lane on the ground scanned by a multi-beam sounder when the survey vessel proceeds along its course

[SOURCE: IHO Hydrographic Dictionary S-32, Fifth Edition]

4.33
image coordinates
coordinates with respect to a Cartesian coordinate system of an image

Note 1 to entry: The image coordinates can be in pixels or in a measure of length (linear measure).

4.34
image formation
<SAR> process by which an image is generated from collected *Phase History Data* (4.48) in a SAR system

[SOURCE: ISO/TS 19130:2010, 4.51]

4.35
incident angle
vertical angle between the line from the detected element to the *sensor* (4.66) and the local surface normal (tangent plane normal)

Note 1 to entry: It is approximately the complement of the *grazing angle* (4.29).

[SOURCE: ISO/TS 19130:2010, 4.57, modified — Note 1 to entry has been added.]

4.36
instantaneous field of view
instantaneous region seen by a single detector element, measured in angular space

[SOURCE: Manual of Photogrammetry]

4.37
intensity
power per unit solid angle from a point source into a particular direction

Note 1 to entry: Typically for *lidar* (4.40), sufficient calibration has not been done to calculate absolute intensity, so relative intensity is usually reported. In *linear mode* (4.41) systems, this value is typically provided as an integer, resulting from a mapping of the *return's* (4.62) signal power to an integer value via a lookup table.

4.38
last return
last reflected signal that is detected by a 3D imaging system, time-of-flight (TOF) type, for a given sampling position and a given emitted pulse

[SOURCE: Adapted from ASTM E2544]

4.39
layover
visual effect in SAR images of ambiguity among *returns* (4.62) from scatterers at different heights that fall into the same range-Doppler-time bin

Note 1 to entry: The effect makes buildings “lay over” onto the ground toward the *sensor* (4.66)*velocity vector* (4.81), akin to perspective views in projective imagery.

4.40
lidar
light detection and ranging
system consisting of 1) a photon source (frequently, but not necessarily, a laser), 2) a photon detection system, 3) a timing circuit, and 4) optics for both the source and the *receiver* (4.59) that uses emitted laser light to measure *ranges* (4.54) to and/or properties of solid objects, gases, or particulates in the atmosphere

Note 1 to entry: Time of flight (TOF) lidars use short laser pulses and precisely record the time each laser pulse was emitted and the time each reflected *return(s)* (4.62) is received in order to calculate the distance(s) to the scatterer(s) encountered by the emitted pulse. For *topographic lidar* (4.80), these time-of-flight measurements are then combined with precise platform location/*attitude* (4.6) data along with pointing data to produce a three-dimensional product of the illuminated scene of interest.

4.41
linear mode
lidar (4.40) system in which output photocurrent is proportional to the input optical incident *intensity* (4.37)

Note 1 to entry: A lidar system which employs this technology typically uses processing techniques to develop the time-of-flight measurements from the full waveform that is reflected from the targets in the illuminated scene of interest. These time-of-flight measurements are then combined with precise platform location/*attitude* (4.6) data along with pointing data to produce a three-dimensional product of the illuminated scene of interest.

[SOURCE: Adapted from Aull et al., 2002]

4.42
look angle
vertical angle from the *platform down direction* (4.50) to the *slant range direction* (4.56), usually measured at the *ARP* (4.4)

Note 1 to entry: It is approximately the complement of the *depression angle* (4.13).

4.43
mean sea level
MSL
average height of the surface of the sea at a tide station for all stages of the tide over a 19-year period, usually determined from hourly height readings measured from a fixed predetermined reference level

[SOURCE: IHO Hydrographic Dictionary S-32, Fifth Edition]

4.44
multibeam sonar
wide *swath* (4.75) echo sounder for use in seabed mapping and surveying using the multi-beam principle

Note 1 to entry: Depths are measured directly below and transverse to the ship’s track. The width of the swath is a function of the number of beams and their aperture.

[SOURCE: IHO Hydrographic Dictionary S-32, Fifth Edition]

4.45
multiple returns
multiple signals returned and detected for a given emitted pulse, such as when a laser beam hitting multiple objects separated in *range* (4.54) is split

[SOURCE: Adapted from ASTM E2544]

4.46
objective
optical element that receives light from the object and forms the first or primary image of an optical system

4.47
passive sonar
type of passive *sensor* (4.66) that only receives sound waves from external sources and does not transmit any sound waves

4.48
phase history data
PHD
video phase history data
raw radar *return* (4.62) signal information after demodulation

Note 1 to entry: Usually stored as a series of *range* (4.54) lines, each containing information from a specific *range bin* (4.55). PHD can be thought of as a table of five columns: In-phase signal, Quadrature signal, *Range* (4.54), *Doppler Angle* (4.15), and Time.

4.49
platform coordinate reference system
engineering coordinate reference system fixed to the collection platform within which positions on the collection platform are defined

[SOURCE: ISO/TS 19130:2010, 4.65]

4.50
platform down direction
downward normal to the platform horizontal plane

4.51
point cloud
collection of data points in 3D space

Note 1 to entry: The distance between points is generally non-uniform and hence all three coordinates (Cartesian or spherical) for each point must be specifically encoded.

4.52
projection centre
perspective centre
point located in three dimensions through which all rays between object points and image points appear to pass geometrically

Note 1 to entry: It is represented by the rear nodal point of the imaging lens system.

[SOURCE: ISO/TS 19130:2010, 4.62, modified — Note 1 to entry has been added.]

4.53
pulse repetition frequency
number of times the system (e.g. *lidar* [4.40]) emits pulses over a given time period, usually stated in kilohertz (kHz)

4.54
range
<SAR> distance between the antenna and a distant object, synonymous with slant range

4.55
range bin
<SAR> group of radar *returns* (4.62) that all have the same *range* (4.54)

[SOURCE: ISO/TS 19130:2010, 4.69]

4.56
range direction
slant range direction
<SAR> direction of the *range vector* (4.58)

Note 1 to entry: It is nominally the direction from a radar antenna to an object, represented by a vector from the *ARP* (4.4) to the GRP for SAR.

[SOURCE: ISO/TS 19130:2010, 4.70, modified — Note 1 to entry has been added.]

4.57
range resolution
spatial *resolution* (4.60) in the *range direction* (4.56)

Note 1 to entry: For a SAR *sensor* (4.66), it is usually measured in terms of the impulse response of the sensor and processing system. It is a function of the bandwidth of the pulse.

[SOURCE: ISO/TS 19130:2010, 4.71]

4.58
range vector
vector from the antenna to a point in the scene

[SOURCE: ISO/TS 19130:2010, 4.72]

4.59
receiver
hardware used to detect and record signals

Note 1 to entry: In *lidar* (4.40) and sonar systems, the receiver detects and records reflected pulse *returns* (4.62).

4.60
resolution (of a sensor)
smallest difference between indications of a *sensor* (4.66) that can be meaningfully distinguished

[SOURCE: ISO/TS 19101-2:2008, 4.34]

4.61
resolution (of imagery)
smallest distance between two uniformly illuminated objects that can be separately resolved in an image

4.62
return
<lidar> sensed signal from an emitted laser pulse which has reflected off of an illuminated scene of interest

Note 1 to entry: There may be *multiple returns* (4.45) for a given emitted laser pulse.

4.63
scan
set of sequential *frames* (4.22) collected during a single full cycle of a mechanical scanner representing a cross-track excursion from one side of the *field of regard* (4.19) to the other and back again

4.64
scan mode
SAR mode in which the antenna beam is steered to illuminate a *swath* (4.75) of ground at various angles relative to flight path throughout the collection

Note 1 to entry: Steering the antenna also allows dwell time to be increased and provides the ability to collect strips at angles non-parallel to the flight direction and with better *resolution* (4.60) than Stripmap mode.

[SOURCE: ISO/TS 19130:2010, 4.77]

4.65
ScanSAR mode
special case of stripmap mode that uses an electronically steerable antenna to quickly change the *swath* (4.75) being imaged during collection to collect multiple parallel swaths in one pass

[SOURCE: ISO/TS 19130:2010, 4.78]

4.66
sensor
element of a measuring system that is directly affected by a phenomenon, body, or substance carrying a quantity to be measured

[SOURCE: ISO/IEC GUIDE 99:2007, 3.8]

4.67
settlement
general lowering in level of a moving vessel, relative to what its level would be were it motionless, due to the regional depression of the surface of the water in which the ship moves

Note 1 to entry: Settlement is not an increase in displacement.

Note 2 to entry: Settlement is measured as an angular tilt about the centre of gravity of the vessel.

[SOURCE: IHO Hydrographic Dictionary S-32, Fifth Edition]

4.68
sensor model
<geopositioning> mathematical description of the relationship between the three-dimensional object space and the two-dimensional plane of the associated image produced by a *sensor* (4.66)

[SOURCE: ISO/TS 19130:2010, 4.80]

4.69
sidescan sonar
type of sonar that transmits sound energy from the sides of a towfish, creating a fanlike beam on either side that sweeps the seafloor, and continuously records **re***turn* (4.62) signals, creating a “picture” of the seafloor and any other objects

Note 1 to entry: Sidescan sonar is used for imaging bottom features and targets in a wide variety of water depths.

Note 2 to entry: This includes synthetic aperture sidescan sonar.

4.70
single beam sonar
type of sonar that produces one narrow sonar beam directly beneath the *transducer* (4.78)/*receiver* (4.59) and receives a *return* (4.62) echo from the closest object

Note 1 to entry: Single beam sonar is commonly called a single beam echosounder (abbr: SBES).

4.71
sonar processing system
system that processes the sonar signals to determine the geopositions of objects sensed by sonar *sensors* (4.66)

4.72
Sound Navigation And Ranging
sonar
sensor (4.66) that uses sound navigation and ranging technology for sensing

4.73
squat
effect that causes a vessel moving through water to create an area of lowered pressure under its bottom that increases the effective *draught* (4.17) (i.e. lowers the vessel in the water)

Note 1 to entry: The effect is a result of Bernoulli's principle of fluid dynamics. The squat represents the increase in effective draught.

Note 2 to entry: For a ship underway, the change of level of the bow and stern from the still water condition in response to the elevation and depression of the water level about the hull resulting from the bow and stern wave systems.

[SOURCE: Implementation Specification — a Draught Information System for the St. Lawrence Seaway, 4.18, modified — Note 2 to entry has been added.]

4.74
stare
scanning mode consisting of a step stair pattern

Note 1 to entry: This applies to a HARLIE transceiver, based on a volume phase holographic optical element.

4.75
swath
<lidar> ground area from which *return* (4.62) data are collected during continuous airborne *lidar* (4.40) operation

Note 1 to entry: A typical mapping mission may consist of multiple adjacent swaths, with some overlap, and the operator will turn off the laser while the aircraft is oriented for the next swath. This term may also be referred to as a Pass.

4.76
sweep sonar
type of sonar that has several single beam *transducer* (4.78)/*receivers* (4.59) mounted on a boom, which is then operated parallel to the water's surface and orthogonal to the vessel's direction of travel

Note 1 to entry: Sweep sounding is commonly called multi-channel echosounding (MCES).

4.77
swipe
set of sequential *frames* (4.22) collected during a single half cycle of a mechanical scanner representing a cross-track excursion from one side of the *field of regard* (4.19) to the other

4.78
transducer
device that converts one type of energy to another

4.79
transmitter
component of sonar that converts an electrical impulse into a sound wave and sends the wave into the water

Note 1 to entry: Transmitter is also called projector in multibeam echosounding.

4.80
topographic lidar
lidar (4.40) system used to measure the topography of the ground surface

Note 1 to entry: Generally referring to an airborne lidar system.

4.81
velocity vector
<Radar> first derivative of the antenna's position vector

5 Symbols and abbreviations

5.1 Symbols

$\mathbf{A}$	3D Affine transform matrix
$\mathbf{a}$	image vector
B	radar pulse bandwidth
$\mathbf{b}$	3D Affine translation vector
C	number of columns (samples) in the image
C_ℓ	correction for row-column to line-sample conversion.
C_S	correction for row-column to line-sample conversion
c	speed of light in a vacuum
c_s	speed of sound in the medium in which the sonar operates
col	column in the row-column coordinate system
D	physical radar antenna aperture
d_x	pixel width in CCS — not applicable to SAR
d_y	pixel height in CCS — not applicable to SAR
f	camera focal length
$\mathbf{G_0}$	Ground Reference Point (GRP)
H	sensor altitude, m HAE; also platform Heading
H_{dg}	heading in reference to the local-vertical coordinate system, e.g. platform Heading
h	height (MSL) of the object the laser intersects, in kilometres.
h	object elevation, m HAE
h_{ae}	elevation relative to elipsoid, e.g. sensor altitude, object elevation
I	In-phase (real) component of phase history data sample
i	index of frames
j	index of points

K	refraction constant, micro-radians
k	arbitrary constant
k_1	first order radial distortion coefficient
k_2	second order radial distortion coefficient
k_3	third order radial distortion coefficient
L	front nodal point of lens
ℓ	line in the line sample coordinate system
l	line number
l_0	location of GRP in line direction in image space
$\mathbf{M_p}$	generic 3D point (in ECEF)
M	rotation matrix (various)
M_{ECEF}	rotation matrix from the ellipsoid-tangential reference frame to the ECEF reference frame
M_{ELL}	rotation matrix from the local vertical reference frame to the ellipsoid-tangential reference frame.
M_{GIM}	rotation matrix from the sensor reference frame to the gimbal reference frame (gimbal angles).
M_{PLA}	rotation matrix from the gimbal reference frame to the platform reference frame (boresight angles).
M_{SEN}	rotation matrix from scanner reference frame to sensor reference frame (scan angles).
M_{VER}	rotation matrix from the platform reference frame to the local vertical reference frame (INS observations).
$\mathbf{M}_\omega$	rotation about the x-axis (roll)
$\mathbf{M}_\varphi$	rotation about the y-axis (pitch)
$\mathbf{M}_\kappa$	rotation about the z-axis (yaw)
$\mathbf{M}_0$	the orientation matrix
mD	Down in the North East Down (NED) Coordinate System, cf. Figure C.4. ("mZ" can also be used to represent down in the North East Down (NED) Coordinate System)
mE	East in the North East Down (NED) or North East Up Coordinate System, cf. Figure C.4.
mN	North in the North East Down (NED) or North East Up Coordinate System, cf. Figure C.4.
N	North in the North East Down (NED) or North East Up Coordinate System
P	pitch in reference to the local-vertical coordinate system

$\mathbf{P_c}$	object point coordinate (ground space)
p_1, p_2	lens decentring coefficients
p_l, p_s	line and sample coordinates of a generic pixel in the image
Q_c	quadrature (imaginary) component of phase history data sample
Q	generic point in the image
$\mathbf{Q_s}$	vector representing a generic point in the image in the slant plane
$\mathbf{Q_0}$	vector representing GRP in the slant plane (ARP as origin)
$\overline{\mathbf{Q}_0}$	vector from ARP to GRP (in ECEF)
R	range
R_G	ground range
R_S	slant range
R'	range from front nodal point (L) to the point on the ground (A)
r	radial distance on image from principal point to point of interest
r_A	azimuth resolution
r_{ECEF}	vector from the ECEF origin to the GNSS antenna phase-centre in the ECEF reference frame (GNSS observations)
r_{EP}	vector from the ECEF origin to the ground point in the ECEF reference frame.
r_{GIM}	vector from the sensor to the gimbal centre of rotation in the gimbal reference frame
r_{GPS}	vector from the GNSS antenna phase-centre to the INS in the platform reference frame
r_{GR}	ground range resolution
r_{INS}	vector from the INS to the gimbal centre of rotation in the platform reference frame.
r_R	range resolution
r_{SCA}	vector from the scanner to the ground point in the scanner reference frame (range).
r_{SR}	slant range resolution
row	row in the row-column coordinate system
S	antenna position vector (in ECEF)
S(*t*)	antenna position vector (in ECEF) as function of time
S_Y	antenna velocity vector (in ECEF)
$S_Y(t)$	antenna velocity vector (in ECEF) as function of time
S_0	Aperture Reference Point (ARP)

S_{Y0}	antenna velocity vector at the ARP (first derivative of ARP)
s	sample in the line-sample coordinate system; symbol has multiple meanings; meaning of the symbol defined in context .
s	adjustment for the range to account for distance from front nodal point to the lens; symbol has multiple meanings; meaning of the symbol defined in context .
s_0	location of GRP in sample direction in image space
T	period of signal
T	radar pulse width
t	time
t_r	round trip travel time
$\hat{U}_R$	unit vector in range direction in slant plane
$\hat{U}_A$	unit vector in azimuth direction in slant plane
X	X coordinates within Earth coordinate system
X_a	platform longitudinal axis
X,Y,Z	right-handed Cartesian ground coordinate system
X_a, Y_a, Z_a	Cartesian coordinates in Local Vertical Coordinate System
$X_LY_LZ_L$	the position of the sensor front nodal point in ground coordinates
X_W,Y_W, Z_W	Cartesian coordinates in World Coordinate System
x'	image coordinate (x-component) adjusted for lens and atmospheric errors
x_{GIM}, y_{GIM}, z_{GIM}	Cartesian coordinates in Gimbal Coordinate System
X_0, Y_0	principal point offset in the x-y frame coordinate system
x_p, y_p, z_p	Cartesian coordinates in Platform Coordinate System
x_s, y_s, z_s	Cartesian coordinates in Sensor Coordinate System
x_{sca}, y_{sca}, z_{sca}	Cartesian Coordinates in Scanner Coordinate System
Y	Y coordinates within Earth coordinate system
Y_a	platform pitch axis
y	y coordinate in the x-y frame coordinate system
y'	image coordinate (y-component) adjusted for lens and atmospheric errors
Z	Z coordinates within Earth coordinate system
Z_a	platform yaw axis
z	various z coordinates, defined by subscripts

α	Doppler angle
$\boldsymbol{\alpha}$	the angle of the laser beam from vertical
α_0	Doppler angle of the GRP
α_L	local Doppler angle of a generic point
a_1, b_1, c_1, a_2, b_2, c_2	parameters for a six parameter transformation, in this case to account for array distortions.
$\dot{B}_{ij}$	coefficients of the unknown corrections to the sensor parameters
$\ddot{B}_{ij}$	coefficients of the unknown corrections to the ground coordinates
β	radar beamwidth
γ	grazing angle
Δd	angular displacement of the laser beam from the expected path
$\Delta \mathrm{x}_{\mathrm{atm}}$	atmospheric correction for image coordinates, x-component
$\Delta \mathrm{y}_{\mathrm{atm}}$	atmospheric correction for image coordinates, y-component
$\Delta \mathrm{x}_{\mathrm{dec}}$	lens decentring errors, x component
$\Delta \mathrm{y}_{\mathrm{dec}}$	lens decentring errors, y component
$\Delta \mathrm{x}_{\mathrm{lens}}$	total lens radial distortion and decentring distortion, x-component
$\Delta \mathrm{y}_{\mathrm{lens}}$	total lens radial distortion and decentring distortion, y-component
$\Delta \mathrm{x}_{\mathrm{radial}}$	radial lens distortions, x-component
$\Delta \mathrm{y}_{\mathrm{radial}}$	radial lens distortions, y-component
$\dot{\Delta}_i$	unknown corrections to the sensor parameters.
$\ddot{\Delta}_j$	unknown corrections to the ground coordinates.
θ	angular displacement of the range vector from the lens optical axis, x-component
E	easting
λ	geodetic longitude
v_{ij}	residuals of the frame coordinates.
Σ	covariance matrix
σ	covariance matrix element
Φ_{ps}	phase shift of signal
φ	geodetic latitude
φ_{eo}	rotation about the y-axis, pitch (equivalent to $\mathbf{M}_{\varphi}$)

φ	angular displacement of the range vector from the lens optical axis, y-component
ω	roll (in reference to the local-vertical coordinate system)

5.2 Abbreviated terms

ANSI	American National Standards Institute
APD	Avalanche Photo Diode (ASTM E2544-07a)
ARDC	Air Research Development and Command
ASTM	Formerly the American Society for Testing and Materials
CCD	Charge Coupled Device
CRS	Coordinate Reference System
CSM	Community Sensor Model
DEM	Digital Elevation Model
DGNSS	Differential Global Navigational Satellite System
ECEF	Earth Centred Earth Fixed
ENU	East North Up
EO	Earth Observation
FOR	Field of Regard
FOV	Field of View
FPA	Focal Plane Array
GmAPD	Geiger-mode Avalanche PhotoDiode
GNSS	Global Navigational Satellite System
GSD	Ground Sample Distance
HAE	Height Above Ellipsoid
IFOV	Instantaneous Field of View
IMU	Inertial Measurement Unit
INS	Inertial Navigation System
InSAR,	Interferometric Synthetic Aperture Radar
IPR	ImPulse Response
IR	InfraRed
Ladar	Laser Detection and Ranging System. This term is used interchangeably with the term lidar. Historically, the term ladar grew out of the Radar community and is more often found in the literature to refer to tracking and topographic systems.
Lidar	LIght Detection and Ranging System

MBIO	Multi Beam Input-Output
MSL	Mean Sea Level
NED	North East Down
PHD	Phase History Data
PPS	Pulses Per Second
PRF	Pulse Repetition Frequency
RAR	Real Aperture Radar
Radar	RAdio Detection And Ranging
SAR	Synthetic Aperture Radar
sonar	SOund Navigation And Ranging
TOF	Time of Flight

5.3 Notation

Clauses 6, 7, 8, 9, 10, and 11 of this Technical Specification present a conceptual schema, specified in the Unified Modeling Language (UML), describing the characteristics of sensor models. Whereas ISO/TS 19103 describes the way in which UML is used in the ISO 19100 family of standards. It differs from standard UML only in the existence and interpretation of some special stereotypes, in particular, “CodeList” and “Union”. ISO/TS 19103 specifies the basic data types used in the UML model and the data dictionary in this Technical Specification.

Annex B contains a data dictionary for the UML diagrams in this schema.

ISO/TS 19103 requires that names of UML classes, with the exception of basic data type classes, include a prefix that identifies the standard and the UML package in which the class is defined. Table 2 lists the prefixes used in this Technical Specification, the International Standard or Technical Specification in which each is defined and the package each identifies. UML classes defined in this Technical Specification belong to a package named Sensor Data Extension and have the prefix SE.

In this Technical Specification, classes taken from other geographic information standards are represented with a dotted outline.

Table 2 — UML class prefixes

Prefix	Standard	Package
CI	ISO 19115	Citation
CV	ISO 19123	Coverages
DQ	ISO 19157	Data quality
GM	ISO 19107	Geometry
MD	ISO 19115	Metadata
MI	ISO 19115-2	Metadata for Imagery
SC	ISO 19111	Spatial Coordinates
SD	ISO 19130	Sensor Data
SE	ISO 19130-2	Sensor Data Extensions
TM	ISO 19108	Temporal Schema

6 Sensor Model Extensions

6.1 Introduction

ISO/TS 19130 specifies the common and sensor-specific components of sensor models for precise geopositioning of imagery data. The specific sensors covered by ISO/TS 19130 are frame, whiskbroom, pushbroom, and SAR sensors. This Technical Specification covers InSAR, lidar, and sonar sensors, extends the SAR sensor model, and defines the sensor model for aerial triangulation. For sonar, the use of non ship based platforms is not covered in this Technical Specification. Clause 6 specifies the extensions to the common sensor model classes defined in ISO/TS 19130. Clauses 7, 8, 9, 10, and 11 specify sensor-specific extensions.

6.2 SE_SensorModel

SE_SensorModel is a specified subclass of SD_SensorModel that contains a description of sensor modeling methods and sensor manufacturer information to further specify the sensor and the modeling approach. The UML for this extension is shown in Figure 1 and the data dictionary for this diagram is located in Table B.1.

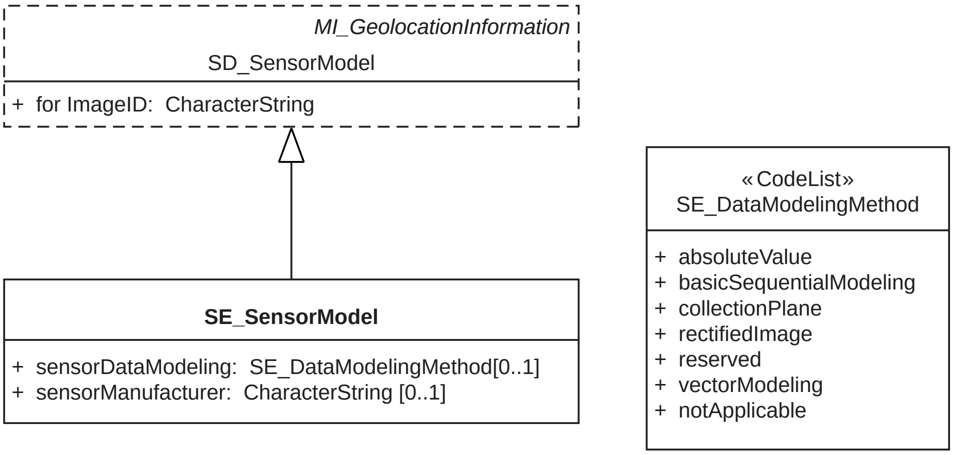

Figure 1 — Extension to the Sensor Model

6.3 SE_Dynamics

The class SD_Dynamics provides a set of elements for describing the rates at which elements of position and attitude change over time. SE_Dynamics is a subclass of SD_Dynamics that allows further specification of the uncertainties in motion and attitude of the sensor platform. The UML for this extension is shown in Figure 2 and the data dictionary for this diagram is located in Table B.2.

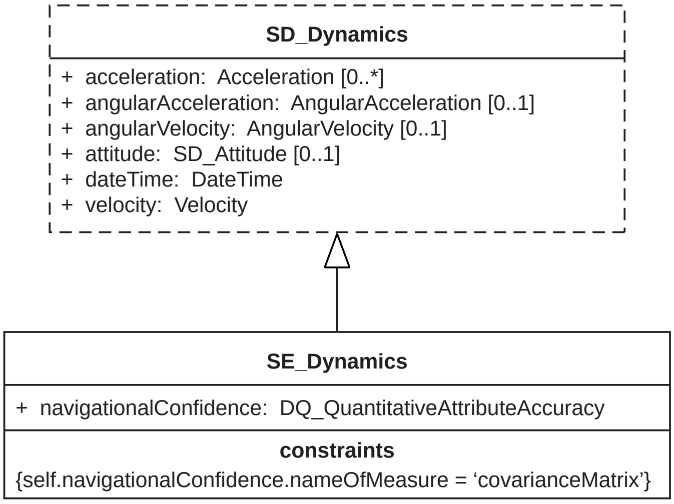

Figure 2 — SE_Dynamics

6.4 SE_PlatformDynamics

SE_PlatformDynamics is a subclass of SD_PlatformDynamics. It specifies additional parameters required to describe the dynamics of platforms for sonar and lidar sensors. The UML for this extension is shown in Figure 3 and the data dictionary for this diagram is located in Table B.3.

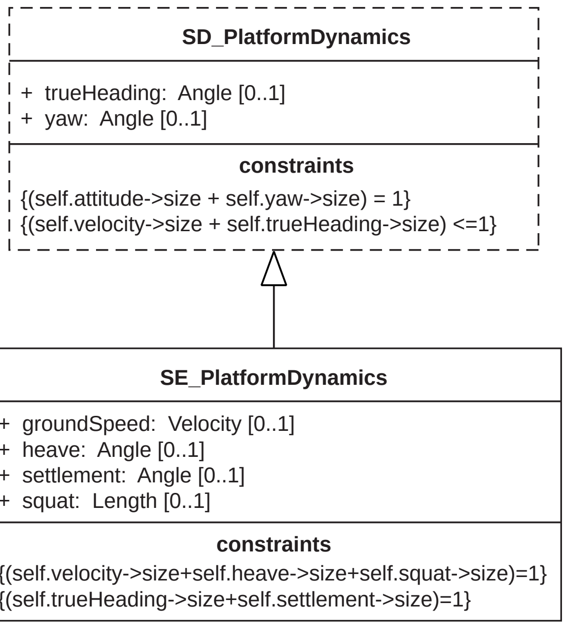

Figure 3 — Extensions to platform dynamics

7 Refinement of SAR physical sensor model

7.1 Introduction

Remote sensing systems using radar (radio detection and ranging) send radio signals towards an object and measure the intensity and phase of the reflected wave. The time difference between the sending of the signal and its return provide the distance to the object. Real Aperture Radar (RAR) images are along a line perpendicular to the flight track; they use the Doppler shift to filter out returns from points ahead of or behind that line. The intensity of the reflectance allows different types of surfaces to be distinguished. In Synthetic Aperture Radar (SAR), the size of the antenna is synthetically enlarged by treating a series of returns from a much smaller physical antenna that is moving relative to the target as one long antenna (aperture). The distance the platform moves in synthesizing the antenna is known as the synthetic aperture. By synthesizing a large array, SAR can enjoy the benefits of improved angular resolution that come with large antennas without the technical and physical problems associated with them. SAR can sum the returns received from any given point over the time in which the physical antenna is moved along the length of the synthetic antenna. Figure 4 shows the geometry of a SAR measurement.

Typically, SARs produce a two-dimensional (2-D) image. One dimension in the image is called range (or cross track) and is a measure of the "line-of-sight" distance from the radar to the target. Range measurement and resolution are achieved in synthetic aperture radar in the same manner as most other radars, from the time from transmission of a pulse to receipt of the echo. In the simplest SAR, range resolution is determined by the transmitted pulse width, i.e. narrow pulses yield fine range resolution. The other dimension is called azimuth (or along track) and is perpendicular to range. To obtain fine azimuth resolution, a large synthetic antenna is needed to focus the transmitted and received energy into a sharp beam. The sharpness of the beam defines the azimuth resolution. A side-looking radar is a SAR-system that records the object space (the ground) on one or both sides of the flight path or of the trajectory. The ground directly below the sensor is not recorded.

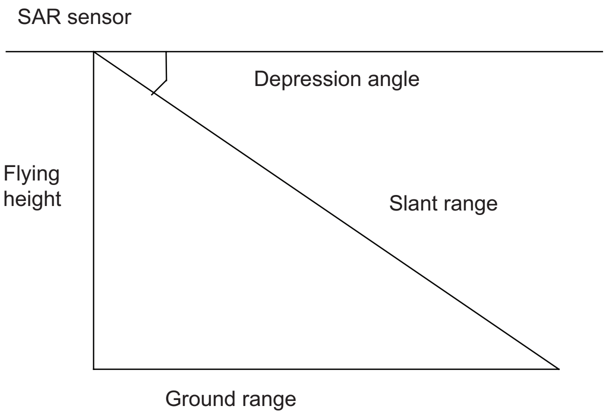

Figure 4 — Geometry of a SAR measurement

ISO/TS 19130:2010 specifies the fundamental metadata models needed for geolocating SAR images. In 7.2, this Technical Specification defines additional metadata for SAR geolocation. In Annex C, it provides an updated informative description of how to use the sensor models defined in ISO/TS 19130:2010 and this Technical Specification for precise geopositioning of SAR images.

7.2 SE_SAROperation

SE_SAROperation is a subclass of SD_SAROperation. It provides further information on the data collection mode used in a SAR operation. Figure 5 defines the extensions required to describe the operation of SAR. The data dictionary for this UML model is located in Table B.4 and the code list B.2.1.7.

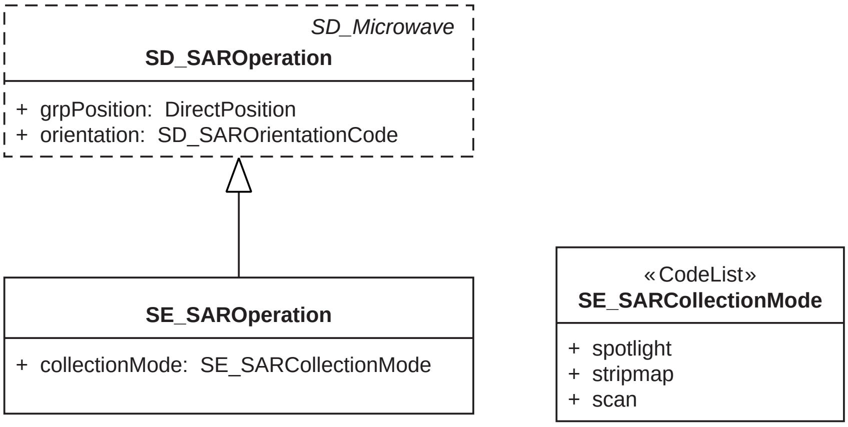

Figure 5 — SE_SAROperation

8 Interferometric SAR

8.1 Introduction

Interferometric SAR, or InSAR, is the application of interferometry to SAR images. An interferogram, the interferometric overlay of two SAR images, taking amplitude (intensity) and phase of both images into account, is produced. InSAR allows for a three-dimensional measurement of a surface and is especially useful for detecting minor surface deformation and mapping topography at millimetre or centimetre scales.

InSAR may be carried out in many ways. Single path interferometry is the interferometry of two SAR images taken from two antennas mounted on a common platform. Repeat-pass interferometry is the interferometry of two SAR images taken from two independent passes of a sensor over the same object. Repeat-pass interferometry of two sensors on two platforms flying almost at the same time and on the same orbit is called tandem interferometry. Differential interferometry is a special form of repeat-pass interferometry to detect local movements of the ground.

ScanSAR interferometry is a method to increase the possible width of the coverage below the flight path by focusing the system at points of interest. The swath is subdivided into several sub-swaths. After the beam has imaged a sub-swath with a certain number of pulses, its depression angle is rapidly steered to a different sub-swath. The result is a pattern of many small SAR image patches without complete coverage of the ground.

After the creation of an interferogram, the phase is ambiguous beyond the interval [0, 2π]. The ambiguities are removed by a process called phase unwrapping. One method of unwrapping the phases of an interferogram uses lines to connect positions with the same phase differences. A line of this type is called a cut.

8.2 InSAR geometry

The distance between the two imaging positions, either from single-pass dual-antennas or from single-antenna repeat passes, is the baseline of InSAR. In dual antenna InSAR, while the baseline vector can be at any orientation, it is often configured to either nearly perpendicular to the platform track, called cross-track InSAR (Figure 6), or nearly parallel to the platform track, called along-track InSAR (Figure 7). Cross-track InSAR is useful in mapping topography and topographic deformations, while along-track InSAR is useful in detecting radial movements such as ocean currents. In single-antenna repeat pass InSAR, the baseline vector is determined by the platform positions, which can be configured to cross-track or along-track geometry. It is also possible to command a platform to return to the exact same position and make another observation at the exact same geometry, in which case the phase difference recorded in the resultant interferogram image reflects, if the elementary scatters within each imaging element are not changed, the movement of the target along the radial direction between the two observations. The amount of the displacement and the elapsed time between the two observations can be used to determine the velocity of the surface movement or deformation. Differential SAR Interferometry (DInSAR) is an application of InSAR for the detection of change in the geometry.

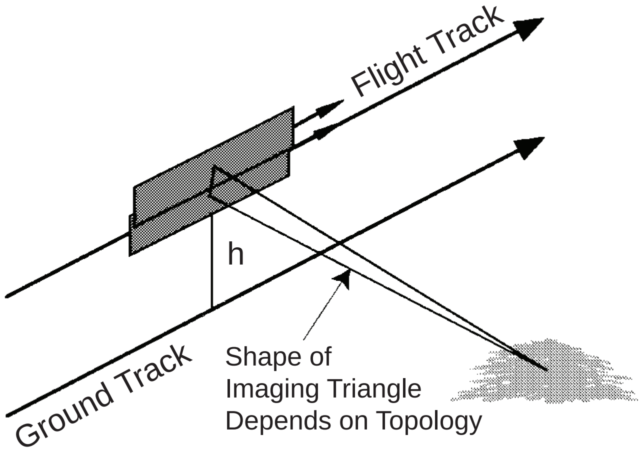

Figure 6 — Cross-track InSAR Configuration (from Rosen et al., 2000)

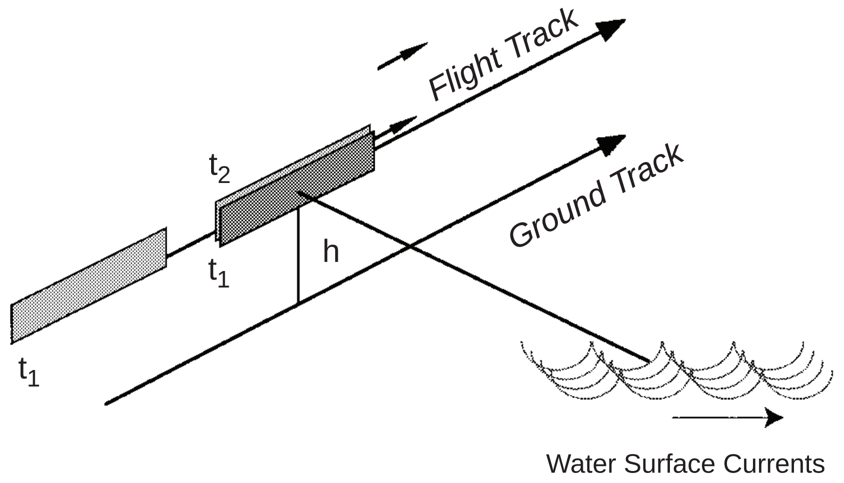

Figure 7 — Along-track InSAR Configuration (from Rosen et al., 2000)

Figure 8 shows the various vectors in an InSAR geometry. The two antennas are positioned at A_1 and A_2, separated by a baseline B. The target position is T. The location O is a reference position, such as the earth centre or nadir point. The vectors from O to the satellite, to the antenna positions, and to the target are .., $\vec{P}_2$, and $\vec{T}$, respectively. The viewing vectors from the antennas to the target are $\vec{l}_1$ and $\vec{l}_2$.

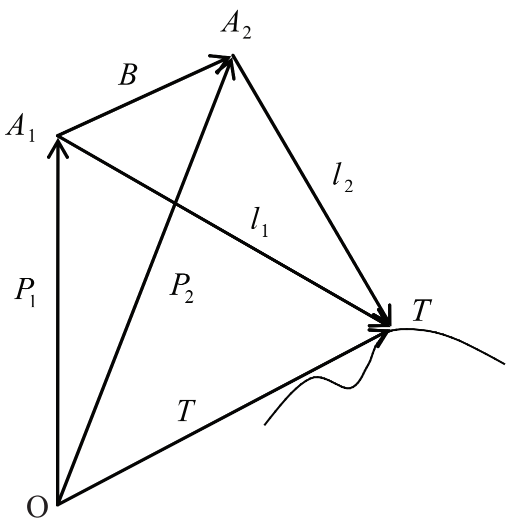

Figure 8 — InSAR Geometry

For cross-track interferometers, two modes of data collection are commonly used: single transmitter, or standard, mode, where one antenna transmits and both interferometric antennas receive, and dual transmitter, or “ping-pong”, mode, where each antenna alternatively transmits and receives its own echoes (Rosen et al., 2000). Single antenna repeat-pass InSAR operates inherently in ping-pong mode.

The following relationship between interferometric phase, ϕ, and baseline and viewing vectors can be derived (Rosen et al., 2000):

$$\begin{aligned}\vec{T} &= \vec{P}_1 + \vec{l}_1 = \vec{P}_1 + \rho_1 \hat{l}_1 \\ &= \vec{P}_2 + \vec{l}_2 = \vec{P}_2 + \rho_2 \hat{l}_2\end{aligned} \tag{1}$$

$$\vec{B} = \vec{P}_2 - \vec{P}_1 \tag{2}$$

$$\begin{aligned}\varphi &= \frac{2\pi p}{\lambda}(\rho_2 - \rho_1) = \frac{2\pi p}{\lambda}\left(\left|\vec{l}_2\right| - \left|\vec{l}_1\right|\right) \\ &= \frac{2\pi p}{\lambda}\rho_1\left[\left(1 - \frac{2\left\langle \hat{l}_1, \vec{B}\right\rangle}{\rho_1} + \left(\frac{B}{\rho_1}\right)^2\right)^{1/2} - 1\right]\end{aligned} \tag{3}$$

where $B = \left|\vec{B}\right|$ is the length of the baseline; ρ_1 and ρ_2 are ranges from the two antennas to the target; p equals *1* for standard mode and *2* for ping-pong mode.

8.3 Interferometric SAR operation

While surface reconstruction of InSAR is different from that of SAR, only a few additional parameters are required in the InSAR sensor model. These parameters include the geometrical relationships between the target and the positions of two antennas or the single repeat-pass antenna. In the two-antenna configuration, all parameters for the two antennas shall be exactly the same except that their positions in the platform are different. In the single antenna repeat pass configuration, the sensor parameters for the different observations shall be the same except that the observation times and positions in the multiple passes are different. Figures 9 and 10 define the extensions required to describe the operation of InSAR. The data dictionaries for this UML model are located in Tables B.5 and B.6 and the code lists in given in B.2.1.11 and B.2.1.12.

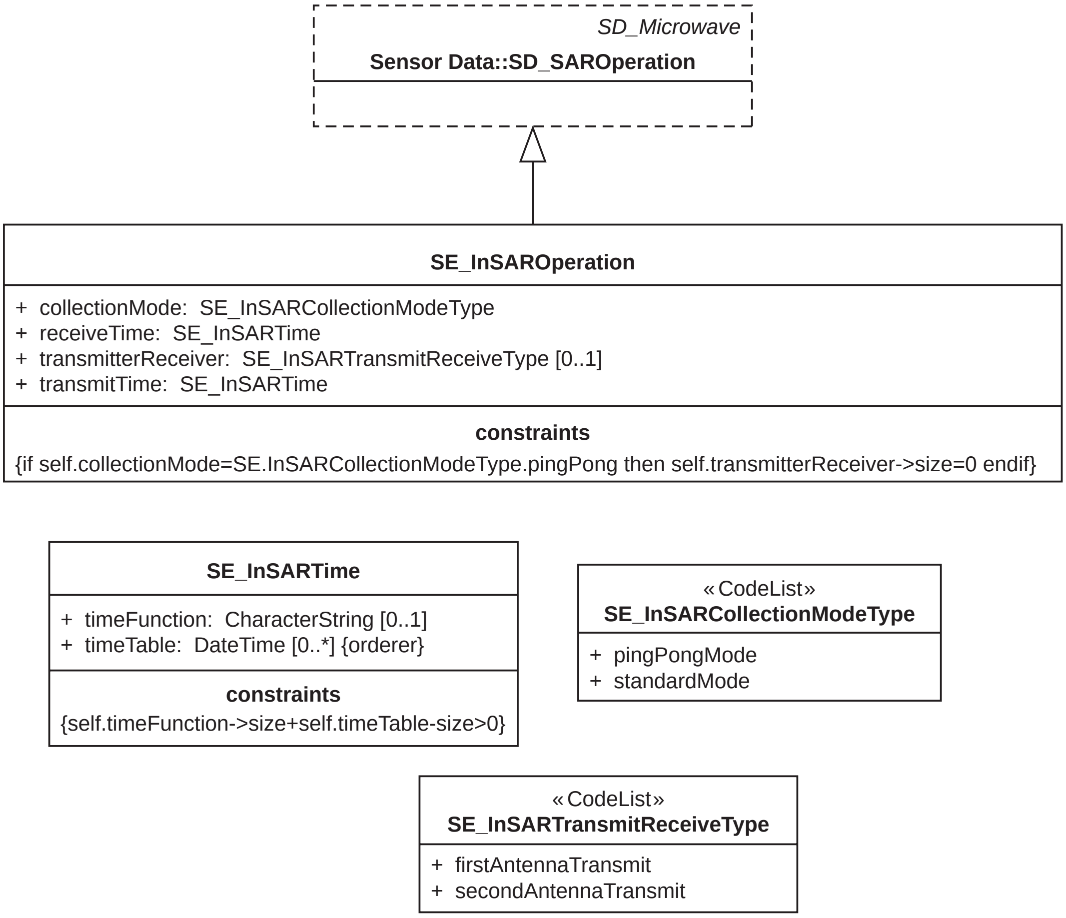

Figure 9 — InSAR Operation

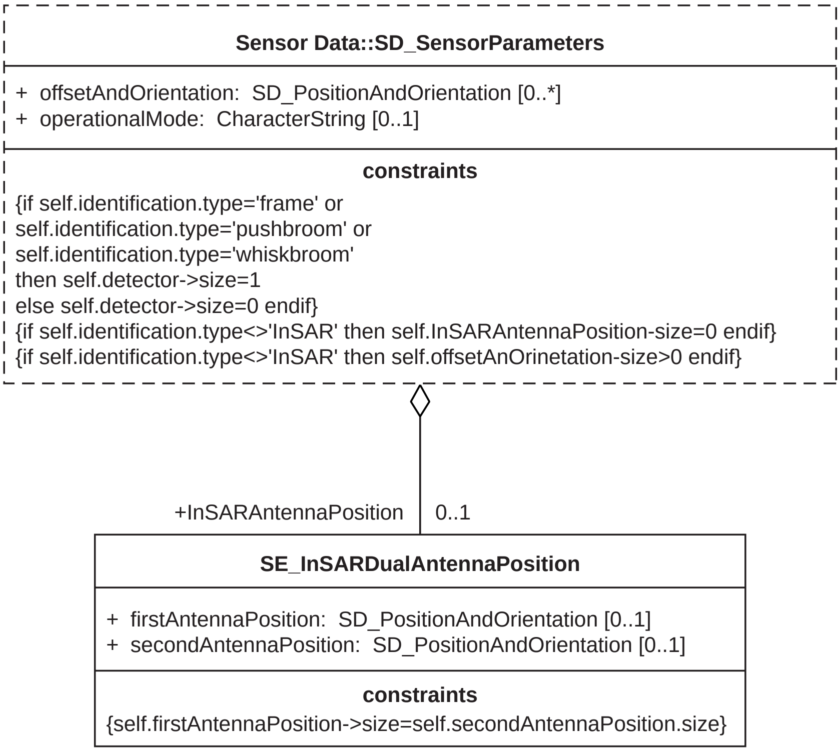

Figure 10 — InSAR dual antenna position

9 Lidar physical sensor model

9.1 Description of sensor

9.1.1 Introduction

A lidar (LIght Detection And Ranging) sensor is often mounted on-board an aircraft or a satellite. During the flight, the lidar sensor pulses a narrow, high frequency laser beam toward the Earth through an opening in the bottom of the platform. The lidar sensor records the time difference between the emission of the laser beam and the return of the reflected laser signal to the platform. Multiple reflections of a signal pulse emission are also possible.

9.1.2 Types of lidar

There are five basic types of lidar systems:

— **Range finder**

Range finders are used to measure the distance from the lidar sensor to a solid or hard target.

— **DIAL**

Differential Absorption lidar (DIAL) is used to measure chemical concentrations (such as ozone, water vapour and pollutants) in the atmosphere. A DIAL lidar uses two different laser wavelengths, which are selected so that one of the wavelengths is absorbed by the molecule of interest while the other wavelength is not. The difference in intensity of the two return signals can be used to deduce the concentration of the molecule being investigated.

— **Doppler lidar**

Doppler lidar is used to measure the velocity of a target. When the light transmitted from the lidar hits a target moving towards or away from the lidar, the wavelength of the light reflected/scattered off the target will be changed slightly. If the target is moving away from the lidar, the return light will have a longer wavelength; if the target is moving towards the lidar, the return light will be at a shorter wavelength.

— **Multiple receiver lidar**

Using multiple receivers at different locations and triangulating the results allows accurate location of a target in three dimensions.

— **Full waveform lidar**

Used for studies of soft targets.

9.2 Information required for geolocating

As a subclass of SD_OpticsOperation, SE_LIDAROperation defines the lidar-specific metadata required for precise geopositioning of lidar data. Geolocation information for lidar shall include the direction and time of each laser pulse, as specified in the UML model shown in Figure 11. The data dictionary for this diagram is defined in Table B.7.

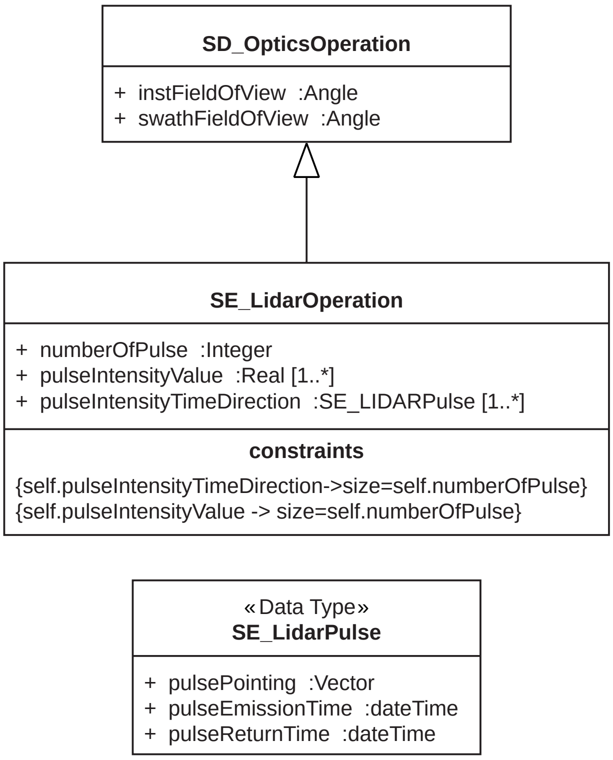

Figure 11 — Lidar operation

10 Sonar physical sensor model

10.1 Description of sensor

10.1.1 Introduction

Hydrographic surveying is usually conducted on a dynamic platform and in an environment that is constantly changing. As far as possible, the many influences that affect accuracy of survey measurements shall be accounted for and applied to the final survey data.

Sonar sensors are used to detect and survey objects in water using sound. Sound or ultrasonic waves are used underwater to obtain imagery of geological and manmade features at the bottom of seas, rivers or lakes, because electromagnetic radiation is generally not usable for imaging through water. Sound waves have many characteristics that are similar to electromagnetic waves, such as reflection, refraction, interference and diffraction. Unlike electromagnetic waves, they are elastic longitudinal waves whereas electromagnetic waves are transverse waves. The higher the frequency used, the greater will be the resolution and the attenuation.

As both horizontal and vertical positioning become increasingly more accurate (using code phase DGNSS [DGPS] and carrier phase DGNSS [kinematic]), knowledge of the vessel's attitude becomes critical for accurate positioning of sonar beams on the ocean floor. The increased path lengths of the outer beams in a multibeam system result in greater errors due to ray bending and require a more detailed knowledge of sound speed through the water column.

10.1.2 Configuration

10.1.2.1 Types of sonar

Four basic types of systems are currently used for hydrographic surveys.

— **Single beam echo sounder system**

A single beam echo sounder system produces one sonar beam directly beneath the transducer and receives a return from the closest point at which it intersects the seabed.

— **Swath (multibeam or interferometric) sonar systems**

Swath sonar systems have a single transducer or pair of transducers that transmit(s) a fan-shaped signal perpendicular to the ship's direction of travel. Returns are received from the points where this fan intersects the seabed and are converted into discrete depth values. Signal backscatter strength can be measured to provide imagery in a way similar to sidescan sonar systems.

— **Sweep or boom systems**

Sweep systems are characterized by several transducers mounted on a boom, which is then operated parallel to the water's surface and orthogonal to the vessel's direction of travel. This is the equivalent of having a number of single beam echo sounders mounted in a line. The transducers are equally spaced. If the echo comes, as is assumed, from the midpoint of the sonar beam, the result will be sonar bottom coverage with a constant width, independent of water depth.

— **Sidescan sonar systems**

Sidescan sonar systems generally have two transducers mounted transversely in a towfish. In a side scan the transmitted energy is formed into the shape of a fan that sweeps the seafloor from directly under the towfish to either side. Sidescan sonar sensors measure backscattered signal strength to provide qualitative information in the form of a "sound image". They do not provide definitive depth measurements. There are significant differences between interferometric and beamforming sonar.

Interferometric sonar, also referred to as Phase Differencing Bathymetric Sonar (PDBS) systems, use the measurement of phase at each of several receive elements to determine the angle from which the acoustic return originates. Once the phase of the acoustic return has been precisely measured, the differences between the phase at each of the receive elements are used to calculate the angle from which the return originated. This angle of origin, in combination with range calculated from the two way travel time, provides a discrete location on the seafloor.

Beamforming is a signal processing technique used in sensor arrays for directional signal transmission or reception.

10.1.2.2 Single beam echo sounder system

A single beam echo sounder system consists of four basic components: a transducer or a transmitter and receiver, and a control and display system. These components are depicted schematically in Figure 12.

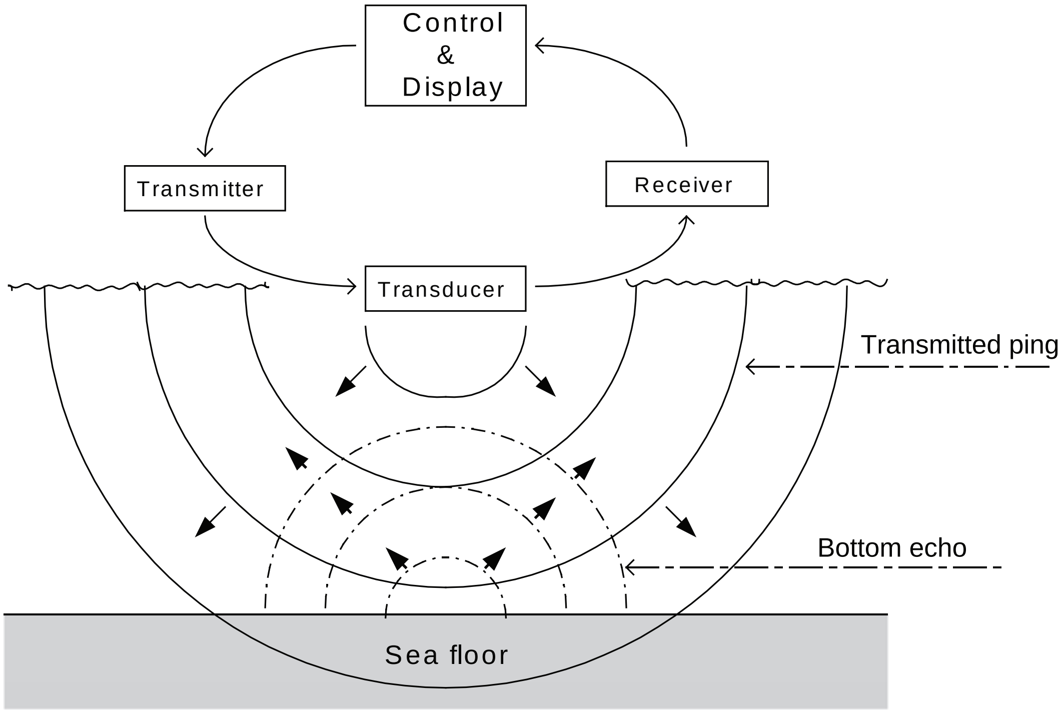

Figure 12 — Single beam sonar systems

10.1.2.3 Swath system

The sounding position coordinates shall be calculated by adjusting for system offsets such as the GNSS antenna, motion reference units, transducer position and alignment.

The cross-track distance and depth shall be calculated from the range (determined by measuring the two-way time travel) and the beam angle, as shown in Figure 13. Depending on the system either phase, amplitude or a combination are used to measure depth.

In the scanning sonar/scanning profiler system for swath sounding, a single beam is mechanically rotated through (part of) a circular arc. A measurement is taken and then the transducer is rotated over an angle equal to the beam angle. A new measurement is taken, the transducer is rotated, and etc.

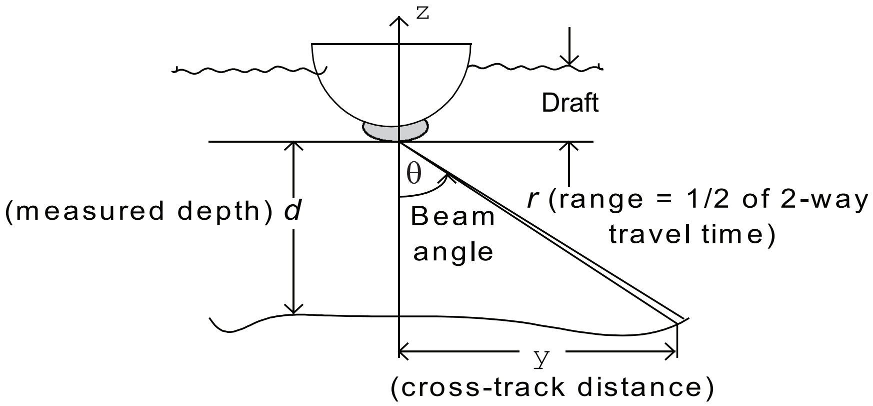

Figure 13 — Swath system

10.1.2.4 Sweep or boom system

Like swath systems, sweep systems produce soundings along a line oriented in the cross-track direction, except that the coordinates of each sounding are simply those of each transducer. Figure 14 shows that there will be separate offset values for each transducer.

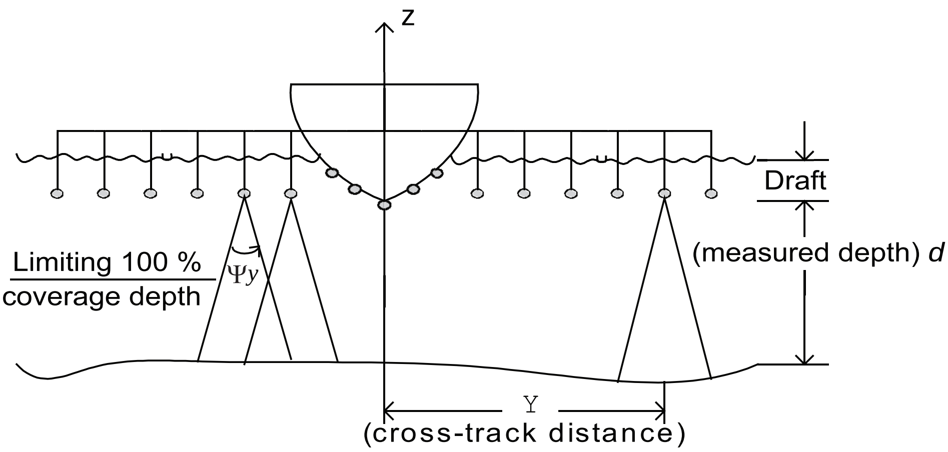

Figure 14 — Sweep system

10.1.2.5 Sidescan sonar system

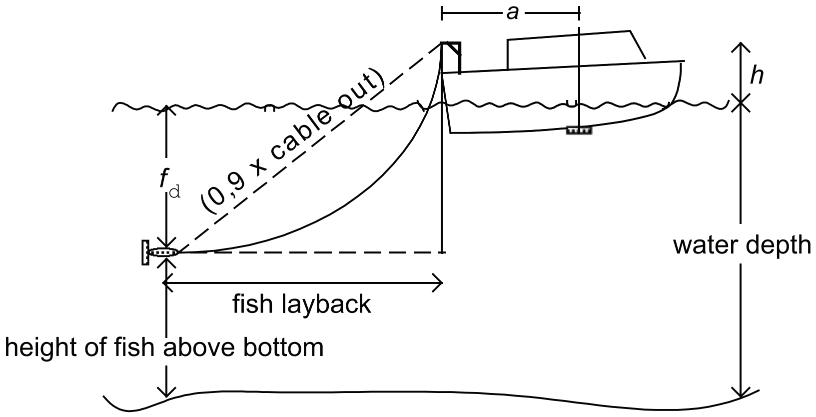

Figure 15 — Height and position determination of sidescan sonar system

Fish layback = sqrt[(0,9 × cable out)^2 – (h+f_d)^2]

where

a offset of tow point from echo sounder transducer;

h height of tow point above waterline;

f_d depth of sidescan sonar fish = water depth – height of fish above bottom.

NOTE 1 A factor of 0,9 of the towing cable length is sometimes used to calculate fish layback length, however this is dependent on the altitude of the sonar fish above the water bottom. This is recommended to be 10 % of water depth but is not always attained. For deep depths different factors may be used or an acoustic positioning system may be used to determine fish relative to either the towing vessel or a 'chase boat'.

Sidescan sonar is used to locate objects. A shallow water multibeam or single beam sonar system is used to determine the smallest depth over the objects. Sidescan sonar data are collected over the seafloor in addition to multibeam or single beam depth data. The operator acquires sidescan sonar data using a towed system. The sidescan sonar system used on the continental shelf can be operated out to a typical maximum range of 500 m although 150 m is commonly used. The towfish should be maintained at a height above the bottom of 8 % to 20 % of the range scale in use. The ideal value is 15 %, as shown in Figure 15.

Since the sonar is pulsing at a fixed rate based on its range scale, the speed that the towfish is being towed will have an effect on the ability to resolve items. In general, the slower the fish is towed, the greater the resolution of the imagery obtained.

NOTE 2 Typically, sidescan sonar is towed at a speed such that objects to be detected would receive a minimum of three pings per pass for a digital system and 5 pings if using a paper recorder. Figure 16 shows an example of how the required towing speed may be computed (if using a paper recorder replace the 3 in the equation for maximum speed with 5).

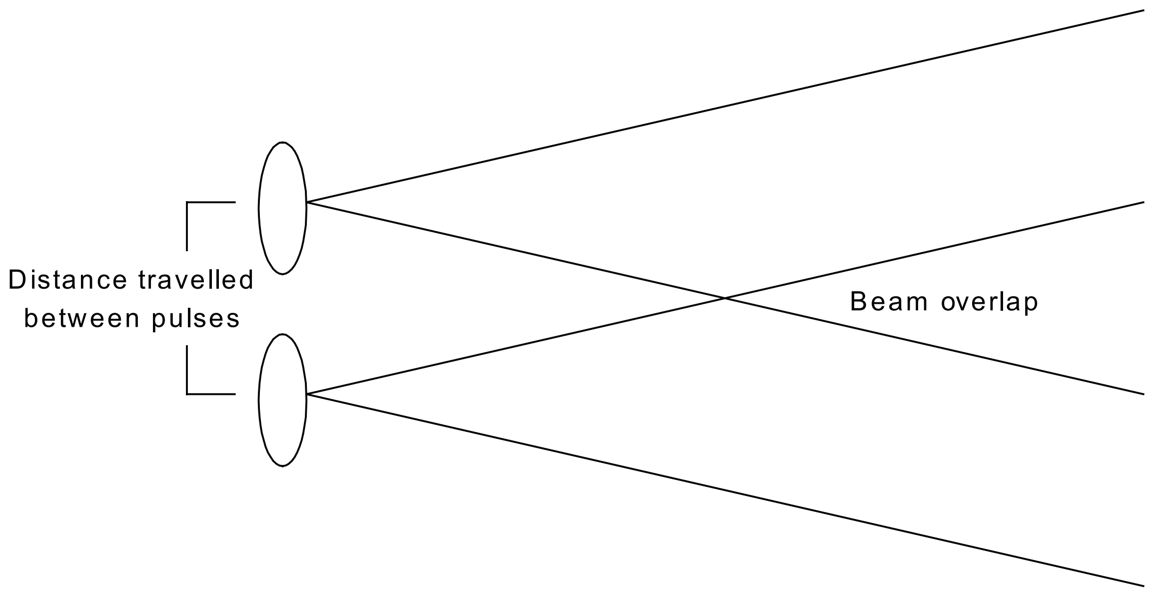

Maximum speed (metres/second) = Target size (metres) × prr/3 (seconds −1)

where prr is the pulse repetition rate = reciprocal of pulse period and knots= metres/second × 1,9

EXAMPLE For a 100 m range scale with 7,5 pulses/second:

— Maximum vessel speed = 4,8 kn

— For a 150 m range scale with 5 pulses/second

— Maximum vessel speed = 3,2 kn

Figure 16 — Speed calculation for sidescan sonar system

10.2 Information required for geolocating

10.2.1 Introduction

The sonar-specific metadata needed for geolocating sonar data are specified in 10.2.2 to 10.2.5. The metadata classes defined here, together with sensor-independent metadata classes defined in ISO/TS 19130 and in this Technical Specification, provide sufficient information to construct a physical sensor model for geolocating the sonar data. The informative Annex E provides a detailed description of Sonar systems and their operation and an example on how to use the metadata defined in ISO/TS 19130 and this Technical Specification to geolocate the sonar data.

10.2.2 SE_SonarOperation

The class SE_SonarOperation is a specified subclass of SD_SensorSystemAndOperation. SE_SonarOperation and its subclasses specify the sonar-specific metadata required to describe sonar operation for precise geopositioning of sonar data. This information shall be provided as shown in the UML model of Figure 17. The classes shown in Figure 17, their attributes and their associations, shall be used as specified in the data dictionary of Table B.8.

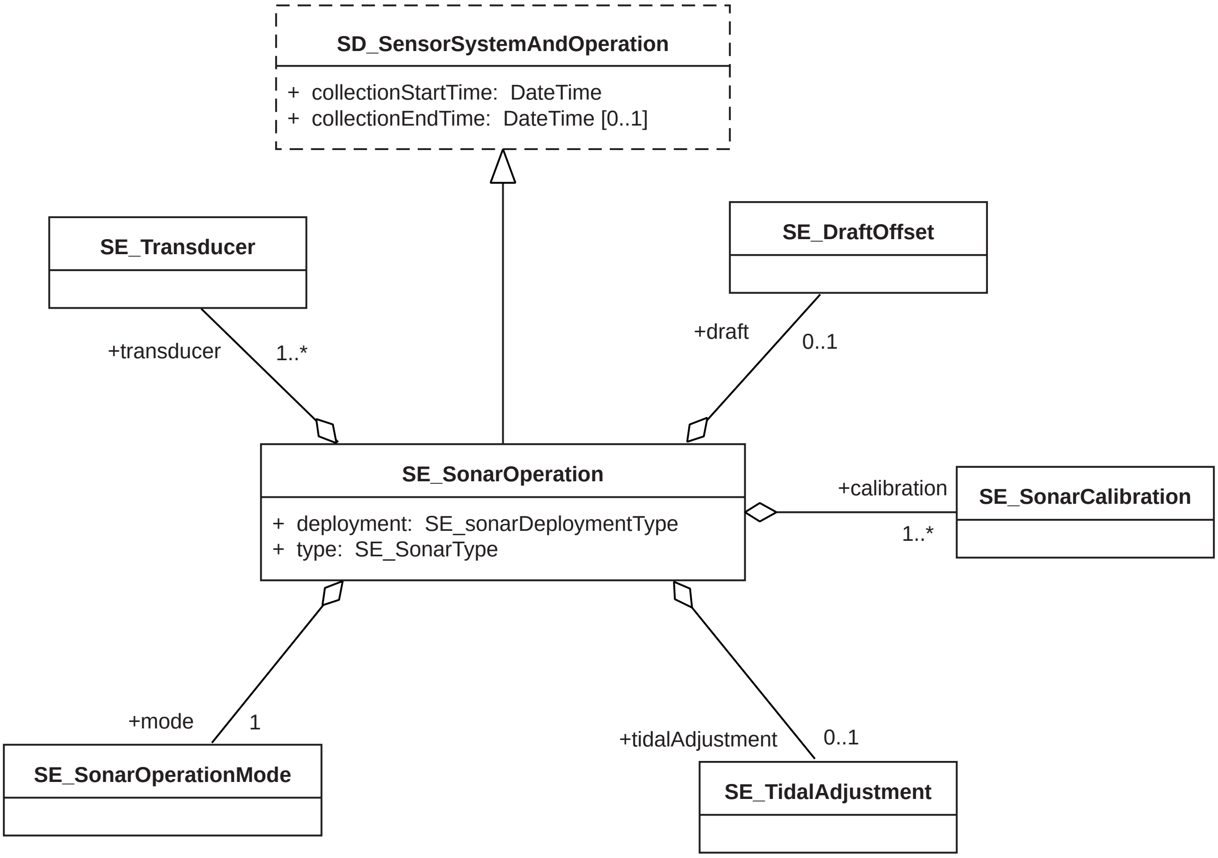

Figure 17 — Sonar operation

10.2.3 SE_SonarOperationMode

The class SE_SonarOperationMode specifies the operation modes of sonar. This information shall be provided as shown in the UML model of Figure 18. The classes shown in Figure 18, their attributes and their associations shall be used as specified in the data dictionary of Table B.9, and the code lists given in B.2.1.7, B.2.1.8 and B.2.1.9.

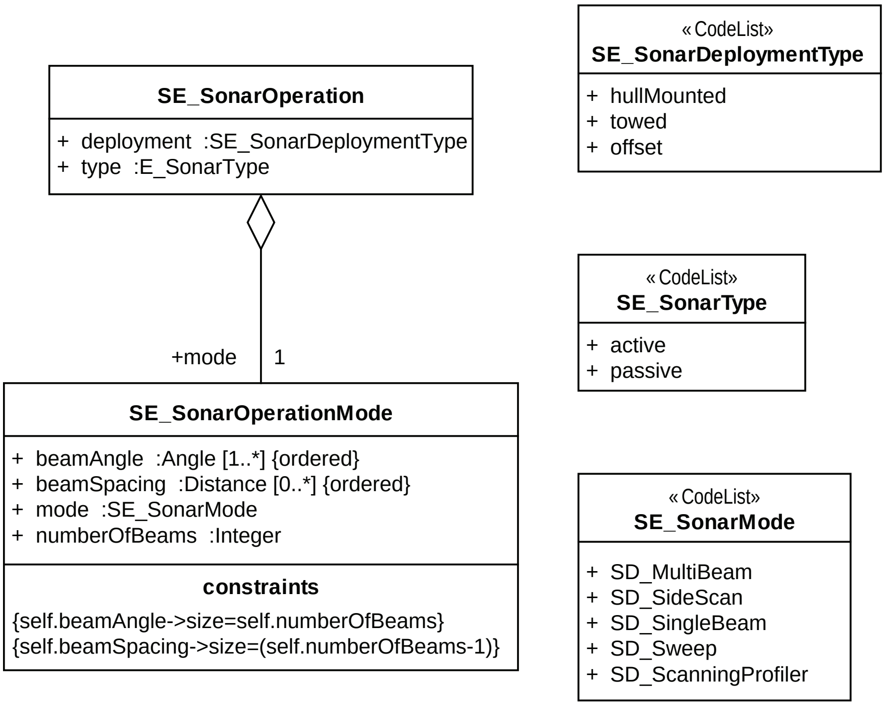

Figure 18 — Sonar operation mode

10.2.4 SE_SonarTransducer

The sonar transducer is a major component of the sonar system. It transmits the sound wave through the transmitter and receives the echo of the wave through the receiver. This information shall be provided as shown in the UML model of Figure 19. The classes shown in Figure 19, their attributes and their associations shall be used as specified in the data dictionary of Table B.10. Position is defined as the x,y,z (layback or offset) distances from the RP (Reference Position). The RP is the 0,0,0 coordinates from which all system equipment is related, and “direction” is defined as the angular orientation from the RP.

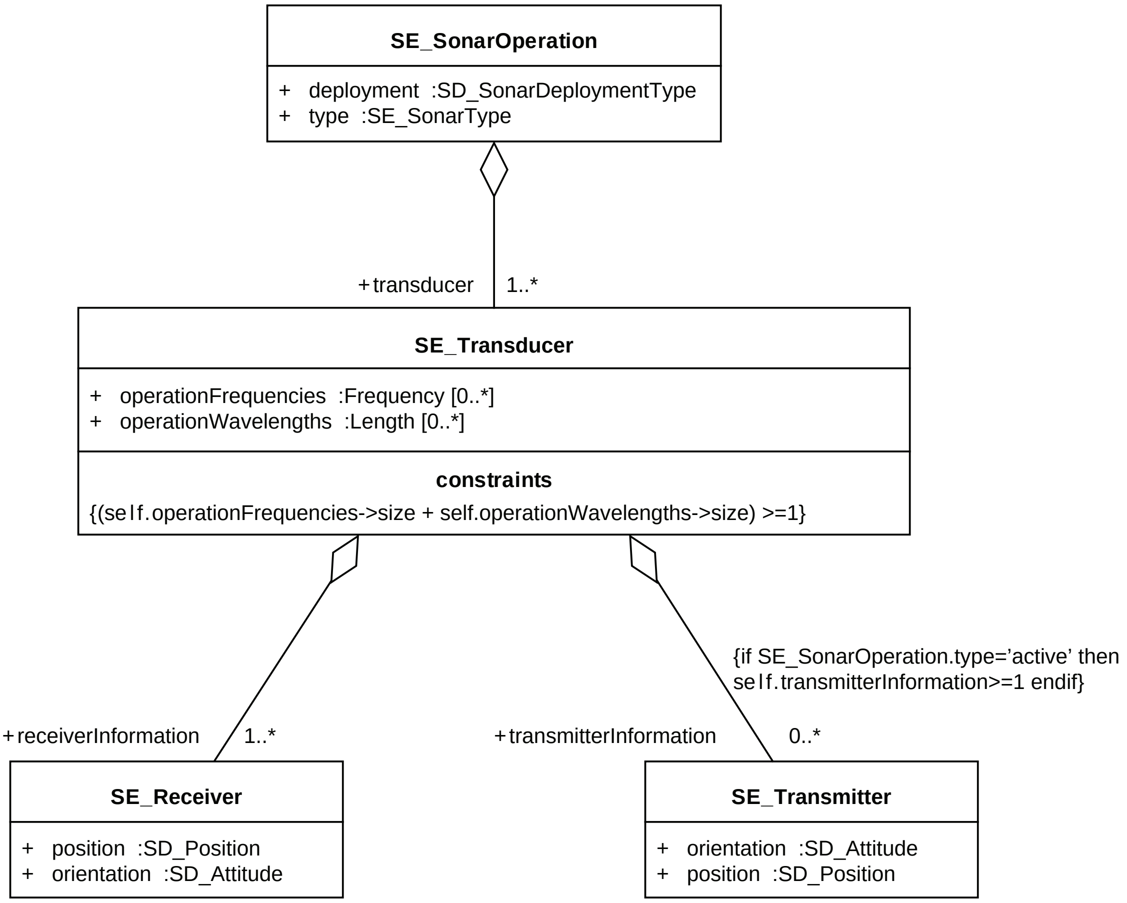

Figure 19 — Sonar transducer

10.2.5 Calibration and adjustment

A set of calibrations and adjustments have to be applied to data collected by a sonar system for geolocating the data. The calibration and adjustment information shall be provided as shown in the UML model of Figure 20. The classes shown in Figure 20, their attributes and their associations shall be used as specified in the data dictionaries of Tables B.11, B.12 and B.13, and the code list given in B.2.1.10. For depths greater than 200 m, it is not always required to correct the measured depths for sound velocity, as a standard sound velocity of 1500 m/s is usually used or values may be selected from the Mathews Correction Tables.

NOTE In some applications a sound velocity profile is used for giving more accurate depths.

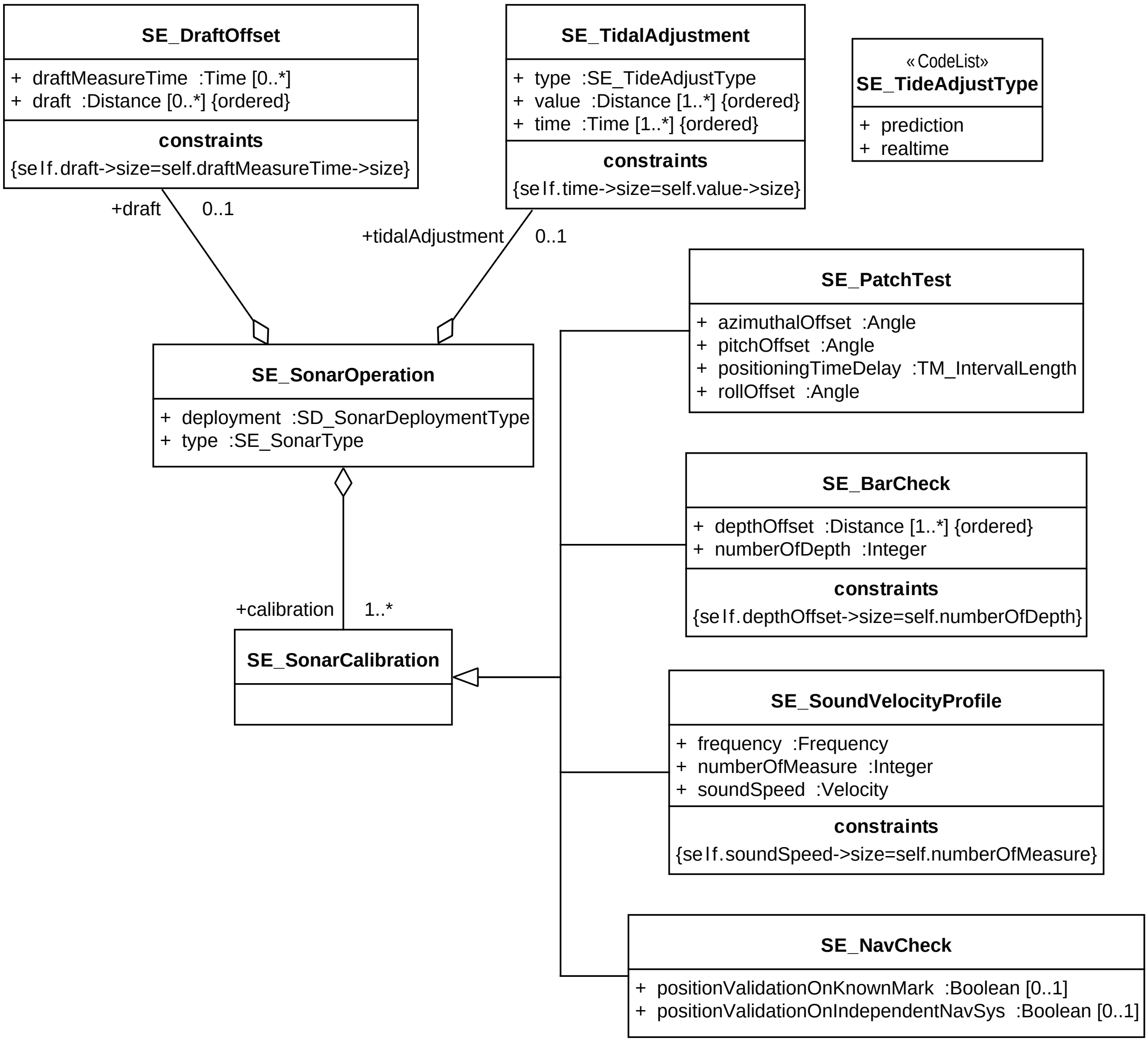

Figure 20 — Calibration and adjustment

11 Aerial triangulation

11.1 Introduction

Aerial triangulation is a method of determining the georeference and other parameters of a sensor and the imagery data taken by this sensor. Aerial triangulation requires an overlap of neighbouring images in order to allow for the creation of a so-called block which is the entirety of all images involved in a project. This requirement restricts aerial triangulation to the physical sensor model of area imaging arrays. This clause addresses only frame camera sensors.

In the past, aerial triangulation was applied in order to restrict the expensive measurement of Ground Control Points to a minimum. Today, a photo flight almost always includes the GNSS (e.g. GPS) measurement of every projection centre. Therefore, aerial triangulation is applied in order to improve the overall accuracy and the reliability. Ground Control Points are used only for a local and mostly unknown datum shift between the coordinate reference system (CRS) of the GNSS and the local CRS.

The heart of aerial triangulation is an adjustment process. The observations include the image coordinates of the tie points, the GNSS-measurements of the projection centres, the IMU-measurements of the projection centres (attitude), the image coordinates of the Ground Control Points, and the image coordinates of the Check Points. The unknowns include the exterior orientation (position and attitude) of every projection centre. The parameters describing the sensor (camera) may be taken as fixed (calibrated) or as unknowns. However, the latter case is not feasible for most aerial applications.

11.2 SE_AerialTriangulation

The information in the classes SE_AerialTriangulation and its subclasses is required for geolocation by aerial triangulation. This information shall be provided as shown in the UML model of Figure 21. The classes shown in Figure 21 their attributes and their associations shall be used as specified in the data dictionary of Table B.14 and the code lists given in B.2.1.1, B.2.1.2, B.2.1.3 and B.2.1.4.

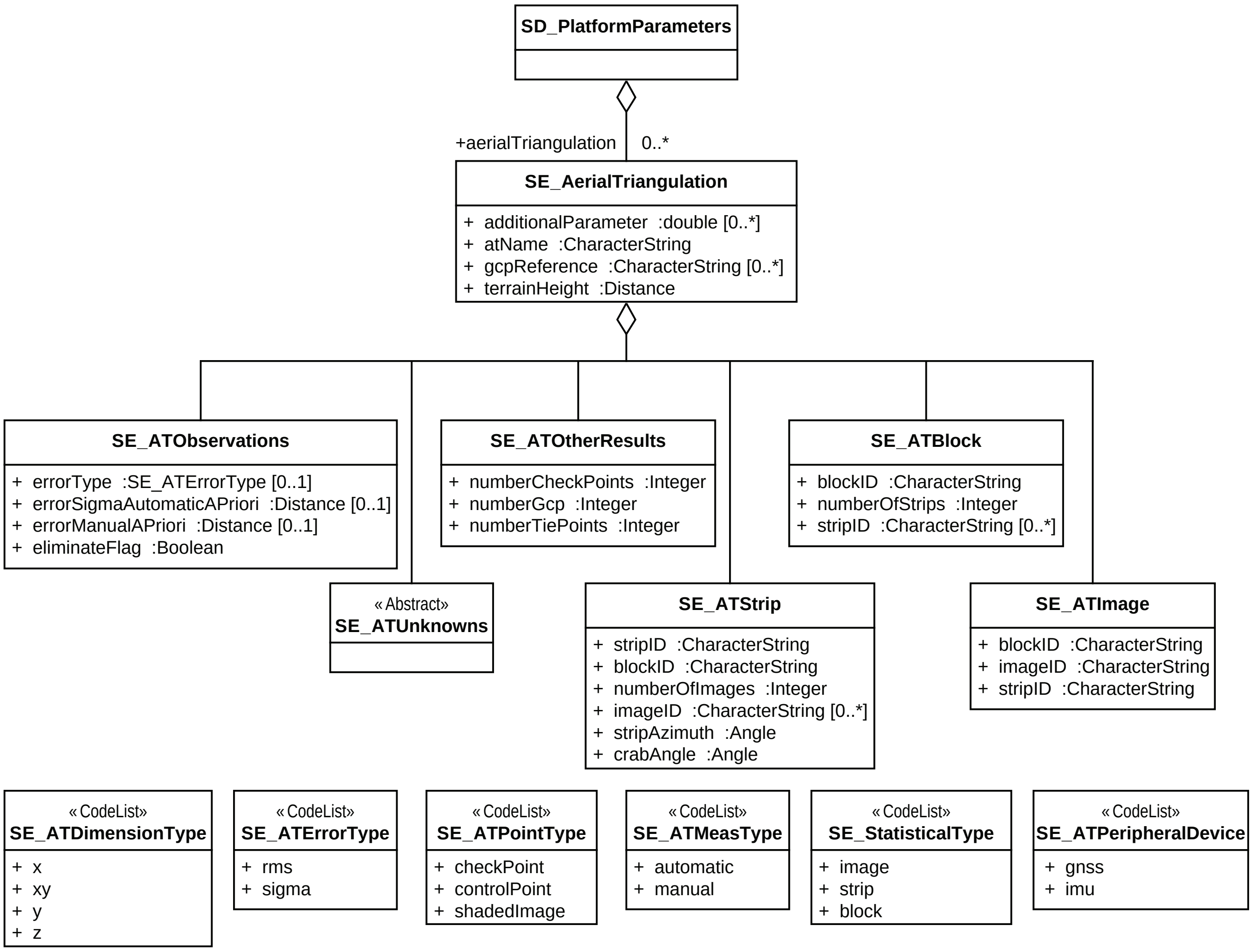

Figure 21 — Aerial triangulation

11.3 SE_ATObservations

Information about the individual observations, as defined in SE_ATObservations and its subclasses, is required for aerial triangulation. This Information shall be provided as shown in the UML model of Figure 22. The classes shown in Figure 22, their attributes and their associations shall be used as specified in the data dictionary of Table B.21.

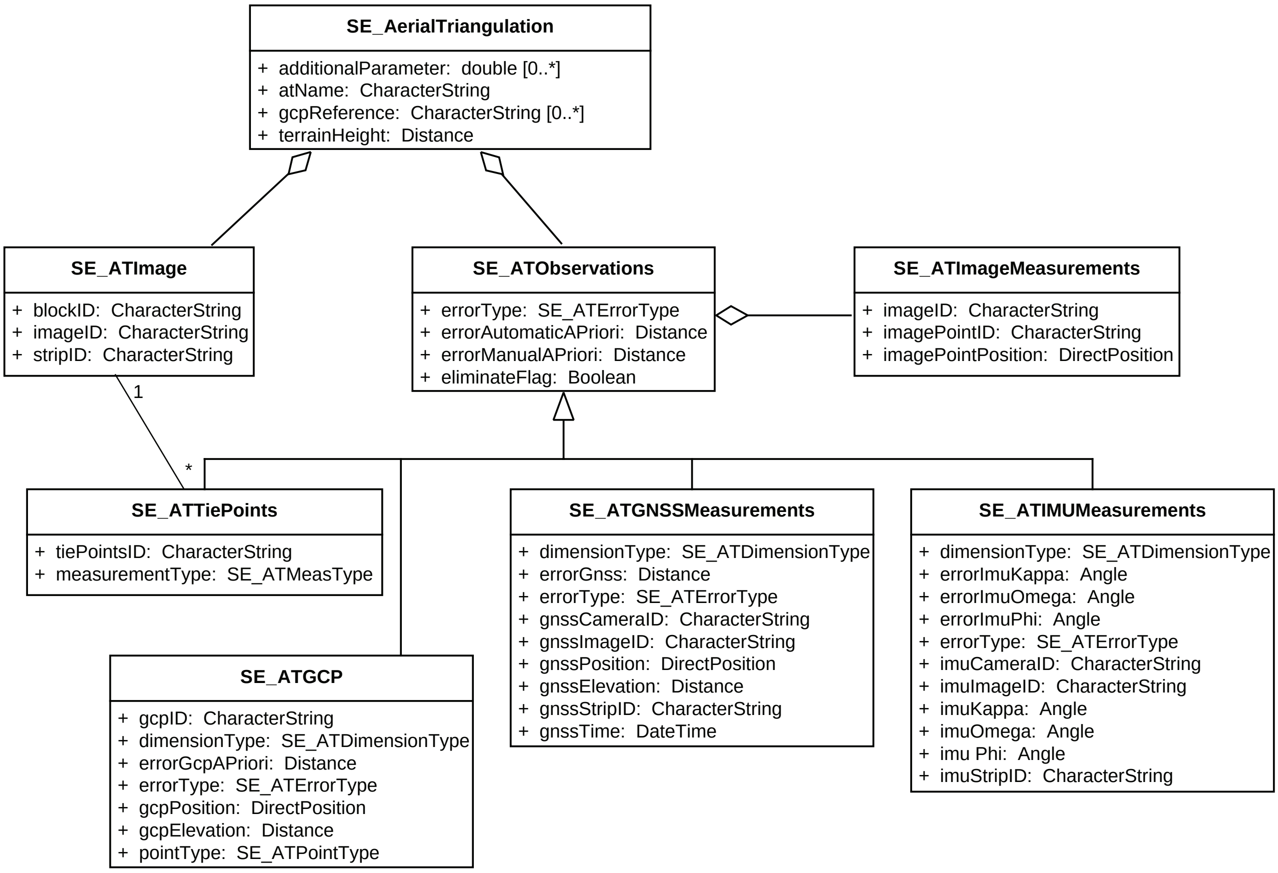

Figure 22 — Aerial triangulation observations

11.4 SE_ATOtherResults

Information about other results of aerial triangulation, as defined in SE_ATOtherResults and its subclasses, is required for aerial triangulation. This Information shall be provided as shown in the UML model of Figure 23. The classes shown in Figure 23, their attributes and their associations shall be used as specified in the data dictionary of Table B.22.

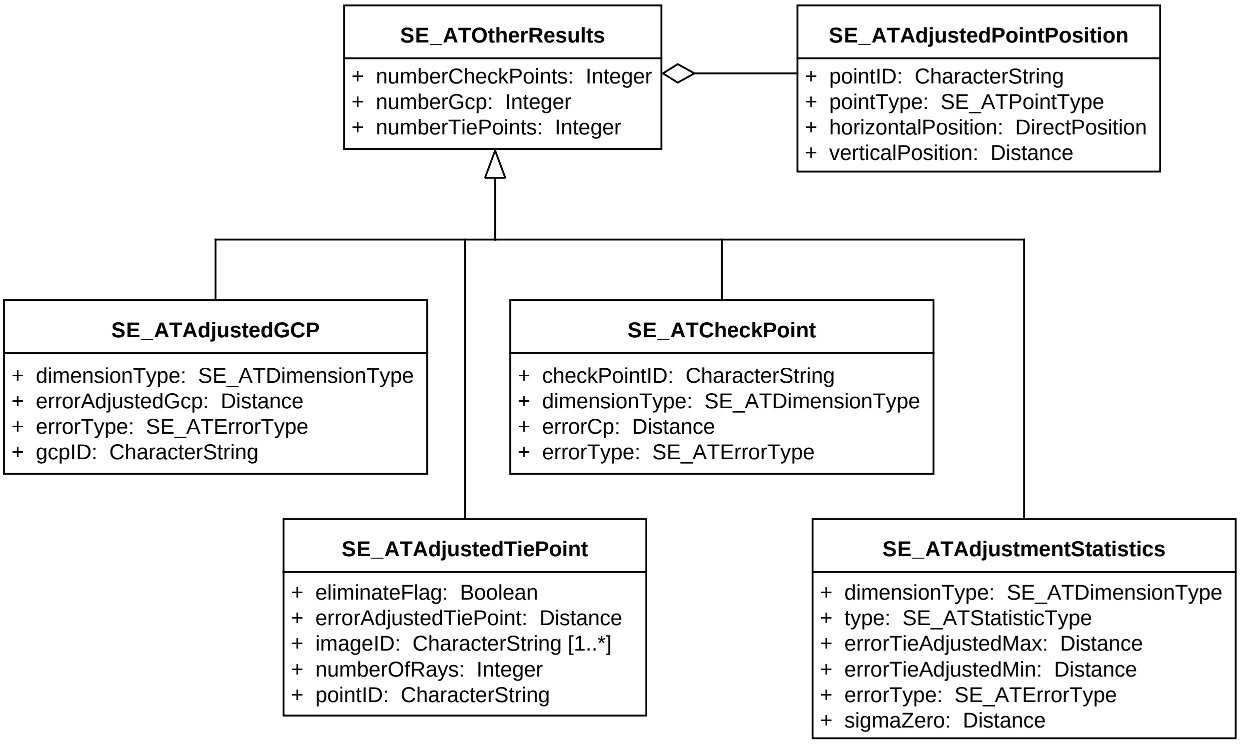

Figure 23 — Other result of aerial triangulation

11.5 SE_ATUnknowns

SE_ATUnknowns and its subclasses define required unknowns for aerial triangulation. This Information shall be provided as shown in the UML model of Figure 24. The classes shown in Figure 24, their attributes and their associations shall be used as specified in the data dictionary of Table B.23.

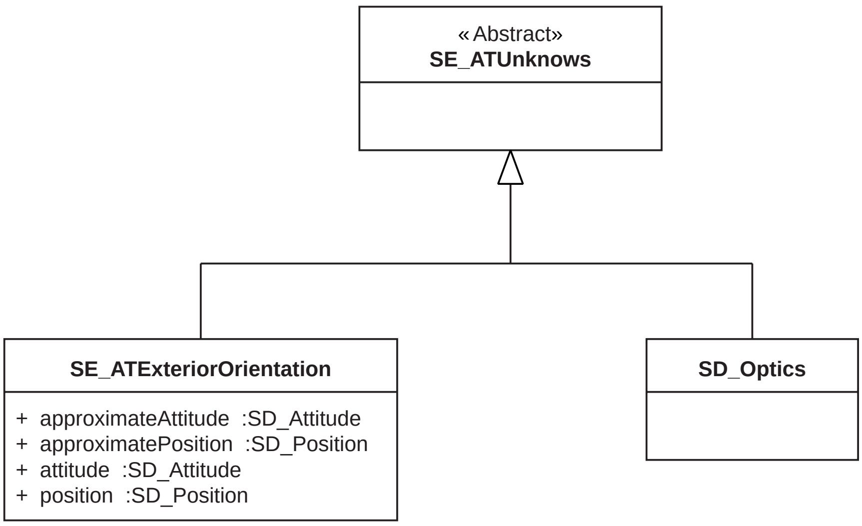

Figure 24 — Exterior orientation of aerial triangulation

Annex A
(normative)

Conformance and testing

A.1 Sensor model extensions

A.1.1 Sensor model completeness

Test purpose: Verify that geopositioning information provided with the image data instantiates SE_SensorModel.

Test Method: Inspect the content of the metadata intended to support geopositioning.

Reference: 6.2

Test Type: Basic

A.1.2 Dynamics

Test purpose: Verify that navigational confidence information provided with the image data instantiates SE_Dynamics.

Test Method: Inspect the content of the metadata intended to support the navigational confidence.

Reference: 6.3

Test Type: Basic

A.1.3 Platform dynamics

Test purpose: If sensor is sonar or lidar, verify that platform dynamics information provided with the image data instantiates SE_PlatformDynamics.

Test Method: Inspect the content of the metadata intended to support the navigational confidence.

Reference: 6.3

Test Type: Capability

A.2 SAR operation

Test purpose: If sensor is SAR, verify that SAR operation description provided with the image data instantiates SE_SAROperation.

Test Method: Inspect the metadata provided with the image.

Reference: 7.2

Test Type: Capability

A.3 InSAR operation and dual antenna position

Test purpose: If sensor is InSAR, verify that metadata about InSAR operation and dual antenna position provided with the image data instantiates SE_InSAROperation and SE_InSARDualAntennaPosition.

Test Method: Inspect the metadata provided with the image.

Reference: 8.3

Test Type: Capability

A.4 Lidar operation

Test purpose: If sensor is lidar, verify that metadata about lidar operation provided with the image data instantiates SE_LIDAROperation.

Test Method: Inspect the metadata provided with the image.

Reference: 9.2

Test Type: Capability

A.5 Sonar operation

Test purpose: If sensor is sonar, verify that metadata about sonar operation provided with the image data instantiates SE_SonarOperation, SE_Transducer, SE_DraftOffset, SE_SonarCalibration, SE_SonarOperationMode, and SE_TidalAdjustment.

Test Method: Inspect the metadata provided with the image.

Reference: 10.2.2, 10.2.3, 10.2.4, and 10.2.5

Test Type: Capability

A.6 Aerial triangulation

Test purpose: If aerial triangulation method is used, verify that metadata provided with the image data instantiates SE_AerialTriangulation and its subclasses.

Test Method: Inspect the metadata provided with the image.

Reference: 11.2, 11.3, 11.4, and 11.5

Test Type: Capability

Annex B
(normative)

Data dictionary

B.1 Overview

B.1.1 Introduction

The layout is as described in ISO 19115-1:2014, Annex B, except as otherwise described here.

B.1.2 Data type/Class

Specifies a set of distinct values for representing the metadata elements: for example, integer, real, string, DateTime and Boolean. The data type attribute is also used to define metadata entities, stereotypes and metadata association. If the data type of an entity or element is a class, specifies the name of the class; if it is an association, specifies the associated class.

B.1.3 Domain

For an entity, specifies the line numbers covered by that entity.

For a metadata element, the domain specifies the values allowed or the use of free text. "Unspecified" indicates that no restrictions are placed upon the content of the field. Integer-based codes shall be used to represent values for domains containing codelists.

B.2 UML models

See Tables B.1 to B.23.

Table B.1 — Sensor model extensions (see Figure 1)

	Name/Role Name	Definition	Obligation/ Condition	Max Occurrence	Data Type/Class	Domain
1.	MI_GeolocationInformation	information used to determine geographic coordinates corresponding to image location	Use obligation/ condition from referencing object	Use maximum occurrence from referencing object	Class << Abstract >>	MI_GeolocationInformation (ISO 19115-2:2009, B.2.3.4)
2.	SD_SensorModel	information on sensor Model for sensor collecting the image	Use obligation/ condition from referencing object	Use maximum occurrence from referencing object	Specialised Class (MI_GeolocationInformation) Aggregated Class (SD_PhysicalSensorModel) (SD_TrueReplacementModel) (SD_CorrespondenceModel)	Lines 3–5 SD_SensorModel (ISO/TS 19130:2010, Table B.1)
3.	SE_SensorModel	method and manufacturer information on sensor Model for sensor collecting the image	Use obligation/ condition from referencing object	Use maximum occurrence from referencing object	Specialised Class (SD_SensorModel)	Lines 4–5
4.	sensorDataModeling	method for modeling the sensor data	O	1	<< Code List >> SE_DataModelingMethod	
5.	sensorManufacturer	maker of sensor	O	1	CharacterString	Unrestricted

Table B.2 — Dynamics extensions — Dynamics (see Figure 2)

	Name/Role Name	Definition	Obligation/ Condition	Max Occurrence	Data Type/Class	Domain
6.	SD_Dynamics	motion of a body	Use obligation/condition from referencing object	Use maximum occurrence from referencing object	Class	Lines 7–8 SD_Dynamics (ISO/TS 19130:2010, B.2.3.4)
7.	SE_Dynamics	uncertainty in motion of a body	Use obligation/condition from referencing object	Use maximum occurrence from referencing object	Specified Class (SD_Dynamics)	Line 8
8.	navigationalConfidence	error matrix for motion of a body	C/ self.navigationalConfidence,nameOfMeasure = 'covariance-Matix'	2	DQ_QuantitativeAttributeAccuracy	ISO 19157:2013, Table C.2

Table B.3 — Dynamics extensions — Platform dynamics (see Figure 3)

	Name/Role Name	Definition	Obligation/ Condition	Max Occurrence	Data Type/Class	Domain
9.	SD_PlatformDynamics	directions of platform travel and pointing	Use obligation/condition from referencing object	Use maximum occurrence from referencing object	Specialised Class (SD_Dynamics)	Lines 10–13 SD_PlatformDynamics (ISO/TS 19130:2010, B2.3.4)
10.	SE_PlatformDynamics	additional parameters describing platform motion and pointing for sonar and lidar sensors	Use obligation/condition from referencing object	Use maximum occurrence from referencing object	Specialised Class (SD_PlatformDynamics)	Lines 11–14
11.	groundSpeed	motion of platform relative to ground	O	1	Velocity	Unrestricted
12.	heave	oscillatory rise and fall of a ship due to the entire hull being lifted by the force of the sea [5]	C /self.velocity- > size + self.heave- > size = 1	1	Length	Unrestricted
13.	settlement	the general lowering in level of a moving vessel, relative to what its level would be were it motionless Note: Settlement is due to the regional depression of the surface of the water in which the ship moves. It is not an increase in displacement. Settlement is a factor to be reckoned in ECHO SOUNDING.		1		
14.	squat	increase in a vessel's draught arising from its motion through the water	O	1	Length	

Table B.4 — SAR operation extensions (see Figure 5)

	Name/Role Name	Definition	Obligation/ Condition	Max Occurrence	Data Type/Class	Domain
15.	SD_SAROperation	operation properties of SAR system	Use obligation/ condition from referencing object	Use maximum occurrence from referencing object	Specialised Class of (SD_Microwave)	SD_SAROperation (ISO/TS 19130:2010, B.2.3.8)
16.	SE_SAROperation	collection properties of SAR system	Use obligation/ condition from referencing object	Use maximum occurrence from referencing object	Specialised Class (SD_SAROperation)	Lines 17–20
17.	collectionMode	method used by SAR system to collect data	M	1	<< Code List >> SD_SARCollectionMode	
18.	receiveTime	receiving time	M	1	SE_InSARTime	
19.	transmitterReceiver	antenna used as transmitter	O	1	SE_InSARTransmitReceiveType	
20.	transmitTime	transmitting time	M	1	SE_InSARTime	
21.	SE_InSARTime	InSAR operation time	Use obligation/ condition from referencing object	Use maximum occurrence from referencing object	Class	Lines 22–23
22.	timeFunction	time function for InSAR operation	C/self.timeFunction- > size + self. timeTable- > size > 0	1	CharacterString	
23.	timeTable	time table for InSAR operation	C/self.timeFunction- > size + self. timeTable- > size > 0	N	DateTime	

Table B.5 — InSAR operation (see Figure 9)

	Name/Role Name	Definition	Obligation/ Condition	Max Occurrence	Data Type/Class	Domain
24.	SD_SAROperation	operation properties of SAR system	Use obligation/ condition from referencing object	Use maximum occurrence from referencing object	Specialised Class of(SD_Microwave)	SD_SAROperation (ISO/TS 19130:2010, B.2.3.8)
25.	SE_InSAROperation	collection properties of InSAR system	Use obligation/ condition from referencing object	Use maximum occurrence from referencing object	Specialised Class (SD_SAROperation)	Line 26
26.	collectionMode	method used by SAR system to collect data	M	1	<< Code List >> SD_SARCollectionMode	

Table B.6 — InSAR dual antenna position (see Figure 10)

	Name/Role Name	Definition	Obligation/ Condition	Max Occurrence	Data Type/Class	Domain
27	SD_SensorParameters	information about sensor properties	Use obligation/ condition from referencing object	Use maximum occurrence from referencing object	Aggregated Class (SD_GSD) (SD_SensorSystemAndOperation) (SD_DetectorArray) (SD_Sensor) (SE_InSARDualAntennaPosition)	Line 28 SD_SensorParameters (ISO/TS 19130:2010, B.2.3.6)
28.	*Role Name:* InSARAntennaPosition	information about the position of InSAR dual antennas	C/if self.identification.type < > 'InSAR' then self.InSARAntennaPosition- > size = 0	1	SE_InSARDualAntennaPosition	
29.	SE_InSARDualAntennaPosition	description of the position of InSAR dual antennas	Use obligation/ condition from referencing object	Use maximum occurrence from referencing object	Class	Line 30–31
30.	firstAntennaPosition	position of the first antenna	C/self.firstAntennaPosition- > size = self.secondAntennaPosition- > size	1	SD_PositionAndOrientation	ISO/TS 19130:2010, B.2.3.5
31.	secondAntennaPosition	position of the second antenna	C/self.firstAntennaPosition- > size = self.secondAntennaPosition- > size	1	SD_PositionAndOrientation	ISO/TS 19130:2010, B.2.3.5

Table B.7 — Lidar operation (see Figure 11)

	Name/Role Name	Definition	Obligation/ Condition	Max Occurrence	Data Type/Class	Domain
32.	SD_OpticsOperation	configuration and operation of sensor optics	Use obligation/ condition from referencing object	Use maximum occurrence from referencing object	Class	SD_OpticsOperation (ISO/TS 19130:2010, B.2.3.9)
33.	SE_LIDAROperation	configuration and operation of lidar	Use obligation/ condition from referencing object	Use maximum occurrence from referencing object	Specified Class (SD_OpticsOperation)	Lines 34–39
34.	numberOfPulse	pulse repetition rate expressed as the number of pulses per second	M	1	Integer	> = 0
35.	pulseTimeDirection	where and when laser pulse is sent	M	N	<< DataType >> SE_LIDARPulse	
36.	SE_LIDARPulse	spatial and temporal information about laser pulse	Use obligation/ condition from referencing object	Use maximum occurrence from referencing object	Class << Data Type >>	Lines 37–39
37.	pulsePointing	direction of laser pulse	M	1	Vector	ISO/TS 19103:2005 Unrestricted
38.	pulseEmissionTime	date and time original laser pulse is sent	M	1	DateTime	ISO/TS 19103:2005 Unrestricted
39.	pulseReturnTime	date and time return laser pulse is received	M	N	DateTime	ISO/TS 19103:2005 > = pulseEmissionTime

Table B.8 — Sonar operation — Overview (see Figure 17)

	Name/Role Name	Definition	Obligation/ Condition	Max Occurrence	Data Type/Class	Domain
40.	SD_SensorSystemAndOperation	specific properties of sensor system and operation	Use obligation/ condition from referencing object	Use maximum occurrence from referencing object	Class	SD_SensorSystemAndOperation (ISO/TS 19130:2010, B.2.3.8) Lines 26–33
41.	SD_SonarOperation	properties and working method of sonar system	Use obligation/ condition from referencing object	Use maximum occurrence from referencing object	Specified Class (SD_SensorSystemAndOperation)	Lines 42–48
42.	deployment	location of sonar relative to ship	M	1	<< CodeList >> SE_SonarDeploymentType	
43.	type	whether sonar system emits sound waves	M	1	<< CodeList >> SE_SonarType	
44.	*Role Name:* mode	component that provides the operation mode of the sonar sensor	M	1	SE_SonarOperationMode	
45.	*Role Name:* transducer	component which defines the parameters of the transducer	M	N	SE_Transducer	
46.	*Role Name:* calibration	component that provides the calibration parameters for all auxiliary systems and environmental factors	M	N	SE_SonarCalibration	
47.	*Role Name:* tidalAdjustment	component that provides information about the values in a tidal model	O	1	SE_TidalAdjustment	
48.	*Role Name:* draft	component that provides the draft value	O	1	SE_DraftOffset	

Table B.9 — Sonar operation — Sonar operation mode (see Figure 18)

	Name/Role Name	Definition	Obligation/ Condition	Max Occurrence	Data Type/Class	Domain
49.	SE_SonarOperationMode		Use obligation/ condition from referencing object	Use maximum occurrence from referencing object	Aggregated Class (SD_Sonar Operation)	Lines 50–52
50.	beamAngle	angle between beam and vertical, as measured from vertical	C/ self.beamAngle- > size = self. numberOfBeams	N	Angle	ISO/TS 19103:2005 > = 0
51.	mode	type of sonar system	M	1	<< CodeList >> SE_SonarMode	
52.	numberOfBeams	number or sounder-transducer combinations	M	1	Integer	ISO/TS 19103:2005 > = 0

Table B.10 — Sonar operation — Transducer (see Figure 19)

	Name/Role Name	Definition	Obligation/ Condition	Max Occurrence	Data Type/Class	Domain
53.	SE_Transducer	positioning of transducer	Use obligation/ condition from referencing object	Use maximum occurrence from referencing object	Aggregated Class (SD_Sonar Operation)	Lines 54–57
54.	operationChannels	wavelength of the sonar	O	N	Length	ISO/TS 19103:2005 Unrestricted
55.	operationFrequencies	frequencies at which sound waves are sent out by transmitter	C/(self.operationFrequencies- > size + self.operationChannels- > size) > = 1	N	Frequency	ISO/TS 19103:2005 Unrestricted
56.	*Role name:* receiverInformation	position and attitude of receiver	M	N	SE_ReceiverInformation	
57.	*Role name:* transmitterInformation	position and attitude of transmitter	O	N	SE_TransmitterInformation	
58.	SE_ReceiverInformation	configuration of receiver	Use obligation/ condition from referencing object	Use maximum occurrence from referencing object	Aggregated Class (SE_Transducer)	Lines 59–60
59.	orientation	mounting direction of receiver	M	1	SD_Attitude (ISO/TS 19130:2010, B.2.3.3)	
60.	position	location of receiver	M	1	SD_Position (ISO/TS 19130:2010, B.2.3.2)	
61.	SE_TransmitterInformation	configuration of transmitter	Use obligation/ condition from referencing object	Use maximum occurrence from referencing object	Aggregated Class (SE_Transducer)	Lines 62–63
62.	orientation	mounting direction of transmitter	M	1	SD_Attitude (ISO/TS 19130:2010, B.2.3.3)	
63.	position	location of transmitter	M	1	SD_Position (ISO/TS 19130:2010, B.2.3.2)	

Table B.11 — Sonar operation — Calibration (see Figure 20)

	Name/Role Name	Definition	Obligation/ Condition	Max Occurrence	Data Type/Class	Domain
64.	SE_SonarCalibration	information required to determine configuration of sonar system	Use obligation/ condition from referencing object	Use maximum occurrence from referencing object	Aggregated Class (SD_Sonar Operation)	Lines 65–76
65.	SE_BarCheck	information to check for sound velocity adjustments	Use obligation/ condition from referencing object	Use maximum occurrence from referencing object	Specified Class (SE_SonarCalibration)	Lines 66–67
66.	depthOffset	depths at which sound speed is measured	C/ self.depthOffset- > size = self. numberofdepth	N	Distance	ISO/TS 19103:2005 Unrestricted
67.	numberOfDepth	depth read from the sonar display to the calibration bar	M	1	Integer	ISO/TS 19103:2005 > = 0
68.	SE_PatchTest	information needed to determine quantified accuracy, precision, and alignment of the sonar system.	Use obligation/ condition from referencing object	Use maximum occurrence from referencing object	Specified Class (SE_SonarCalibration)	Lines 69–72
69.	azimuthalOffset	angle between centre of sensor and ship in the azimuthal direction	M	1	Angle	ISO/TS 19103:2005 Unrestricted
70.	pitchOffset	angle between centre of sensor and ship in the pitch direction	M	1	Angle	ISO/TS 19103:2005 Unrestricted
71.	positioningTimeDelay	time interval between initial receipt of time positioning data and the time the computed position reaches the logging module			TM_IntervalLength	ISO 19108:2002
72.	rollOffset	angle between centre of sensor and ship in the roll direction	M	1	Angle	ISO/TS 19103:2005, 5.2.3.7 Unrestricted

Table B.11 — *(Continued)*

	Name/Role Name	Definition	Obligation/ Condition	Max Occurrence	Data Type/Class	Domain
73.	SD_SoundVelocityProfile	record of the sound velocities vertically through the water column	Use obligation/ condition from referencing object	Use maximum occurrence from referencing object	Specified Class (SE_SonarCalibration)	Lines 74–76
74.	frequency	frequency at which sound wave is emitted and received	M	1	Frequency	ISO/TS 19103:2005 Unrestricted
75.	numberOfMeasure	number of sound velocity profiles observed	M	1	Integer	ISO/TS 19103:2005 > = 0
76.	soundSpeed	speed of sound in medium where sonar is operating	C/ self.soundSpeed- > size = self.NumberofMeasure	1	Velocity	ISO/TS 19103:2005 > = 0

Table B.12 — Sonar operation — Draft offset (see Figure 20)

	Name/Role Name	Definition	Obligation/ Condition	Max Occurrence	Data Type/Class	Domain
77.	SE_DraftOffset	draft of the transducer	Use obligation/ condition from referencing object	Use maximum occurrence from referencing object	Aggregated Class (SD_Sonar Operation)	Lines 78–79
78.	draft	depth of transducer head below waterline of vessel	O	N	Distance	ISO/TS 19103:2005 Unrestricted
79.	draftMeasureTime	time at which depth of transducer is measured	C/(self. draft- > size = self. draftMeasureTime- > size)	N	Time	ISO/TS 19103:2005 Unrestricted

Table B.13 — Sonar operation — Tidal adjustment (see Figure 20)

	Name/Role Name	Definition	Obligation/ Condition	Max Occurrence	Data Type/Class	Domain
80.	SE_TidalAdjustment	the vertical adjustment for tidal observations referred to a local datum	Use obligation/ condition from referencing object	Use maximum occurrence from referencing object	Aggregated Class (SD_Sonar Operation)	Lines 81–83
81.	time	reference time for the tidal adjustment	C/ self.depthOffset- > size = self. numberofdepth	N	Time	ISO/TS 19103:2005 Unrestricted
82.	type	prediction or observed tide	M	1	<< Code List >> SE_TideAdjustType	
83.	value	tide adjustment value	C/	N	Distance (height of tide reduced to local datum)	ISO/TS 19103:2005 Unrestricted

Table B.14 — Aerial triangulation — General (see Figure 21)

	Name/Role Name	Definition	Obligation/ Condition	Max Occurrence	Data Type/Class	Domain
84.	SE_AerialTriangulation	method for determining the exterior orientation of more than two images in one calculation	Use obligation/ condition from referencing object	Use maximum occurrence from referencing object	Aggregated Class (SD_PlatformParameters)	Lines 85–88
85.	additionalParameter	additional parameters used to control adjustment, from ISO/TS 19159	O	N	Double	Unrestricted
86.	atName	sequence of alphanumerical characters describing the aerial triangulation project	M	1	CharacterString	Unrestricted
87.	gcpReference	name of the registry for Ground Control Points	O	N	CharacterString	Unrestricted
88.	terrainHeight	average terrain height in the project area used for various reasons e.g. to support image matching	O	1	Distance	ISO/TS 19103

Table B.15 — Aerial triangulation — Aerial triangulation of a single image (see Figure 21)

	Name/Role Name	Definition	Obligation/ Condition	Max Occurrence	Data Type/Class	Domain
89.	SE_ATImage	characteristics of a single image of the aerial triangulation block	Use obligation/ condition from referencing object	Use maximum occurrence from referencing object	Aggregated Class (SE_AerialTriangulation)	Lines 90–92
90.	blockID	alphanumerical identifier of the adjustment block	O	1	CharacterString	Unrestricted
91.	imageID	alphanumerical identifier of an aerial image	M	N	CharacterString	Unrestricted
92.	stripID	alphanumerical identifier of a photo-flight strip	O	N	CharacterString	Unrestricted

Table B.16 — Aerial triangulation — Aerial triangulation of one strip (see Figure 21)

	Name/Role Name	Definition	Obligation/ Condition	Max Occurrence	Data Type/Class	Domain
93.	SE_ATStrip	Characteristics of a single strip of the aerial triangulation block	Use obligation/ condition from referencing object	Use maximum occurrence from referencing object	Aggregated Class (SE_AerialTriangulation)	Lines 94–99
94.	stripID	alphanumerical identifier of a photo-flight strip	M	1	CharacterString	Unrestricted
95.	blockID	alphanumerical identifier of the adjustment block	O	1	CharacterString	Unrestricted
96.	numberOfImages	number of images that form the strip	O	1	Integer	Unrestricted
97.	imageID	alphanumerical identifier of aerial images	M	N	CharacterString	Unrestricted
98.	stripAzimuth	average direction of the plane's flight track when the images of the strip were taken	O	1	Angle	Unrestricted
99.	crabAngle	angle between the strip azimuth and the pointing direction of the plane's fuselage	O	1	Angle	Unrestricted

Table B.17 — Aerial triangulation — Aerial triangulation of a block (see Figure 21)

	Name/Role Name	Definition	Obligation/ Condition	Max Occurrence	Data Type/Class	Domain
100.	SE_ATBlock	Characteristics of the aerial triangulation block	Use obligation/ condition from referencing object	Use maximum occurrence from referencing object	Aggregated Class (SE_AerialTriangulation)	lines101–103
101.	blockID	alphanumerical identifier of the adjustment block	M	1	CharacterString	Unrestricted
102.	numberOfStrips	number of strips that form the block	O	1	Integer	Unrestricted
103.	stripID	alphanumerical identifier of a photo-flight strip	O	N	CharacterString	Unrestricted

Table B.18 — Aerial triangulation — Characteristics of aerial triangulation observations (see Figure 21)

	Name/Role Name	Definition	Obligation/ Condition	Max Occurrence	Data Type/Class	Domain
104.	SE_ATObservations	observations of the aerial triangulation	Use obligation/ condition from referencing object	Use maximum occurrence from referencing object	Aggregated Class (SE_AerialTriangulation)	Lines 105–108, 118–150
105.	errorType	specification of the formula that shall be applied for calculating the error-value	C	1	SD_ATErrorType	
106.	errorAutomaticAPriori	known geometric quality of the automatically measured tie points as set before the adjustment (*a priori*)	O	1	Distance	ISO/TS 19103
107.	errorManualAPriori	known geometric quality of the manually measured tie points as set before the adjustment (*a priori)*	O	1	Distance	ISO/TS 19103
108.	eliminateFlag	flag that indicates whether an observation is activated or deactivated before the adjustment	O	1	Boolean	True, False

Table B.19 — Aerial triangulation — Unknowns (see Figure 21)

	Name/Role Name	Definition	Obligation/ Condition	Max Occurrence	Data Type/Class	Domain
109.	SE_ATUnknowns	information about the unknowns of the triangulation	Use obligation/ condition from referencing object	Use maximum occurrence from referencing object	<< abstract >> Aggregated Class (SE_AerialTriangulation)	Lines 175–179

Table B.20 — Aerial triangulation — Other properties (see Figure 21)

	Name/Role Name	Definition	Obligation/ Condition	Max Occurrence	Data Type/Class	Domain
110.	SE_ATOtherResults	other results of the adjustment process	Use obligation/ condition from referencing object	Use maximum occurrence from referencing object	Aggregated Class (SE_AerialTriangulation)	Lines 111–113, 151–174
111.	numberCheckPoints	number of Check Points applied	M	1	Integer	> = 0
112.	numberGcp	number of Ground Control Points applied	M	1	Integer	> = 0
113.	numberTiePoints	number of tie points applied	M	1	Integer	> = 0.

Table B.21 — Aerial triangulation — Observations (see Figure 22)

	Name/Role Name	Definition	Obligation/ Condition	Max Occurrence	Data Type/Class	Domain
114.	SE_ATImageMeasurements	observations of image coordinates	Use obligation/ condition from referencing object	Use maximum occurrence from referencing object	Aggregated Class (SE_ATObservations)	Lines 115–117
115.	imageID	alphanumerical identifier of the aerial image	M	1	CharacterString	ISO/TS 19103
116.	imagePointID	alphanumerical identifier of an image point	M	1	CharacterString	ISO/TS 19103
117.	imagePointPosition	2-dimensional coordinates that describe the geometric position of the image point	M	1	DirectPosition	ISO 19107
118.	SE_ATTiePoints	points with a location on an image that are used to link two of more neighbouring images	Use obligation/ condition from referencing object	Use maximum occurrence from referencing object	Specified Class (SE_ATObservations)	Lines 119–120
119.	tiePointID	alphanumerical identifier of the tie point	M	1	CharacterString	Unrestricted
120.	measurementType	flag that indicates whether a tie point is manually or automatically determined	O	1	SE_ATMeasType	Unrestricted
121.	SE_ATGCP	Ground Control Point that is prepared and eventually used within the aerial triangulation	Use obligation/ condition from referencing object	Use maximum occurrence from referencing object	Specified Class (SE_Observations)	Lines 122–128

Table B.21 — *(Continued)*

	Name/Role Name	Definition	Obligation/ Condition	Max Occurrence	Data Type/Class	Domain
122.	gcpID	alphanumerical identifier of the Ground Control Point	M	1	CharacterString	ISO/TS 19103
123.	dimensionType	dimensionality of the GCP such as horizontal and vertical	C	1	SE_ATDimensionType	
124.	errorGcpAPriori	value that characterizes the geometric quality as known before the adjustment is computed	O	1	Distance	ISO/TS 19103
125.	errorType	specification of the formula that shall be applied for calculating the error-value	C	1	SE_ATErrorType	
126.	gcpPosition	planar 2-dimensional coordinates of the gcp	M	1	DirectPosition	ISO 19107
127.	gcpElevation	vertical 1-dimensional coordinate of the gcp	O	1	Distance	ISO/TS 19103
128.	pointType	whether a point is a Ground Control Point, Check Point or something else, if a priori known	O	1	SE_ATPointType	
129.	SE_ATGNSSMeasurements	information on the GNSS-measurement involved in the aerial triangulation	Use obligation/ condition from referencing object	Use maximum occurrence from referencing object	Specified Class (SE_ATObservations)	Lines 130–138
130.	dimensionType	dimensionality of the GNSS-measured point such as horizontal and vertical	C	1	SE_ATDimensionType	
131.	errorGnss	value that characterizes the geometric quality of the GNSS-position	O	1	Distance	ISO/TS 19103

Table B.21 — *(Continued)*

	Name/Role Name	Definition	Obligation/ Condition	Max Occurrence	Data Type/Class	Domain
132.	errorType	specification of the formula that shall be applied for calculating the error-value	C	1	SE_ATErrorType	
133.	gnssCameraID	alphanumerical identifier of a camera related to the GNSS-positions	O	1	CharacterString	Unrestricted
134.	gnssImageID	alphanumerical identifier of an image related to the GNSS-positions	M	1	CharacterString	Unrestricted
135.	gnssPosition	position provided by a GNSS	M	1	DirectPosition	ISO 19107
136.	gnssElevation	elevation provided by a GNSS	O	1	Distance	ISO/TS 19103
137.	gnssStripID	alphanumerical identifier of a photo-flight strip related to the GNSS-positions	O	1	CharacterString	Unrestricted
138.	gnssTime	time at which the position measurement was made	M	1	DateTime	ISO/TS 19103
139.	SE_ATIMUMeasurements	information on the Inertial Measurement Unit (IMU)-measurement involved in the aerial triangulation	Use obligation/ condition from referencing object	Use maximum occurrence from referencing object	Aggregated Class (SE_ATObservations)	Lines 140–150
140.	dimensionType	dimensionality of the IMU-measured point such as horizontal and vertical	C	1	SE_ATDimensionType	
141.	errorImuKappa	value that characterizes the geometric quality of the kappa-value of the IMU- position	O	1	Angle	ISO/TS 19103

Table B.21 — *(Continued)*

	Name/Role Name	Definition	Obligation/ Condition	Max Occurrence	Data Type/Class	Domain
142.	errorImuOmega	value that characterizes the geometric quality of the omega-value of the IMU- position	O	1	Angle	ISO/TS 19103
143.	errorImuPhi	value that characterizes the geometric quality of the phi-value of the IMU- position	O	1	Angle	ISO/TS 19103
144.	errorType	specification of the formula that shall be applied for calculating the error-value	C	1	SE_ATErrorType	
145.	imuCameraID	alphanumerical identifier of a camera related to the IMU-positions	O	1	CharacterString	Unrestricted
146.	imuImageID	alphanumerical identifier of an image related to the IMU-positions	M	1	CharacterString	Unrestricted
147.	imuKappa	kappa value of the IMU-position	M	1	Angle	ISO/TS 19103
148.	imuOmega	omega value of the IMU-position	M	1	Angle	ISO/TS 19103
149.	imuPhi	phi value of the IMU-position	M	1	Angle	ISO/TS 19103
150.	imuStripID	alphanumerical identifier of a photo-flight strip related to the IMU-positions	O	1	CharacterString	Unrestricted

Table B.22 — Aerial triangulation — Other results (see Figure 23)

	Name/Role Name	Definition	Obligation/ Condition	Max Occurrence	Data Type/Class	Domain
151.	SE_ATAdjustedTiePoint	information about sensor model for sensor collecting the image	Use obligation/ condition from referencing object	Use maximum occurrence from referencing object	Specialised Class (SE_ATOtherResults))	Lines 152–157
152.	eliminateFlag	flag that indicates whether a tie point is activated or deactivated during the adjustment	O	1	Boolean	True, False
153.	errorAdjustedTiePoint	value that characterizes the geometric error	O	1	Distance	ISO 19103
154.	imageID	image in which the tie point was found	M	N	CharacterString	Unrestricted
155.	numberOfRays	number of images in which the point is located	O	1	Integer	> = 0
156.	pointID	alphanumerical identifier of the point that is located in the image	M	1	CharacterString	Unrestricted
157.	positionAdjustedTiePoint	position of the adjusted tie point	M	1	DirectPosition	ISO 19103
158.	SE_ATAdjustmentStatistics	statistical values describing the geometric quality of the adjustment	Use obligation/ condition from referencing object	Use maximum occurrence from referencing object	Specialized Class (SE_ATOtherResults))	Lines 159–163
159.	dimensionType	dimension in which the error is valid	C	1	SE_ATDimensionType	
160.	errorTieAdjustedMax	maximum geometric error	O	1	Distance	ISO 19103
161.	errorTieAdjustedMin	minimum geometric error	O	1	Distance	ISO 19103
162.	errorType	specification of the formula that shall be applied for calculating the error-value	C	1	SE_ATErrorType	
163.	sigmaZero	value that characterizes the geometric quality of the aerial triangulation block	M	1	Distance	ISO 19103

Table B.22 — *(Continued)*

	Name/Role Name	Definition	Obligation/ Condition	Max Occurrence	Data Type/Class	Domain
164.	SE_ATAdjustedGCP		O	Use maximum occurrence from referencing object	Specified Class (SE_ATOtherResults)	Lines 165–169
165.	dimensionType	dimension in which the error is valid	C	1	SE_ATDimensionType	
166.	errorAdjustedGcp	accuracy in one dimension	O	1	Distance	ISO 19103
167.	errorType	definition of formula that is applied to compute the error such as sigma or rm	C	1	SE_ATErrorType	
168	gcpID	alphanumerical identifier of the Ground Control Point	M	1	CharacterString	Unrestricted
169.	positionAdjustedGcp	position of the Ground Control Point as a result of the adjustment process	M	1	DirectPosition	ISO 19103
170.	SE_ATCheckPoint	check point that is prepared and eventually used within the aerial triangulation	Use obligation/ condition from referencing object	Use maximum occurrence from referencing object	Specified Class (SE_ATOtherResults)	Lines 171–174
171.	checkPointID	position of the Check Point as a result of the adjustment process	O	1	CharacterString	Unrestricted
172.	dimensionType	dimension in which the error is valid	C	1	SE_ATDimensionType	
173.	errorCp	value that characterizes the geometric quality	O	1	Distance	ISO 19103
174.	errorType	specification of the formula that shall be applied for calculating the error-value	C	1	SE_ATErrorType	

Table B.23 — Aerial triangulation — Unknowns (see Figure 24)

	Name/Role Name	Definition	Obligation/ Condition	Max Occurrence	Data Type/Class	Domain
175.	SE_ATExteriorOrientation	Exterior Orientation of every image	Use obligation/ condition from referencing object	Use maximum occurrence from referencing object	Specialized Class (SE_ATUnknowns)	Lines 176–179
176.	approximateAttitude	approximate values necessary for the aerial triangulation calculation	M	1	SD_Attitude	ISO/TS 19130
177.	approximatePosition	approximate values necessary for the aerial triangulation calculation	M	1	SD_Position	ISO/TS 19130
178.	attitude	attitude of the adjusted image	M	1	SD_Attitude	ISO/TS 19130
179.	position	position of the adjusted image	M	1	SD_Position	ISO/TS 19130

B.2.1 Codelists

B.2.1.1 SE_Aerial Triangulation Dimension Type codes (see Figure 21)

	Name	Definition
1.	SE_ATDimensionType	
2.	x	error in x-dimension
3.	xy	error in the xy-plane
4.	y	error in y-dimension
5.	z	error in z-dimension

B.2.1.2 SE_Aerial Triangulation Error Type codes (see Figure 21)

	Name	Definition
1.	SD_ATErrorType	``
2.	rms	root Mean Square error
3.	sigma	sigma error

B.2.1.3 SE_AerialTriangulation Measurement Type codes (see Figure 22)

	Name	Definition
1.	SE_ATMeasType	
2.	Automatic	point positions are determined by an automatic process
3.	Manual	point positions are measured manually

B.2.1.4 SE_Aerial Triangulation PointType codes (see Figure 21)

	Name	Definition
1.	SD_ATPointType	
2.	checkPoint	ground Control Point applied as Check Point
3.	controlPoint	ground Control Point applied as Ground Control Point
4.	shadedimage	ground control point applied as a shaded part of the image

B.2.1.5 SE_Aerial Triangulation StatisticType Codes (see Figure 21)

	Name	Definition
1.	SE_ATStatisticType	
2.	image	statistical attributes valid for a single image
3.	strip	statistical attributes valid for a single strip
4.	block	statistical attributes valid for the block

B.2.1.6 SE_DataModelingMethod code (see Figure 1)

	Name	Definition
1.	SE_DataModelingMethod	
2.	absoluteValue	
3.	basicSequentialModeling	
4.	collectionPlane	
5.	rectifiedImage	
6.	Reserved	
7.	vectorModeling	
8.	notApplicable	

B.2.1.7 SE_SARCollectionMode (see Figure 5)

	Name	Definition
1.	SE_SARCollectionMode	way in which SAR operates
2.	scan	beam is steered to illuminate a strip of terrain that can be at any angle with respect to the direction of motion
3.	spotlight	antenna is steered to keep approximately the same ground area illuminated by the beam
4.	stripmap	beam sweeps a swath along a strip of terrain that is parallel to the path of motion

B.2.1.8 SE_SonarDeploymentType Code (see Figure 18)

	Name	Definition
1.	SE_SonarDeploymentType	location of sonar relative to platform
2.	hullMounted	sensor that is mounted (attached) to the hull of a vessel
3.	offset	sensor that is mounted on a pole which is attached to the vessel
4.	Towed	measuring device/sensor that is towed (pulled) behind a primary survey platform (e.g. vessel)

B.2.1.9 SE_SonarMode Code (see Figure 18)

	Name	Definition
1.	SE_SonarMode	method of operation of sonar
2.	SD_MultiBeam	sonar system that emits multiple “beams” of sound waves in a fan-shaped pattern to produce a swath of sounding data in a single pass over an area of the seafloor
3.	SD_SideScan	fixed acoustic beams that are directed (in water) perpendicularly to the direction of travel in order to scan the bottom and generate a record of the bottom configuration
4.	SD_SingleBeam	echosounders that use one emitting and receiving “transducer”, which releases a series of energy pulses ensonifying a small area underneath the platform
5.	SD_Sweep	several single beam transducers operating simultaneously, sequentially or in interleave phase and measurement of the amplitude is used for target detection
6.	SD_ScanningProfiler	profiler comprises a small transducer array mounted on an electro-mechanical stepper motor operate at much higher frequencies than echo sounders and consequently have much reduced ranges and very little material penetrative capability

B.2.1.10 SE_SonarType Code (see Figure 18)

	Name	Definition
1.	SE_SonarType	class of sonar
2.	Active	transmits and receives sound waves
3.	Passive	receives but does not transmit sound waves

B.2.1.11 SE_TideAdjustType Code (see Figure 20)

	Name	Definition
1.	SE_TideAdjustType	
2.	Prediction	predicted tidal heights (related to chart datum) calculated using historical tidal values, for a fixed location
3.	Realtime	tidal values derived in realtime for a fixed location

B.2.1.12 SE_InSARCollectionModeType Code (see Figure 9)

	Name	Definition
1.	SE_InSARCollectionModeType	InSAR data collection modes
2.	pingPongMode	ping pong mode
3.	standardMode	standard mode

B.2.1.13 SE_InSARTransmitReceiveType Code (see Figure 10)

	Name	Definition
1.	SE_InSARTransmitReceiveType	InSAR antenna transmit/receive arrangement
2.	firstAntennaTransmit	first antenna used for transmit
3.	secondAntennaTransmit	second antenna used for transmit

Annex C
(informative)

Synthetic aperture radar sensor model metadata profile supporting precise geopositioning

C.1 Introduction

The purpose of this annex is to show how to use metadata defined in this Technical Specification and ISO/TS 19130:2010 to accomplish precise geopositioning of images from Synthetic Aperture Radar (SAR) imagery systems. This annex is intended to give an example for using the common terminology and a common frame of reference established in this Technical Specification and ISO/TS 19130:2010 to perform precise geopositioning using a physical SAR sensor model. This annex provides additional information to Annex F of ISO/TS 19130:2010.

C.2 Overview for coordinate reference system descriptions and relationships

C.2.1 General coordinate reference system considerations

The purpose of a sensor model is to develop a mathematical relationship between the position of an object on the Earth's surface and the position of the image of that object as recorded by an overhead sensor. An object's spatial position may be given either in relation to a coordinate system locally defined or relative to an Earth reference. A horizontal (latitude and longitude) datum and a vertical (elevation) datum will be required to define the origin and orientation of the coordinate systems. Likewise, the corresponding object's position in an image may be defined with respect to a local sensor or platform coordinate system or an Earth-based datum. For purposes of this metadata profile, transformation between the various coordinate systems may be accomplished via a sequence of translations and rotations of the sensor's coordinate system origin and axes until it coincides with an Earth-based coordinate system origin and axes.

An overview of some of the coordinate reference system frames to be considered for an airborne SAR collection platform is shown in Figure C.1. SAR geopositioning is dependent primarily upon the accurate measurement of the sensor position and sensor velocity, with acceleration being a secondary factor. SAR geometric sensor models are completely independent of the *sensor's pointing attitude*, which is quite different from geopositioning with passive light-sensing systems, such as Frame and Pushbroom sensors. This is because SAR images or other products are created by processing the radar signal's time and frequency characteristics, rather than physical pointing characteristics. Raw SAR data can be processed into many products, one of which, known as a "detected image," is commonly referred to as a SAR image. Only the quality of the product (e.g. noise level, dynamic range) is a function of the pointing direction of the antenna, since the magnitude of the returned signal is dependent upon the amount of energy illuminating the region processed into the image, which is a function of the antenna beam pointing. (This is analogous to a camera with an independently pointed light source, in which the camera can point in any direction, but the quality of the image depends upon where the light is pointing relative to the camera.)

The platform attitude information *is relevant* to SAR geopositioning to the extent that the information must be used to determine accurate position and velocity vectors of the sensor relative to a reference coordinate system. However, it is expected that these transformations are accomplished within the SAR product formation processor, and should not be needed to perform geopositioning from a SAR product. This will be discussed in more detail in C.3.6. Hence, the discussion of platform coordinate systems and angles is included in C.2.3 for reference only.

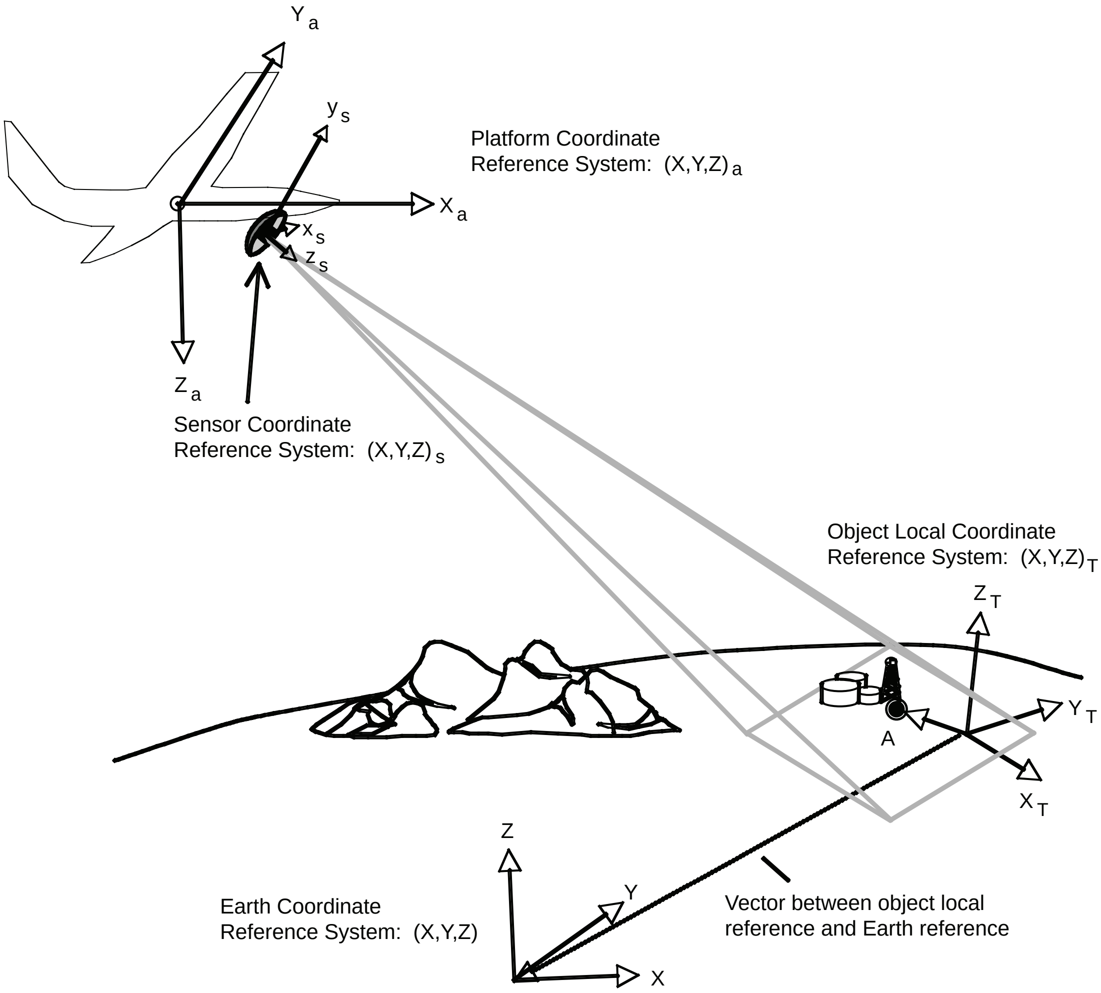

Figure C.1 — Multiple coordinate reference systems

C.2.2 Earth coordinate reference system

To simplify sensor model development, a stationary, non-time dependent coordinate reference frame is needed to which all other reference frames may be mathematically defined. Consider a coordinate system (X,Y,Z) which is Earth-centred, Earth-fixed (ECEF), as shown in Figure C.2; with the X-Y plane coincident with the equatorial plane. The **X** axis intersects, in the positive direction, the Greenwich Meridian (from where longitude is measured; longitude equals 0-degrees at Y equal to zero), **Z** is parallel to the Earth's rotation axis and has a positive direction toward the North pole, **Y** is in the equatorial plane and perpendicular to **X** and completes a right-handed coordinate system; i.e. the cross-product of **X** and **Y** is a vector in the direction of **Z**.

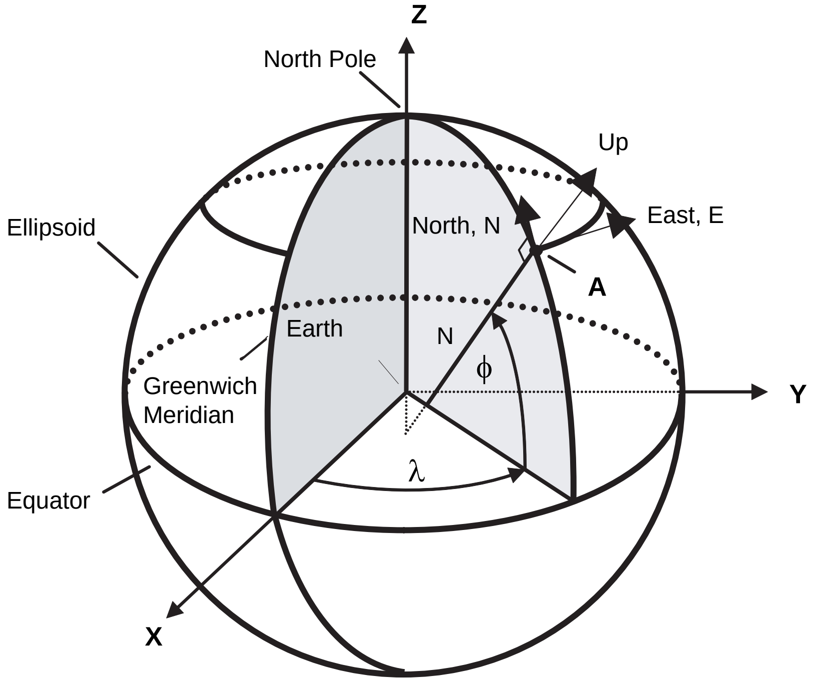

Key

ϕ latitude

λ longitude

Figure C.2 — Earth-centred and local surface (ENU) coordinate frames

Therefore any point (A) on the reference surface may be described in (X,Y,Z) coordinates, or alternatively in the equivalent longitude, latitude, and elevation terms. Likewise, this point, the "object" point, can be described relative to a local reference system attached to the surface, specifically in an East-North-Up (ENU) orientation; where North is tangent to the local prime meridian and pointing North, Up vector pointing to the local zenith, and East completes a right-hand Cartesian coordinate system.

C.2.3 Platform coordinate reference system

A platform coordinate reference system is defined with respect to its centre of navigation, fixed to the platform structure; e.g. the aircraft as shown in Figure C.3. The axes are defined as: X_a positive along the heading of the platform, along the platform roll axis; Y_a positive in the direction of the starboard (right) wing, along the pitch axis such that the X_aY_a plane is horizontal when the platform is at rest; and Z_a positive down, along the yaw axis. The platform coordinate reference system is also closely related to a North-East-Down (NED) reference system with its origin at the centre of navigation. In horizontal flight, the platform Z_a axis is aligned with the Down (mD) axis, and the North-East plane is parallel to the tangent plane to the Earth surface reference at the intersection of the mD axis, Figure C.4. Therefore, the platform reference system orientation defined in terms of its physical relation (rotation) with this local NED reference, Figure C.5, is as follows:

— Platform heading — horizontal angle from north to the NED horizontal projection of the platform positive roll axis, X_a (positive from north to east).

— Platform pitch — angle from the NED horizontal plane to the platform positive roll axis, X_a-axis (positive when positive X_a is above the NED horizontal plane, or nose up).

— Platform roll — rotation angle about the platform roll axis; positive if the platform positive pitch axis, Y_a, lies below the NED horizontal plane (right wing down).

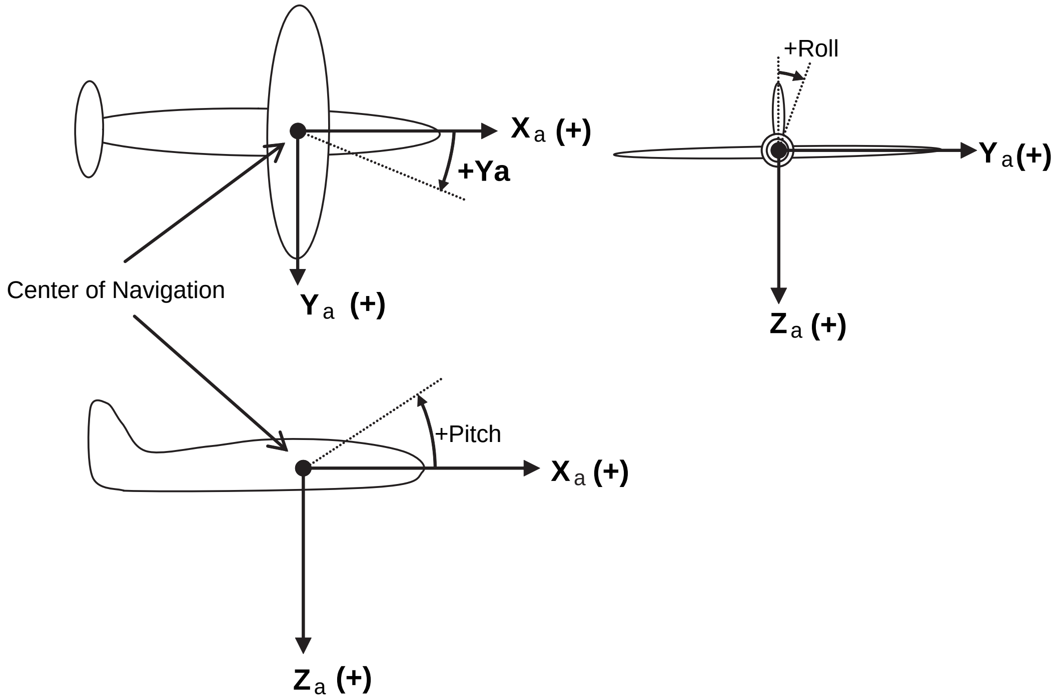

Figure C.3 — Platform coordinate reference system and local (NED) frame

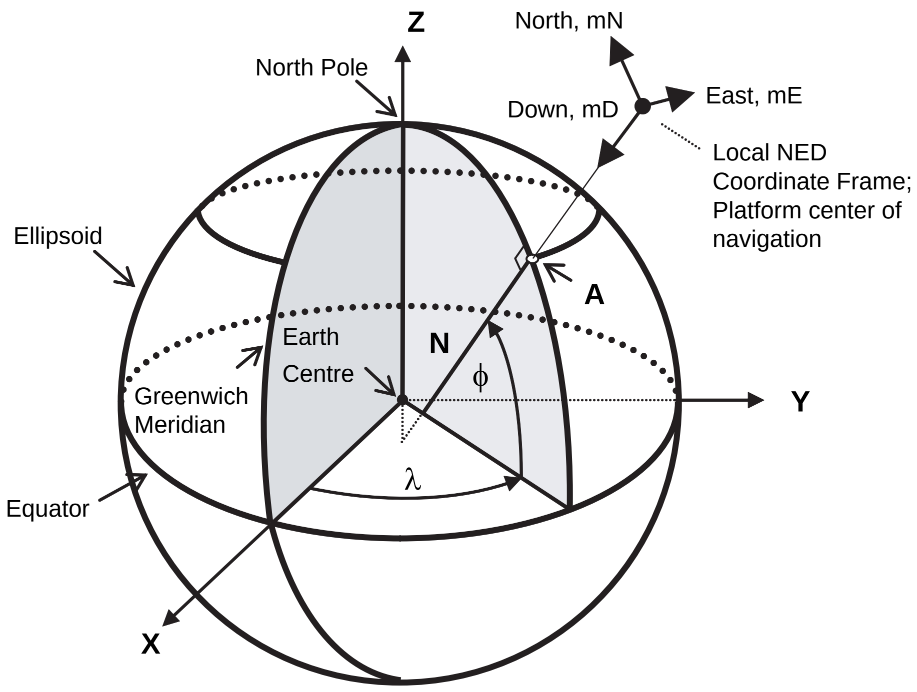

Key

ϕ latitude

λ longitude

Figure C.4 — Earth and local platform (NED) coordinate frames

The NED can be further defined to relate the local platform centre of navigation through a sequence of angular rotations to the local Earth surface (ENU) reference; that is, the latitude, longitude and height, relative to an Earth-based horizontal datum (e.g. WGS-84, Tokyo, etc.) and a vertical datum such as an

Earth ellipsoid or an Earth Geoid. In turn, the local surface-based ENU reference can be translated and rotated into the ECEF frame; that is latitude, longitude, and a gravity vector-based reference such as WGS-84 or latitude (positive north), longitude (positive east), and gravity vectors relative to an Earth-based vertical datum (e.g. OSU91A, EGM-96).

A reference ellipsoid is typically defined for a given reference system (e.g. WGS-84) and is mathematically defined by semi-major and semi-minor axes (or alternatively an eccentricity). Conversely, the Earth Geoid is a theoretical surface of equal gravity potential that is often used to define Mean Sea Level (MSL) anywhere on the Earth's surface. Geoids are mathematically defined by a set of sinusoidal harmonic equations[1)] and are referenced by a particular gravity model, such as EGM-96. Generally, the Up or Down directions for local coordinate systems are given by to the local gravity acceleration vector, which is the normal to the Geoid surface. However, many positioning systems now use the Global Navigational Satellite System (GNSS), which generally provides height relative to the WGS-84 ellipsoid. Thus, collection systems must define the reference for any height or elevation fields contained in metadata. Height above the ellipsoid should be referred to as HAE, height above the geoid should be referred to as HMSL or MSL (Height above Mean Sea Level), and height above the actual ground terrain level should be referred to as AGL.

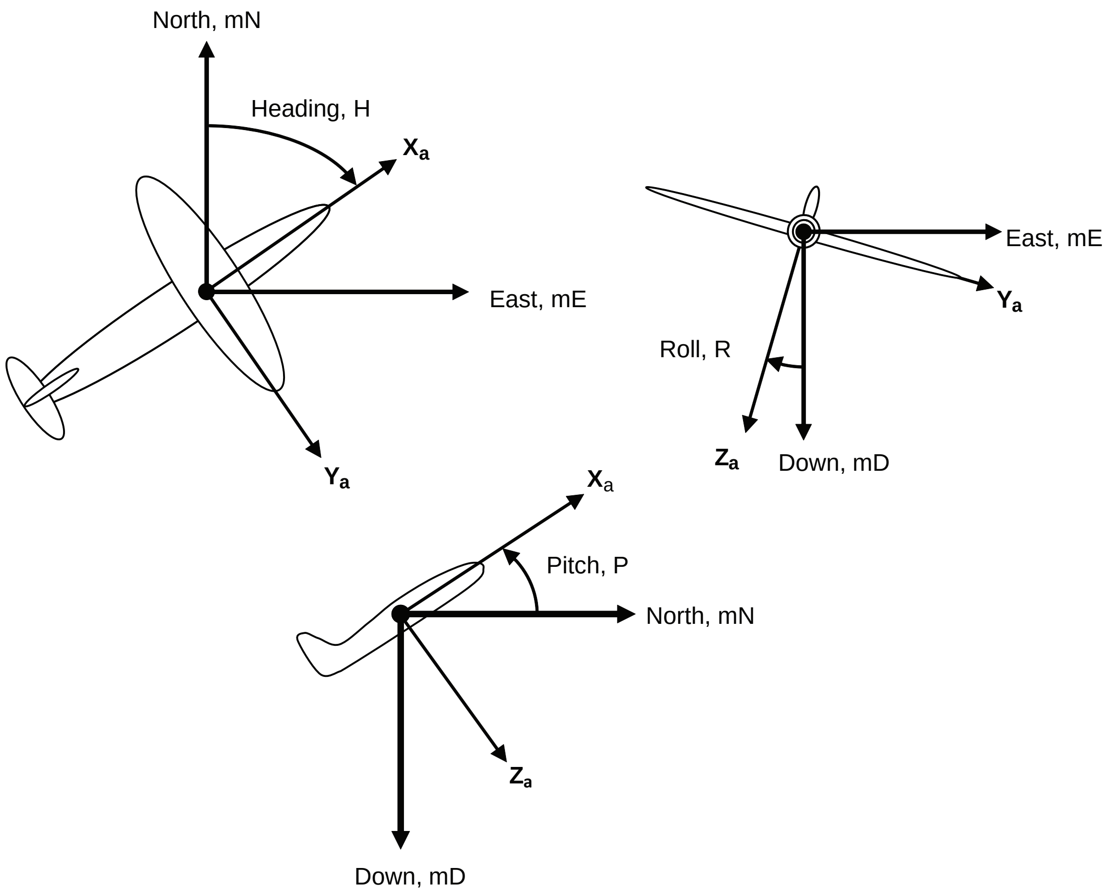

Figure C.5 — Platform body coordinate reference frame and local (NED) frame

C.2.4 Typical imagery sensor storage layout

In common imagery formats, and in particular ISO/IEC 12087-5, picture elements (pixels) are indexed according to placement within a "Common Coordinate System" (CCS), a two-dimensional array of rows and columns as illustrated in the array examples in Figure C.6. Three coordinate systems associated with digital and digitized imagery are commonly referred to: row, column (r,c), line, sample (ℓ,s), and x,y. The units used in the first two systems are pixels (and decimals thereof), while the x,y are linear

1) c.f., Manual of Photogrammetry, 5th Edition, ASPRS, 2004, pg. 192.

measures such as mm (and decimals thereof), as will be introduced in C.2.5 and Figure C.6. The origin of the CCS, as shown in Figure C.6, is the upper left corner of the first (or 0,0) pixel, which in turn is the upper left of the array. Because the CCS origin is the pixel corner, and the r,c associated with a designated pixel refers to its centre, the coordinates of the various pixels, (0.5,0.5), (0.5,1.5), ..., etc., are as shown in Figure C.6.

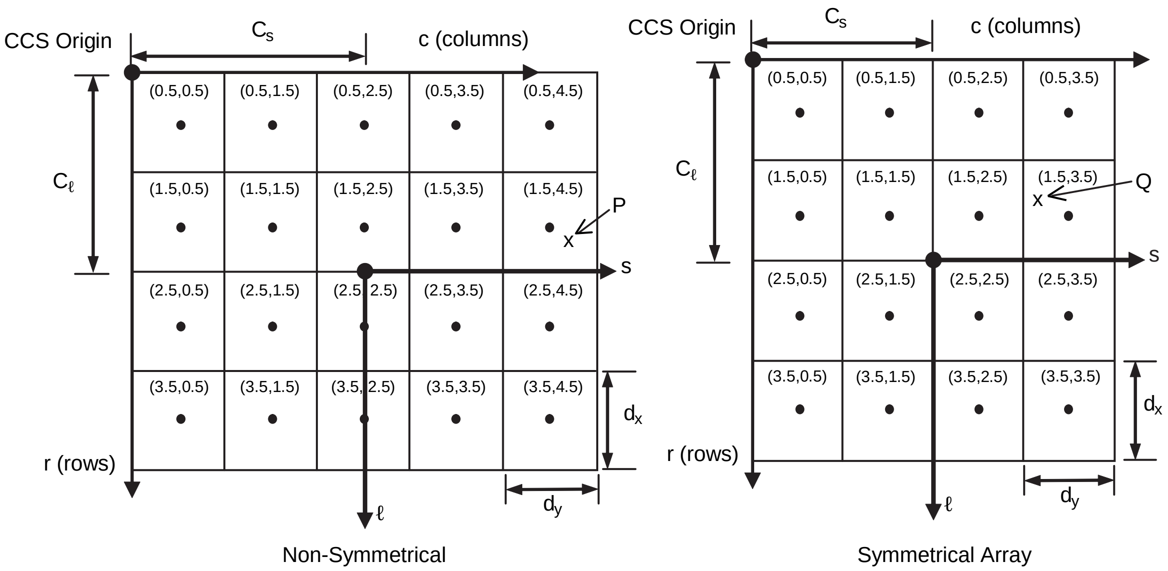

Figure C.6 — Pixel orientation within the frame sensor coordinate system

C.2.5 Row, Column (r,c) to Line, Sample (ℓ,s) coordinate transformation

The mathematical developments that follow are based on a Line-Sample, (ℓ, s), coordinate system, with the geometric centre of the image as the origin. The (ℓ,s) coordinates are computed from their (r,c) coordinates by two simple translations:

$$\begin{aligned} \ell &= r - C_\ell \\ s &= c - C_s \end{aligned} \quad (C.1)$$

where C_ℓ and C_s are each half of the image pixel array size, in pixels, in the row and column directions, respectively.

EXAMPLE 1 Figure C.6 (Non-symmetrical Array): For C_ℓ = 4/2 = 2,0 and C_s = 5/2 = 2,5, then r_P = 1,6 pixels and c_P = 4,7 pixels and

$$\begin{aligned} \ell_p &= r_p - C_\ell = 1{,}6 - 2{,}0 = -0{,}4 \text{ pixels} \\ s_p &= c_p - C_s = 4{,}7 - 2{,}5 = 2{,}2 \text{ pixels} \end{aligned} \quad (C.2)$$

EXAMPLE 2 Figure C.6 (Symmetrical Array): For C_ℓ = 4/2 = 2,0 and C_s = 4/2 = 2,0, then r_Q = 1,4 pixels and c_Q = 3,1 pixels and

$$\begin{aligned} \ell_Q &= r_Q - C_\ell = 1{,}4 - 2{,}0 = 0{,}6 \text{ pixels} \\ s_Q &= c_Q - C_s = 3{,}1 - 2{,}0 = 1{,}1 \text{ pixels} \end{aligned} \quad (C.3)$$

C.3 SAR sensor imagery systems

C.3.1 Introduction

SAR is an *active* sensor system that uses a series of radar pulses transmitted and received over time from a moving platform to create an image. SAR differs from other types of radars, known as “Real Aperture

Radars" (RAR), by creating a large "virtual antenna", known as the *synthetic aperture*, which allows tight focusing of the "virtual beam" along the direction of travel, known as the *along-track direction*. This allows a SAR system to achieve much higher image resolution in the along-track direction than is possible with a RAR system.

C.3.2 SAR resolution

Resolution is a loosely used word; however, it has a very specific meaning that is important to understanding SAR. Resolution is frequently, and loosely, used to describe the size of image pixels as they are projected onto the ground or some other surface. This is not resolution, but rather the *ground sample distance* (GSD) or *pixel sampling distance*. The proper definition of image resolution is:

The smallest distance between two uniformly illuminated objects that can be separately resolved in an image.

Resolution has an additional linguistic ambiguity, because "higher resolution" means smaller values of resolution metrics and to "increase resolution" means to decrease those metric values making the resolution better. Conversely, "lower resolution" means larger values of resolution metrics and to "decrease resolution" means to increase the value of the metrics making the resolution poorer. This language is illogical, but generally accepted. In this document, the use of ambiguous terms has been avoided.

Resolution, in general, can be limited by many different factors, one of which is the rate at which information is sampled. The GSD of an image is the result of a sampling process. If an image is sampled below its theoretical maximum resolution – *undersampling* – then the sampling rate will determine the resolution; however, the sample rate is not the same as the resolution. Sampling at higher than the theoretical maximum resolution – *oversampling* – will not change the resolution, but will waste storage space or bandwidth by retaining significantly redundant information. GSD is important to photogrammetric calculations, because it defines the sample spacing in the image coordinate system and is usually related to the actual resolution of the system; however, it should not be confused with resolution in either optical or SAR systems.

The resolution of a SAR system is measured in terms of the system's *Impulse Response (IPR)*. This is the width (e.g. in metres) of the return generated by a small *point reflector*, which equates to the smallest distance between two point reflectors that can be distinguished as two objects (see Figure C.7). SAR images are very often oversampled in order to retain as much information as possible. The Nyquist–Shannon Sampling Theorem states:

> "Exact reconstruction of a continuous-time baseband signal from its samples is possible if the signal is bandlimited and the sampling frequency is greater than twice the signal bandwidth."

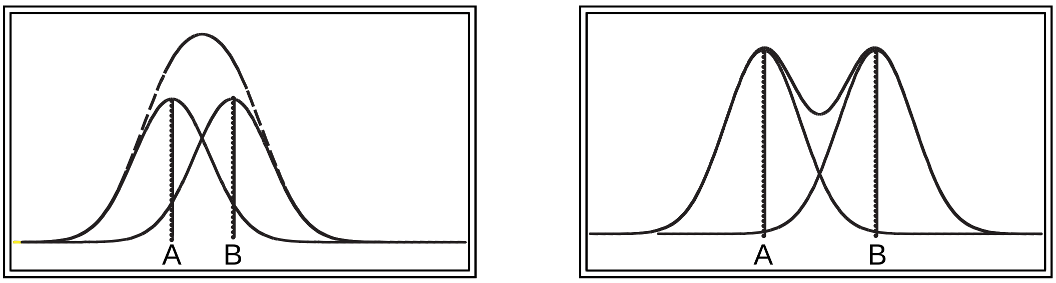

Distance between A and B is less than IPR

Two point reflectors are indistinguishable from one large reflector

Distance between A and B is greater than IPR

Two point reflectors are identified as two independent objects

Figure C.7 — Impulse Response (IPR) is how resolution is defined for SAR systems

The optimal sampling rate is sometimes referred to as the **Nyquist Rate** or the **Nyquist Frequency**. This theorem also applies to spatial signals, such as images, and the practical application of this to imaging is that in order to retain all of the information acquired by a sensor (e.g. radar or optical), the image should be sampled at twice the resolution of the signal reaching the sampling device. Other considerations, such as cost, efficiency, and value, may result in decisions to sample at lower rates. For SAR, it is common to see sampling rates in the range from the Nyquist Rate to 1/2 the Nyquist Rate, which translates to GSDs of 1/2 the IPR width to the IPR width, respectively. From the standpoint of SAR photogrammetry, the GSD of the pixels is more important than the IPR; although understanding the range and azimuth resolution equations are fundamental to the photogrammetric process.

C.3.3 Basic radar principles

Radar systems, in general, are *ranging* devices. They measure the time it takes for a signal transmitted by an antenna to return to that antenna (or, in some cases, a different antenna), as well as the magnitude of the returned signal, as shown in Figure C.8. The resolution (i.e. the smallest spacing between two objects that can be differentiated) in the range direction (i.e. radially away from the antenna) is dependent upon the ability to accurately measure the pulse arrival times, which is highly accurate in modern radar systems. For a general radar system, range resolution in the range direction is given by the following equation

$$r_R = \frac{cT}{2} \tag{C.4}$$

where

c is the speed of light;

T is the pulse duration.

Unlike in optical systems the range resolution in Formula (C.4) is independent of the range.

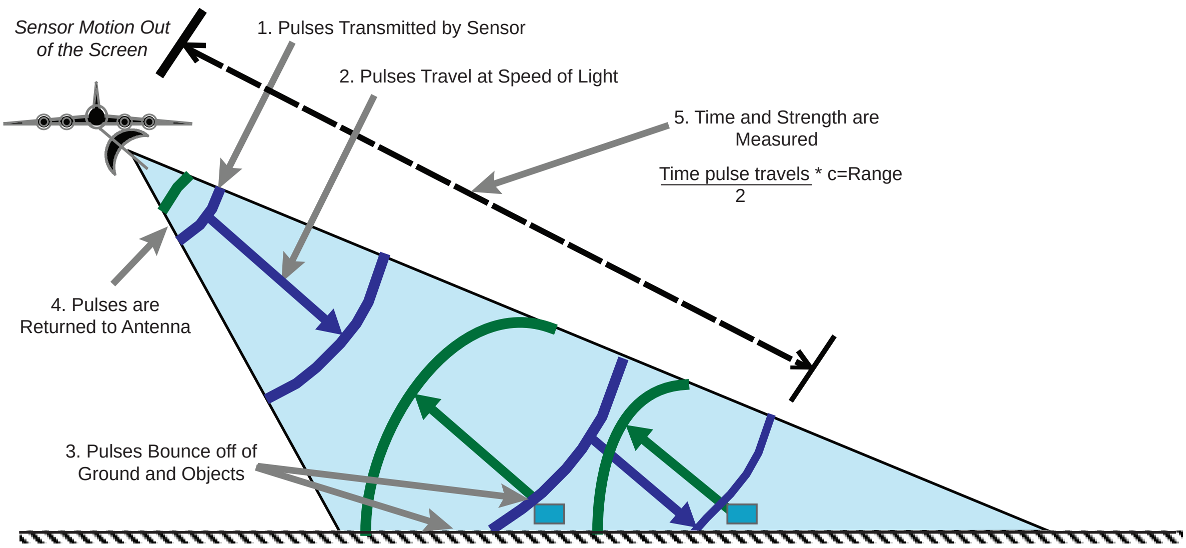

Figure C.8 — RADAR is a ranging system for determining distance using the time for transmitted electromagnetic pulses to return

When a radar system is used to image the ground, the term *slant range resolution* is used to refer to the resolution in the range direction. *Ground range resolution*, r_{GR}, refers to the resolution of the radar information projected onto the ground surface, which varies with the grazing angle – the angle between the ground surface and the direction of travel of the radar energy. Thus, the ground range resolution is always larger than the slant range resolution, and the ground range resolution is poorer (i.e. decreasing resolvability) at nearer ranges. See Figure C9. This is opposite of the range-to-resolution relationship for optical systems as the ground range resolution approaches infinity. This explains why radar imaging systems cannot image directly along the ground track of the platform, and have a near-range limit for practical utility. In practice, the grazing angle is set to around 60°, at which the ground range resolution is twice the slant range resolution [see Formula (C.5)].

$$r_{GR} = \frac{cT}{2\cos(\gamma)} \tag{C.5}$$

RAR systems change the position or pointing of the antenna in order to measure signal returns in different directions. Their resolution in the direction of rotation or translation, known as *azimuth resolution*, r_A, is dependent upon the width of the beam at the target.

$$r_A = r_{SR}\beta \tag{C.6}$$

where r_{SR} is the (slant) range to the target and β is the beam width, approximated by 0.89 * wavelength / antenna_size.

Since the azimuth resolution is inversely proportional to antenna size and proportional to range to the target, long range imaging at even moderate resolution may require an antenna size that exceeds what can be practically built and carried on an aircraft. The invention of Synthetic Aperture Radar resolved this problem by using motion of the radar to synthesize a very large antenna.

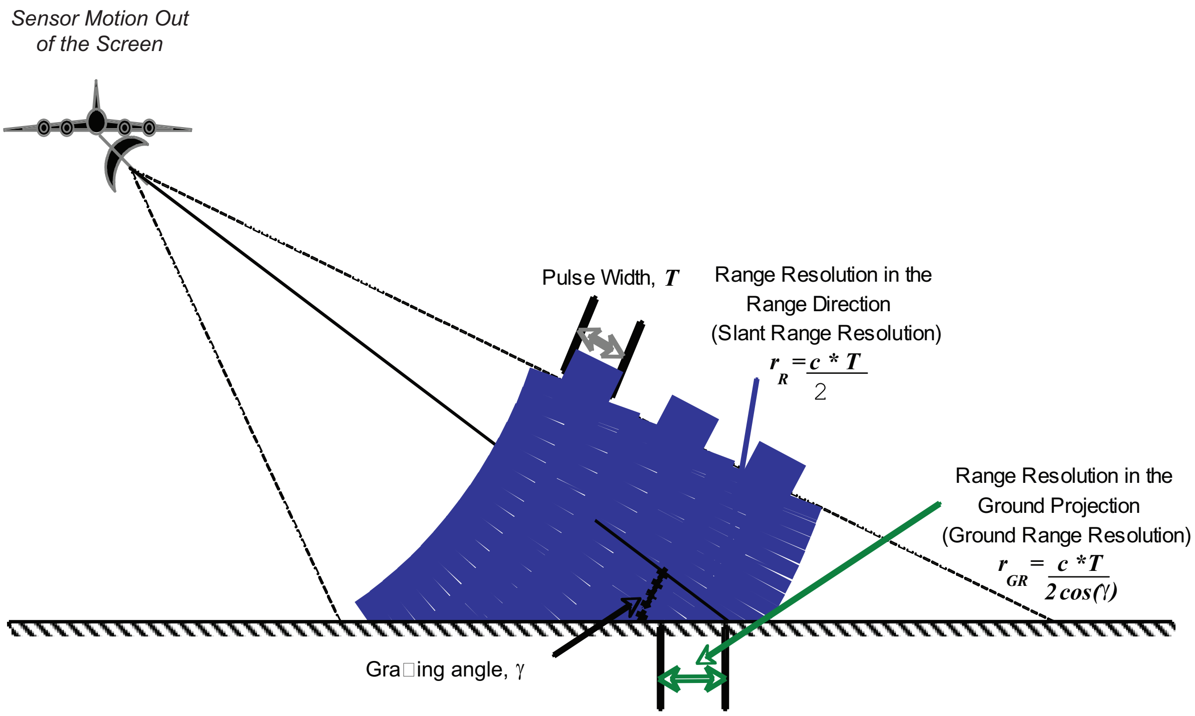

Figure C.9 — Slant Range Resolution vs. Ground Range Resolution

C.3.4 SAR radar principles

C.3.4.1 Introduction

The unique aspect of SAR is the method it uses for improving upon azimuth resolution by forming a synthetic virtual antenna that can be much larger than any plausible real antenna. In addition, SAR systems use more advanced ranging techniques than those described in D.3 to improve range resolution.

C.3.4.2 Range resolution in SAR

SAR systems employ a *chirped pulse*, in which a frequency modulation is imposed on each radar pulse. Using this technique, the radar can distinguish between overlapping pulses to a much higher degree, so that the effective range resolution becomes

$$r_R = \frac{c}{2B} \tag{C.7}$$

where B is the bandwidth of the chirped pulse. Chirped pulses are used by many types of radars, not just SARs.

C.3.4.3 Azimuth resolution in SAR

SAR systems use information collected over many pulses along a path to synthesize a virtual antenna. This is only possible when there is relative motion between the antenna and the fixed object or scene being imaged. This motion creates a Doppler shift (slight increases or decreases in the frequency) on the returning signal. The amount of the Doppler shift is related to the velocity of the antenna relative to the object that caused the signal to return. Objects that lie on a path orthogonal to the antenna's velocity vector, $\dot{S}$, (i.e. broadside to the motion) impose no Doppler shift on the returning signal because there is no relative motion in the range direction between that object and the aircraft. Objects forward of broadside impart a positive Doppler shift and objects aft of broadside impart a negative Doppler shift, as shown in Figure C.10. Moreover, all objects lying along a radial from the antenna position (i.e. at the same angle from broadside) have the same Doppler shift, hence the term *Doppler Angle* is often used. Doppler angle is represented by α.

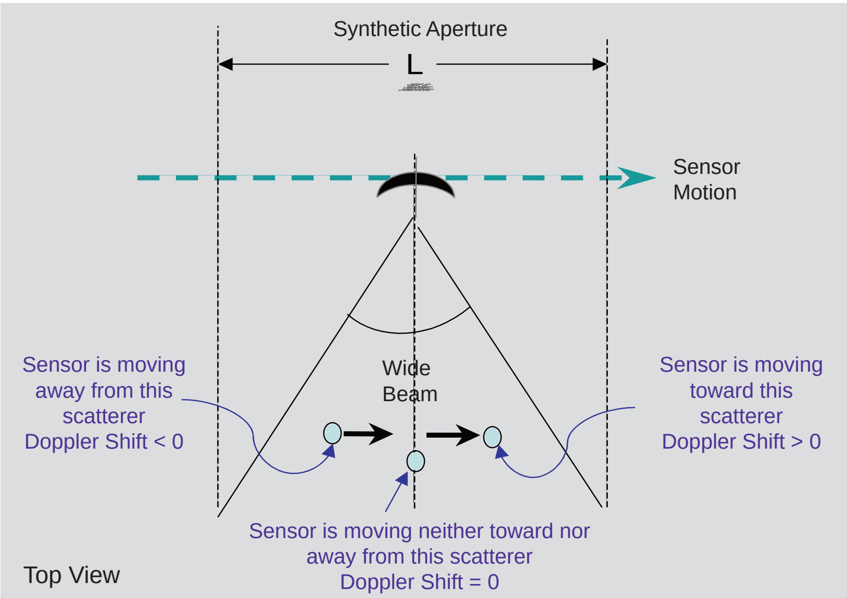

Figure C.10 — Doppler shift of a returning pulse's frequency is due to forward motion of the sensor relative to the scene

In order to discern the Doppler shift of a returning pulse, the phase of the signal must be recorded in addition to the magnitude. The phase information provides the information that allows a SAR processor to identify returning signals based on their Doppler shift. For every transmitted pulse, almost every point on the ground and in the beam reflects some return signal. These points are called *scatterers*. The returned signal is the sum of all returns from all scatterers. Since the antenna moves between pulses, the range and Doppler angle for each scatterer will change. The total distance travelled by the sensor while a scatterer stays illuminated is called the *Synthetic Aperture*, as illustrated in Figure C.11.

As the pulses are decoded, the signals for each discrete range bin are collected into a *range line*. The name "range line" is a misnomer based on the assumption that the surface being imaged is a plane. The range line data actually represents a *range sphere*, since the location of the ground surface has not yet been defined. The range line contains a collection of the radar signal's magnitude and phase for each of many returning pulses at that range. This information is usually represented by a complex number with a Real or in-phase component, *I*, and an *imaginary* or quadrature component, *Q*) The set of range lines recorded during a contiguous time-period is known as the *Phase History Data (PHD)*, or sometimes the *Video Phase History Data (VPHD)*. The PHD is the fundamental data collected by a SAR.

PHD can be processed in different ways to produce various products, the most common of which is a SAR image, which is more properly referred to as a *detected SAR image*. A detected SAR image is typically a single-banded, 8-bit or 16-bit fixed point image that can be displayed or printed. It is important to understand that the detected image (or any SAR product, for that matter) is simply one way to visualize the SAR PHD that was collected. A common intermediate product is a *complex SAR image*, wherein each pixel value is a complex number that represents the accumulated in-phase and quadrature signal from the scatterers within an area on the ground represented by a range value (±1/2 range resolution) and a Doppler angle value (±1/2 azimuth resolution). The detected SAR image is generated from the complex SAR image by taking the magnitude of the complex pixels, adjusting the dynamic range of the result, and, often, applying a coordinate transformation to a desired output projection.

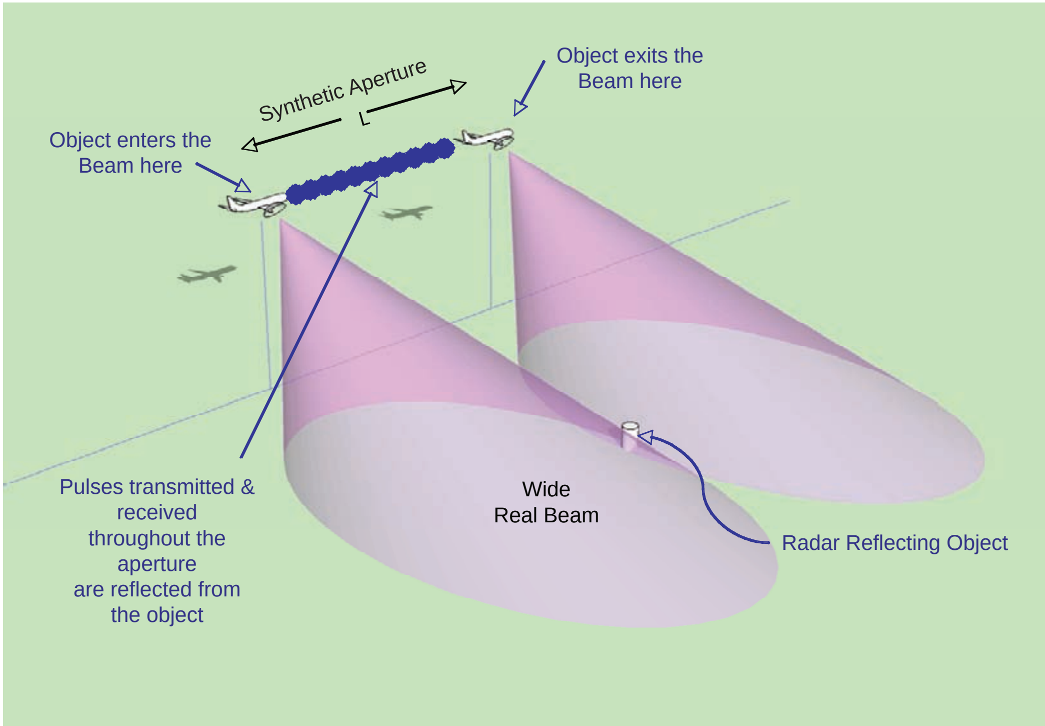

Figure C.11 — The synthetic aperture

C.3.5 SAR imaging Modes

C.3.5.1 Introduction

There are three primary types of *SAR imaging modes* used for ground imaging from aircraft and satellites: *Stripmap*, *Spotlight*, and *Scan*. In addition, a fourth mode used by some systems is called *ScanSAR*, which is not related to the general Scan mode. The modes are a function of the way in which the synthetic apertures are created. Scatterers contribute to the radar signal only during the time that they are in the synthetic aperture, with longer times resulting in better resolution. Thus, different modes have different equations for defining their azimuth resolution.

C.3.5.2 Stripmap Mode

In Stripmap Mode, the antenna pointing is fixed relative to the flight path, as shown in Figure C.12. Often, but not always, the beam is pointed at broadside (i.e. orthogonal to the velocity vector). As the platform moves, the beam sweeps a swath along a strip of terrain that is parallel to the path of motion. This mode is used primarily for continuous mapping applications. The synthetic aperture length, L, is equal to the real antenna beam width on the ground. More importantly, the synthetic aperture for each range line is different, even though its length, L, remains constant. The azimuth resolution for Stripmap mode is defined by:

$$r_A \approx \frac{D}{2\sin(\alpha)} \quad \text{(C.8)}$$

where D is the physical antenna aperture and α is the Doppler angle. For many SAR systems, the Stripmap mode uses a Doppler angle of 90°, which is directly broadside. For this case, Formula (C.8) simplifies to

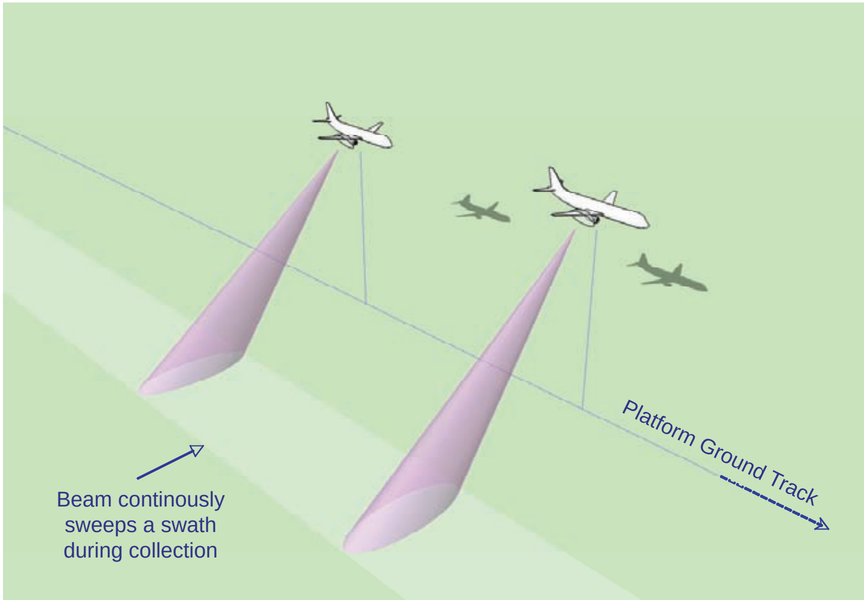

Figure C.12 — SAR stripmap imaging mode

$$r_A \approx \frac{D}{2} \quad \text{(C.9)}$$

C.3.5.3 Spotlight Mode

In the Spotlight mode, the antenna is steered to keep approximately the same ground area illuminated by the beam, as illustrated in Figure C.13. The illuminated area can be anywhere in the acquisition region of the SAR. This means that the synthetic aperture can be very large, resulting in better resolution than Stripmap mode. Every line in a Spotlight image has the same synthetic aperture, unlike Stripmap images. Spotlight mode is used primarily for acquisition of point or small area collections at higher resolution than would be achievable with other modes. The azimuth resolution for spotlight mode is defined by:

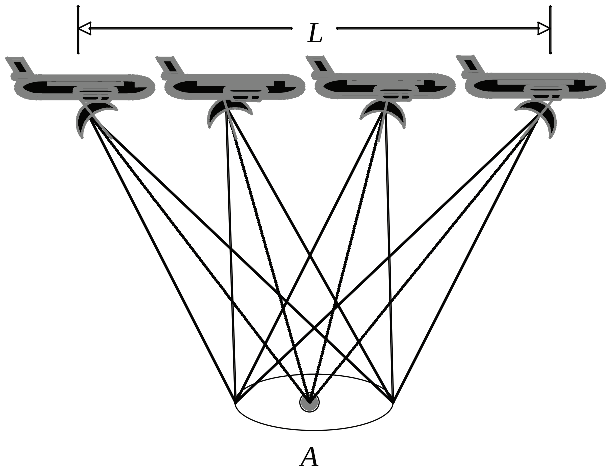

Figure C.13 — Spotlight mode imaging concept

$$r_A \approx \frac{0.89 r_{SR} \lambda}{2L\sin(\alpha)} \tag{C.10}$$

where

r_{SR} is the slant range;

L is the length of the synthetic aperture;

λ is the wavelength of the radar;

α is the Doppler angle.

The synthetic aperture, L, for Spotlight is not dependent on the real antenna beam width, as with Stripmap mode. Hence, the resolution can be improved by increasing the dwell time (i.e. the time that is spent illuminating the same target area) by moving the antenna beam. This allows for efficient imaging of many small scenes during one flight. Spotlight mode requires an antenna that can steer the beam during flight. This requires additional complexity in the antenna system to either electronically or physically steer the real antenna aperture.

C.3.5.4 Scan Mode

Scan mode SAR is actually the most general SAR mode. It combines the characteristics of Spotlight mode and Stripmap mode, each of which can be formulated as special cases of Scan mode. In Scan mode, the beam is steered to illuminate a strip of terrain that can be at any angle with respect to the direction of motion. Because of this, scatterers may be illuminated for differing amounts of time. Moreover, the beam can be steered to both scan and increase dwell, thereby allowing better resolution than Stripmap mode by scanning more slowly than would result from the platform motion alone. Scan mode is used primarily for imaging, at medium to high resolution, large scenes that are not parallel to the flight path. The use of scan mode can increase collection efficiency particularly for satellites, because their flight paths are fixed. The azimuth resolution for Scan mode imagery depends upon the scan rate relative to each pixel.

C.3.5.5 ScanSAR Mode

ScanSAR mode is an additional mode that has been defined by some SAR data providers. ScanSAR is not a true Scan mode, but rather a special case of Stripmap mode. ScanSAR incorporates a process for time-sharing an electronically-steered phased array antenna to quickly move the beam from one strip to a parallel one, so that multiple strips can be illuminated in one pass. However, because the strips are not continuously illuminated for as long as they are in Stripmap mode, not as many range lines are collected and, thus, ScanSAR modes have poorer resolution. The strips are typically processed into slightly overlapping images that can then be mosaicked into large area maps at medium resolution. Individual strips from the ScanSAR collections can be treated photogrammetrically as separate Stripmap mode images.

C.3.6 SAR sensor coordinate systems

C.3.6.1 Characteristics of SAR sensor coordinate systems

SAR sensor coordinate systems have many unique terms and quantities. The fundamental reference data needed for performing photogrammetric processing with SAR images are the *Aperture Reference Point (ARP)*, $\mathbf{S_0}$, the *Ground Reference Point (GRP)*, $\mathbf{G_0}$, and the *Sensor Velocity Vector*, $\dot{\mathbf{S}}$. Unlike passive projective imaging sensors (e.g. frame or pushbroom optical sensors), SAR sensors do not strictly have an “interior orientation” that can be physically modelled. This is because the SAR images or image-like products are generated synthetically from the PHD. Pulses are transmitted by the radar part of the sensor, the magnitude, phase, range, Doppler-angle, and time of the returned signal are sensed by the radar system; and then the SAR processor calculates an aggregate magnitude and phase for each range-Doppler cell, or pixel, within the desired footprint. These can be output in any desirable coordinate system or projection, although there are a few common methods, which will be discussed below.

In the PHD, the return from a given scatterer actually exists in many different Range-Doppler cells. The aggregation process, known as *image formation*, combines the relevant signals into one complex value, and associates the value with a single range-Doppler cell relative to a fixed reference point within the synthetic aperture. This reference point is the ARP and it is frequently defined by the physical location of the sensor at the centre of the synthetic aperture. In some cases, however, the ARP may be defined in other ways, such as the mean of several way points along the antenna path, *S(t).* For purposes of geopositioning, it is not critical to know just how the ARP is derived, but knowing the ARP that is used as the reference to form a product (or part of a product) is sufficient.

For Spotlight mode imagery, there is almost always one synthetic aperture and one ARP for all pixels in the image. For Stripmap and Scan mode imagery, the synthetic aperture varies continuously along the strip or scan, so the ARP is defined as a function of time, with each image line having its own ARP. For Stripmap mode, the Doppler angle is identical for every line; whereas for Scan mode, the Doppler angle may vary from line-to-line or possibly even pixel-to-pixel.

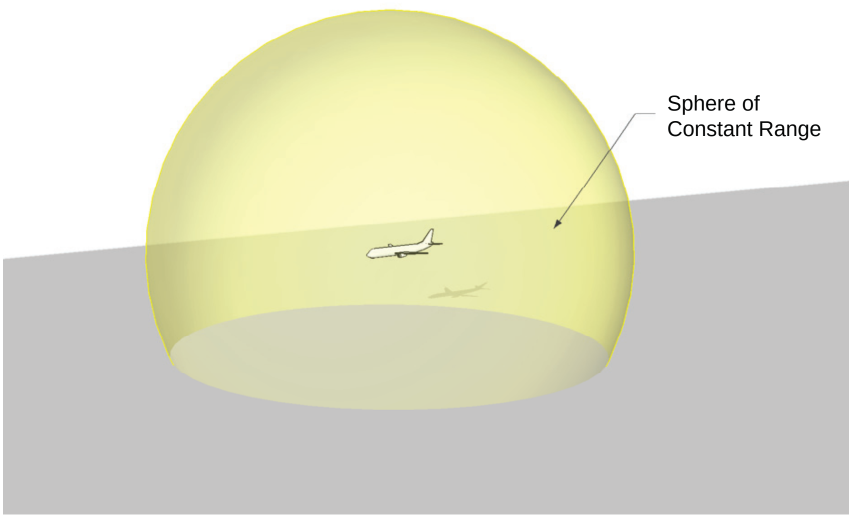

Figure C.14 — Each range “line” represents signals returned from a spherical shell

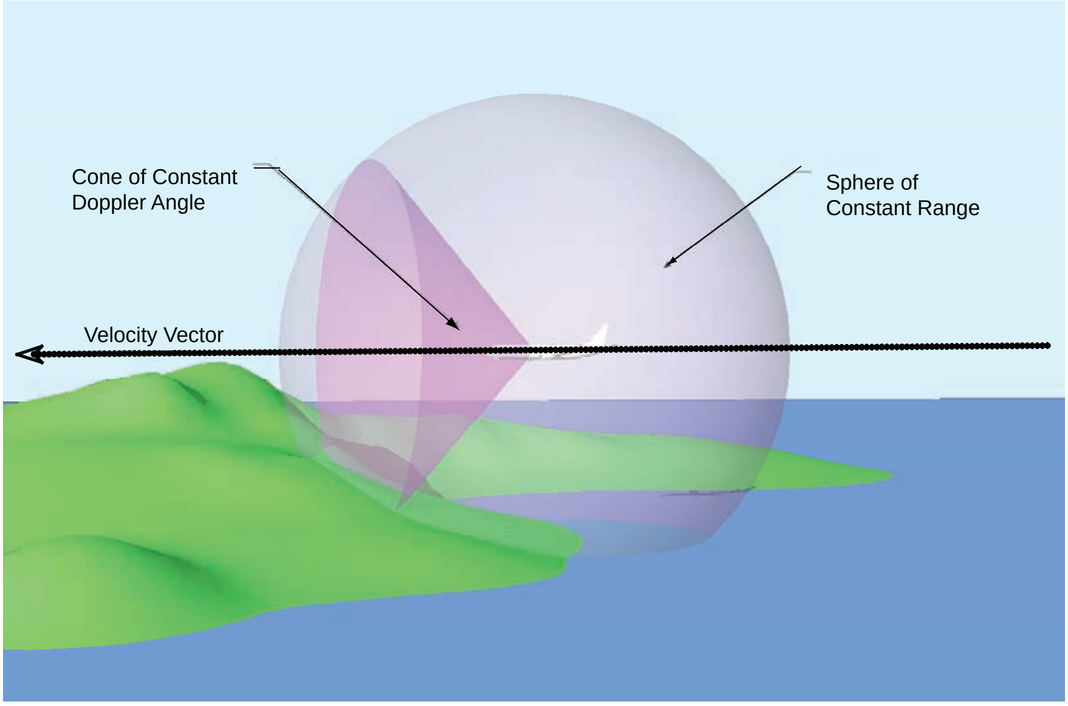

Figure C.15 — Range-Doppler "cell" represents the signals from the circle that is the intersection of the range sphere and the Doppler cone

This view can be generalized mathematically for image products from all SAR modes, with pixel values (either real or complex) being a function of slant range R_S, Doppler angle α, and time t:

$$\text{pixel\_value} = f(R_S, \alpha, t) \tag{C.11}$$

For Spotlight mode, t = *constant*, and for Stripmap mode, α = *constant*. In this general formulation, the ARP, the GRP, and the velocity vector are all functions of time. Since time is constant for Spotlight mode, a single set of data must be provided for each image. For other modes, sufficient sets of data must be provided either directly (e.g. one set for each image line) or indirectly (e.g. periodic sets with time stamps, from which each line's values can be accurately estimated, or polynomial coefficients that can be used to compute them).

Each range bin represents a spherical shell of constant distance from the sensor, shown in Figure C.14. It is called a shell because it represents a volume having a width equal to the range resolution. Similarly, each Doppler bin represents a conical shell having a width of the azimuth resolution and defined by a constant angle from the velocity vector of the sensor, the Doppler angle. As shown in Figure C.15, the intersection of these two shells is a circular ring, or shell, with a cross section of range resolution by azimuth resolution. Thus, each pixel's value is an aggregation of all signals received from anywhere within that circular shell. This viewpoint is analogous to representing a pixel in an optical sensor as an aggregation of all light energy received within a single cylindrical ray.

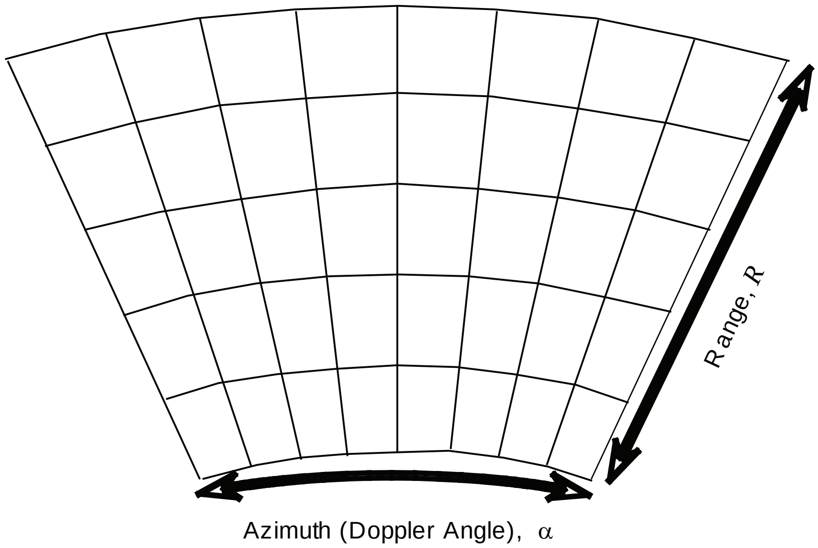

Figure C.16 — Polar format image projected to a ground plane (angular variation exaggerated)

Thus, a natural coordinate system to use for addressing Spotlight SAR pixels is defined by the two axes: slant range R_S and Doppler-angle α. When an image is formed in this coordinate system, it is usually referred to as the "polar form" of a SAR image, since it forms a 2-D polar coordinate system when projected to a plane that passes through the velocity vector, as shown in Figure C.16. However, with SAR, the choice of a particular product's output surface and coordinate system is arbitrary – the pixel values can be computed on a plane referenced to the SAR sensor, on a plane referenced to the Earth, or even onto a terrain surface, such as one might do to create an orthographic image.

The three most common methods for image formation are to use the *Slant Plane*, the *Ground Plane*, or an *Inflated Ellipsoid*.

C.3.6.2 Slant Plane coordinates

The slant plane is a plane that passes through the sensor velocity vector and the *Ground Reference Point (GRP)* for an image. The sensor velocity vector is usually close to a straight line, however, it often has some variation from it. As a result, the velocity vector is defined at the ARP for practical purposes in Spotlight mode imagery. In the other modes, the variation in the velocity vector is accommodated by the time-dependent nature of the metadata. The GRP is somewhat of a misnomer, as there is no assurance that the GRP is actually located on the "ground." Instead, it is a predefined coordinate for a target location or targeted centreline that is presumed to be "on the ground" (based, for example, on a DEM or other information with unknown reliability). SAR products are almost always formed with the GRP at the centre of the image in the range direction. For Spotlight mode, it is usually placed at the centre of the image in azimuth, as well. For other modes, the centre of each product line is defined as the GRP for that line. For non-Spotlight modes, the variable nature of the GRP and velocity vector implies that the *slant plane* may vary with each line and so the image may not actually be formed on a single plane. Regardless, it is still usually called a *slant plane image*.

The slant plane coordinate system is defined by a unit vector in the range direction, $\hat{\mathbf{U}}_R$, that points from the GRP to the ARP, and an azimuth unit vector, $\hat{\mathbf{U}}_A$, that is in the slant plane, but orthogonal to $\hat{\mathbf{U}}_R$

and parallel to the velocity vector. Typically, the image row / sample direction (x-axis) is aligned with $\hat{\mathbf{U}}_A$ and the column / line direction (y-axis) is aligned with $\hat{\mathbf{U}}_R$.

NOTE 1 If an image is collected off broadside (i.e. with a non-zero squint angle), then the slant plane image will be approximately a parallelogram when projected to the ground.) While a polar format can be used for the coordinate system, images are usually generated, either directly or via resampling, onto a pixel coordinate system with pixel spacings that are equidistant along both orthogonal axes – as opposed to the polar format, which is equidistant in range and equiangular in azimuth. The mapping from pixel coordinates to range and Doppler angle is accomplished as follows:

Given the line, *l*, and sample, *s*, of a pixel, calculate the offset of the pixel from the GRP in pixel coordinates,

$$\Delta l = l - l_0 \text{ and } \Delta s = s - s_0 \qquad \text{(C.12)}$$

where l_0 and s_0 are the line and sample coordinates of the GRP, and calculate the vectors $\overline{\mathbf{Q}_0}$ from the ARP vector, $\dot{\mathbf{S}}$ to the GRP vector, and $\mathbf{G}_0$, in the ECEF coordinate system.

$$\overline{\mathbf{Q}_0} = S_0 - \mathbf{G}_0 \qquad \text{(C.13)}$$

Project the vector $\overline{\mathbf{Q}_0}$ into the slant plane (ARP as origin)

$$\mathbf{Q}_0 = \left|\overline{\mathbf{Q}_0}\right| \hat{\mathbf{U}}_R \qquad \text{(C.14)}$$

Then, calculate the pixel's 3D vector in the slant plane (ARP as origin)

$$\mathbf{Q} = \mathbf{Q}_0 + \begin{vmatrix} \Delta l & p_1 \\ \Delta s & p_s \\ 0 & \end{vmatrix} \qquad \text{(C.15)}$$

where p_S and p_l are the slant plane pixel sampling distances (e.g. in metres) in the sample and line directions, respectively. SAR images are often oversampled during image formation in order to retain maximum information, with pixel sampling distances being smaller than the image resolution. Thus, fields labelled as “Resolution” or “IPR” should not be used for this calculation. Rather, fields marked as “Sample Distance” or “Ground Sample Distance” (a misnomer, since it is actually measured in the slant plane) should be used. The slant range, R_S, and the local Doppler angle, α_L, for the pixel can now be computed using

$$R_s = |\mathbf{Q}| \text{ and } \alpha_L = \cos^{-1}\left(\frac{\mathbf{Q} \bullet \mathbf{Q}_0}{|\mathbf{Q}||\mathbf{Q}_0|}\right) + \alpha_0 \qquad \text{(C.16)}$$

where α_0 is the Doppler angle of the GRP, calculated as the complement of the squint angle at the GRP:

$$\alpha_0 = 90^\circ - \tau \qquad \text{(C.17)}$$

Alternatively, the Doppler angle can be computed directly using the antenna's velocity vector, $\dot{\mathbf{S}}$

$$\alpha_L = \cos^{-1}\left(\frac{\mathbf{Q} \bullet \dot{\mathbf{S}}}{|\mathbf{Q}||\dot{\mathbf{S}}|}\right) \qquad \text{(C.18)}$$

NOTE 2 The slant plane is sometimes called the *SAR plane*, because the SAR image is generally formed in that plane.

C.3.6.3 Ground Plane coordinates

The ground plane is defined as a plane that is tangent to the Earth's surface at the GRP. Interestingly, this can be somewhat ambiguous. First, as stated above, the GRP may not be on the Earth's surface, and second, “the Earth’s surface” can be defined in a number of ways. Most commonly, the plane that is used is orthogonal to the Earth ellipsoid normal and passes through the GRP for Spotlight mode, or through a central GRP for other modes. Ground plane images are most often created by projecting the slant plane image into the ground plane, requiring a resampling of the slant plane image. However, sometimes images are formed directly into the ground plane. Regardless, the mapping from slant plane to ground plane is accomplished using a plane-to-plane coordinate transform called a 3D affine transform.

$$Y = AX + b \tag{C.19}$$

where **X** is the slant plane coordinate in ECEF, **Y** is the ground plane coordinate in ECEF, **A** is the 3X3 Affine matrix and **b** is a 3x1 translation vector. The range and Doppler angle can be calculated from ground plane pixel coordinates by first inverting the affine transform to recover the equivalent slant plane pixel coordinates, then applying the method given above. The projected slant plane coordinates will likely not fall directly on slant plane pixel coordinates, so floating point numbers are used to encode pixel coordinates. The affine transform parameters used to perform the coordinate transform from slant plane to ground plane or their inverse must be provided with a ground plane SAR product in order to allow photogrammetric processing.

The ground plane is also sometimes called the *focus plane*, because the image formation process must focus each pixel at a particular range. Commonly, the range used is that to the pixel point projected into a plane tangent to an ellipsoid inflated to the tasked elevation.

C.3.6.4 Inflated Ellipsoid coordinates

The inflated ellipsoid coordinate system uses a fixed height, *h*, above the Earth’s ellipsoid. The height is usually that of the GRP, for Spotlight mode, or some average height for the other modes. This coordinate system is primarily used with non-Spotlight modes that cover large areas, for which the Earth’s curvature makes planar projections impractical. In order for an ellipsoidally projected SAR product to be useful photogrammetrically, the method that the SAR provider uses for defining a pixel’s coordinate must be clear. Typically, one axis (usually the x-axis) is defined along the surface of the Earth’s ellipsoid in the instantaneous ground range direction, and the other axis (usually the y-axis) is defined in the instantaneous velocity vector direction. So for any pixel in the image or product, the x and y coordinates will uniquely determine a three-dimensional point, **M**, in the ECEF coordinate system, on the ellipsoid. **M** must be calculated by inverting the data provider’s method for defining the pixel’s coordinate.

For example, for an ellipsoid inflated by h, and image coordinates x and y, determine the geographic coordinates, latitude λ, and longitude, Φ, from

$$\begin{aligned}\Phi &= F(x,y)\\ \lambda &= G(x,y)\end{aligned} \tag{C.20}$$

using the product provider's conversion method. Then convert these coordinates using standard code, such as GEOTRANS, which implements something like the following:

$$\begin{aligned}X &= \frac{(a+h)\cdot\cos(\varphi)\cdot\cos(\lambda)}{\sqrt{1-(e'\cdot\sin(\varphi))^2}}\\ Y &= \frac{(a+h)\cdot\cos(\varphi)\cdot\sin(\lambda)}{\sqrt{1-(e'\cdot\sin(\varphi))^2}}\\ Z &= \frac{(1-e'^2)\sin(\varphi)}{\sqrt{1-(e'\cdot\sin(\varphi))^2}}\end{aligned} \tag{C.21}$$

Here

$$e' = \sqrt{1-\{(b+h)/(a+h)\}^2} \tag{C.22}$$

The slant range, R_S, and the local Doppler angle, α_L, can now be computed directly.

$$R_s = |\mathbf{M}-\mathbf{S}(t)| = \sqrt{\left[M_x - S_x(t)\right]^2 + \left[M_y - S_y(t)\right]^2 + \left[M_z - S_z(t)\right]^2} \tag{C.23}$$

$$\alpha_L = \cos^{-1}\left\{\frac{S_x(t)\left[M_x - S_x(t)\right] + S_y(t)\left[M_y - S_y(t)\right] + S_z(t)\left[M_z - S_z(t)\right]}{R_s\left|\dot{\mathbf{S}}(t)\right|}\right\} \tag{C.24}$$

C.3.6.5 Important SAR terms

A number of different terms, including *Range* or *Slant Range*, *Ground Range*, *Azimuth Angle*, *Squint Angle*, *Depression Angle*, *Look Angle* or *Elevation Angle*, *Grazing Angle*, and *Incident Angle* are unique to SAR and are defined in Clause 4. Figure C.17 and Figure C.18 illustrate these terms.

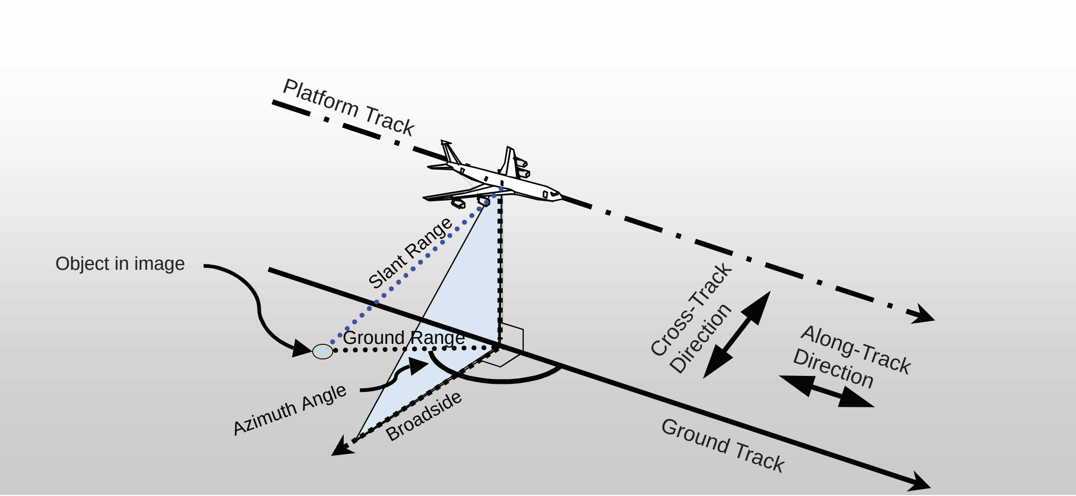

Figure C.17 — Some important SAR terms

C.4 SAR geometry

C.4.1 Equations

As discussed previously, SAR pixel coordinates are characterized by their range and Doppler angle, each of which places a condition on the pixel's location in space. As described in C.3, any pixel location in line-sample space can be converted to a coordinate in Range-Doppler space. The range value of a pixel identifies the surface of a sphere of radius R_S that is governed by the *range equation* or *range condition* of Formula (C.25):

$$R_S = |\mathbf{Q}| = \left[(X - S_X)^2 + (Y - S_Y)^2 + (Z - S_Z)^2 \right]^{\frac{1}{2}} \tag{C.25}$$

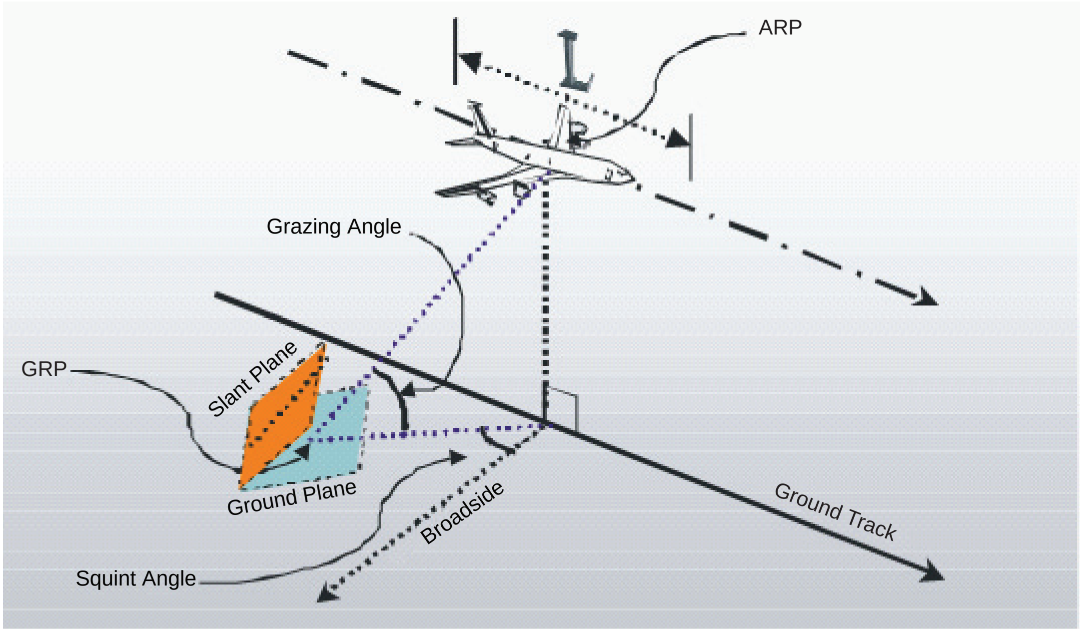

Figure C.18 — Important SAR geometry parameters

where $[X, Y, Z]^T$ in ECEF coordinates, is the location of a point on the range sphere, and $S_0 = [S_{X0}, S_{Y0}, S_{Z0}]^T$ is the location of the ARP in ECEF coordinates. R_S is the slant range to the scatterer from Formula (C.16). The Doppler angle value of a pixel identifies the surface of a cone of angle α, from the antenna's velocity vector that is defined by the *Doppler Cone equation* or *Doppler Cone condition* of Formula (C.26):

$$\dot{S}_X (X - S_X) + \dot{S}_Y (Y - S_Y) + \dot{S}_Z (Z - S_Z) = \cos\alpha \cdot \left(\dot{S}_X{}^2 + \dot{S}_Y{}^2 + \dot{S}_Z{}^2 \right)^{\frac{1}{2}} \left[(X - S_X)^2 + (Y - S_Y)^2 + (Z - S_Z)^2 \right]^{\frac{1}{2}} \tag{C.26}$$

The solution to these two equations traces a circle that represents the intersection of the Doppler Cone with the Range Sphere. The correct 3D location of the radar return could lie anywhere on that circle. When the Doppler angle is 90°, the Doppler Cone becomes a plane, and the right side of Formula (C.26) goes to zero. This is the case for many Stripmap mode imaging systems.

A single Range-Doppler pair does not uniquely define the 3D location for a radar return or its associated position on the Earth's surface. Rather, the slant plane image is simply a convenient way to store the radar signal information gathered from each Range-Doppler circle collected and processed by the SAR system. However, knowing the 3D location of an object point does allow one to calculate to which Range-Doppler circle it corresponds, and, hence, its corresponding location in the 2D image.

C.4.2 External Influences

Atmospheric Refraction. The atmospheric refraction of the microwave radiation should be adjusted for within the image formation processor. Errors in the estimation of this factor during image formation may affect accuracy at longer ranges. Generally, geopositioning should not need to consider this factor.

Curvature of the Earth. The curvature of the Earth should be adjusted for within the image formation processor. Generally, geopositioning should not need to consider this factor.

Land cover. Land cover, such as a vegetation canopy layer on the ground, also affects the back scattering, depending on the frequency and polarization.

Topography. Topography can cause image distortions such as foreshortening, layover and shadowing.

C.5 Application of Sensor Model

C.5.1 SAR geopositioning

C.5.1.1 Introduction

Geopositioning from SAR images relies on the ability to associate image coordinates and ground coordinates. In general, two sets of photogrammetric (some use the term *radargrammetric*) equations are needed to perform geopositioning: (1) the Ground-to-Image function and (2) the Image-to-Ground function. In general, the Ground-to-Image function is well-defined as a direct transformation, or projection, using the sensor model equations, from an object point in 3D space to a 2-D coordinate in image space. Conversely, the Image-to-Ground function cannot generally be determined directly, because, for most sensors, a single-image coordinate maps into a large number (possibly infinite) of possible 3D object coordinates.

For SAR images and products, Formula (C.25) and Formula (C.26) together form the Ground-to-Image Function. Because of the nonlinearity of these equations, however, the Image-to-Ground function can be directly solved for only the simplest of cases. Thus, the Image-to-Ground function is nearly always implemented in an iterative fashion using the Ground-to-Image equations, with an initial estimate of ground coordinates using a simplified model, such as the corner coordinates commonly provided in the metadata (see Box below).

As with projective sensors and their collinearity equations, there are two methods for photogrammetric geopositioning from SAR images. These are:

a) to intersect the Range-Doppler circle for a given pixel with a known elevation, such as a DEM, and

b) to use two or more images of the same ground area and find the “intersection” of the two or more Range-Doppler circles associated with the corresponding pixels.

NOTE As with optical images, SAR images often come with Earth coordinates that can be used for rudimentary positioning. For example, given a slant plane or ground plane image, the corners of the image are often projected to a tangent plane or some other simple model of the Earth’s surface, such as the Earth Ellipsoid or the Geoid. Combined with the pixel count or pixel GSD, this can be used to estimate surface coordinates. However, since the true location of a pixel from a single image is ambiguous, these methods are only rough approximations. One can think of these ambiguities as analogous to the perspective distortion seen in optical images taken at oblique angles.

C.5.1.2 Mono image with an elevation source

Given an elevation source, such as a known object height or a DEM of the Earth’s surface, and the equation of the circle for a given pixel, we can calculate the intersection of the two. (This is equivalent to using the collinearity equations for an image from an optical sensor in the same fashion.) Generally, there will be two intersections – one on the left side of the velocity vector and one on the right. Since the pointing direction from the ARP to the GRP is known, only one of these makes sense. This effect is illustrated using a tangent plane in Figure C.19. The equations must be solved iteratively due to the nonlinear nature of the Range-Doppler condition equations. Techniques such as those in [3] can be applied.

When a DEM is used, it is possible for the circle to intersect the DEM more than once on the same side of the sensor, though. This can occur, for example, in mountainous areas where there is significant terrain relief or in urban areas where a high-resolution surface DEM can represent buildings and other structures in great detail. The cause of this multiple-intersection is radar return information in a single Range-Doppler cell that comes from more than one surface location. This is an ambiguity in SAR data that cannot be resolved. The visual image effect of this ambiguity is known as *layover*, since it appears in the image that the near-vertical face of an object (e.g. mountain, building) appears to "lay-over" the surfaces in front of the object. When geopositioning, layover becomes a concern if the resolution of the DEM results in ambiguities where multiple 3D ground or object points map to the same image point.

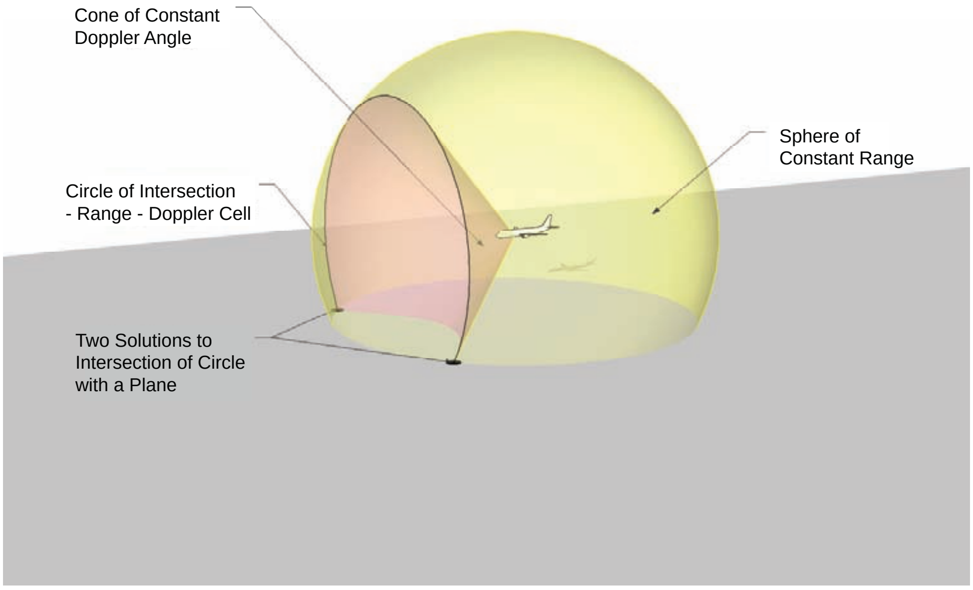

Figure C.19 — Two solutions when the range-Doppler circle intersects with a plane

C.5.1.3 Stereo intersection

When two images of the same ground location are collected (assuming different ARPs), the pixels in each image associated with that location will define distinct Range-Doppler circles. The intersection of those two circles, or more properly the intersections of the two Range Spheres and two Doppler Cones, will define a 3D point. The simultaneous solution of the two Range and two Doppler equations is then over-determined, as there are four equations and three unknowns. Hence, any errors in the range or Doppler information in either image will result in a variety of close solutions. Pictorially, this means that the Range-Doppler circles do not directly intersect, but come very close. Iterative least squares techniques, such as those discussed in [3], must be used to solve for the optimal (in a least squares sense) result.

C.5.2 Adjustable parameters

Adjustable parameters are those parameters in the sensor model that have uncertainty associated with them and that can be adjusted during triangulation, resection, or model-based registration operations. For SAR, the primary measured parameters are the ARP, $\mathbf{S_0}$, and its first derivative, the sensor velocity vector, $\dot{\mathbf{S}}$. The other key parameter, the GRP, $\mathbf{G_0}$, is not measured but rather is given, and, thus, is not adjustable.

C.5.3 Covariance matrices

In all the metric applications of imagery, the quality of the extracted information is considered as important as the information itself. This is particularly true for geopositioning applications that require high levels of accuracy and precision. The location of an object in the three-dimensional ground space is given either by its geodetic coordinates of longitude (λ), latitude (ϕ), and height above the ellipsoid, h, or by a set of Cartesian coordinates (X,Y,Z). Although there are many ways to express the quality of the coordinates, the most fundamental is through the use of a *covariance matrix*. For example:

$$\Sigma = \begin{bmatrix} \sigma_X^2 & \sigma_{XY} & \sigma_{XZ} \\ \sigma_{XY} & \sigma_Y^2 & \sigma_{YZ} \\ \sigma_{XZ} & \sigma_{YZ} & \sigma_Z^2 \end{bmatrix} \quad \text{(C.27)}$$

in which $\sigma_X{}^2$, $\sigma_Y{}^2$, $\sigma_Z{}^2$ are the marginal variances of the coordinates, and σ_{XY}, σ_{XZ}, σ_{YZ} are covariances between the coordinates, which reflect the correlation between them. The practice is often to reduce these six different numbers to only two: one expressing the quality of the horizontal position and the other the quality in the vertical position. The first is called *circular error*, or CE, and the second *linear error*, or LE. Both of these can be calculated at different probability levels, CE50 for 0.5 probability, CE90 for 0.9 probability, etc. Commonly used measures, particularly by NGA under “mapping standards”, are CE90 and LE90. The CE90 value is derived from the 2x2 submatrix of **Σ** that relates to X,*Y*, or

$$\begin{bmatrix} \sigma^2{}_X & \sigma_{XY} \\ \sigma_{XY} & \sigma^2{}_Y \end{bmatrix} \quad \text{(C.28)}$$

The LE90 is calculated from $\sigma_Z{}^2$. In these calculations, the correlation between the horizontal (*X,Y*) and vertical (*Z*) positions, as represented by σ_{XZ}, σ_{YZ}, are ignored (i.e. assumed to be zero). The X,Y,Z system in these equations usually refers to the local coordinate system where Z represents elevation.

In order to have a realistic and reliable value for the estimated covariance matrix, Σ, of the geoposition, all the quantities that enter into calculating the coordinates *X,Y,Z* must have realistic and dependable variances and covariances. These latter values present the image sensor modellers and exploiters with the most challenge. Sensor designers frequently do not provide any reasonable estimates of the expected errors associated with their sensor parameters. For well-calibrated sensors, it is usually reasonable to have the values of the needed sensor parameters as well as their quality.

The quality of the six adjustable SAR parameters can be determined via analytical or empirical methods during a calibration process. Since these parameters are carried as adjustable parameters, it is not critical to have good prior error estimates. These prior values can be approximate since, through the adjustment process, they will be refined through rigorous error propagation associated with least squares adjustment. These updated parameter covariances are, in turn, used in a rigorous propagation to produce the final covariance matrix Σ associated with each object.

For a SAR sensor, the corresponding covariance matrix is given by:

$$\Sigma_{EO} = \begin{bmatrix} \sigma^2_{S_X} & \sigma_{S_X S_Y} & \sigma_{S_X S_Z} & \sigma_{S_X \dot{S}_X} & \sigma_{S_X \dot{S}_Y} & \sigma_{S_X \dot{S}_Z} \\ & \sigma^2_{S_Y} & \sigma_{S_Y S_Z} & \sigma_{S_Y \dot{S}_X} & \sigma_{S_Y \dot{S}_Y} & \sigma_{S_Y \dot{S}_Z} \\ & & \sigma^2_{S_Z} & \sigma_{S_Z \dot{S}_X} & \sigma_{S_Z \dot{S}_Y} & \sigma_{S_Z \dot{S}_Z} \\ & & & \sigma^2_{S_X} & \sigma_{S_X \dot{S}_Y} & \sigma_{\dot{S}_X \dot{S}_Z} \\ & & \text{symmetric} & & \sigma^2_{\dot{S}_Y} & \sigma_{\dot{S}_Y \dot{S}_Z} \\ & & & & & \sigma^2_{\dot{S}_Z} \end{bmatrix} \quad \text{(C.29)}$$

The diagonal elements of the square symmetric non-singular matrix in Formula (C.29) are the variances of the sensor position parameters *(S_X, S_Y, S_Z)* and their corresponding velocities $(\dot{S}_X, \dot{S}_Y \dot{S}_Z)$. The off-diagonal elements of the matrix Σ_{EO}, in Formula (C.29) are the covariances among all six components of the position and velocity.

Covariances will always exist if the image has been processed through either single image resection or as part of multi-image triangulation. For an unprocessed image, Σ_{EO} may simply be a diagonal matrix containing variances, with all off-diagonal elements being zero. On the other hand, for a processed image, Σ_{EO}, will be a full matrix. In fact, for two processed images, i, j, their total covariance matrix Σ_{EO}, will be a 12-by-12 symmetric non-singular matrix of the form:

$$\Sigma_{EOT} = \begin{bmatrix} \Sigma_{EOi} & \Sigma_{EOij} \\ \Sigma^T_{EOij} & \Sigma_{EOj} \end{bmatrix} \quad \text{(C.30)}$$

For a pair of correlated images, the matrix in Formula (C.30) needs to be provided in order to calculate quality measures associated with physical sensor models.

The greatest difficulty is encountered when no adjustability is allowed and the information is based solely on the mission support data. In this case, if the input values for the quality of the parameters are either grossly in error, or non-existent, the propagated geolocation covariance matrix, Σ, can be considerably in error. This is of particular concern when performing Stereo Intersections using SAR, as discussed in C.5.1.3.

Annex D
(informative)

Lidar sensor model metadata profile supporting precise geopositioning

D.1 Introduction

The purpose of this annex is to show how to use metadata defined in this Technical Specification and ISO/TS 19130:2010 to precisely geoposition images from lidar sensor systems. This annex is intended to give an example for using the common terminology and a common frame of reference established in this Technical Specification and ISO/TS 19130:2010 to perform precise geopositioning using a physical lidar sensor model.

D.2 Lidar overview

D.2.1 Overview of lidar sensor types

D.2.1.1 Introduction

LIght Detection And Ranging (lidar) or Laser Detection And Ranging (ladar) refers to a radar system operating at optical frequencies that uses a laser as its photon source. This annex focuses on topographic lidar systems, or systems used to make a map or 3D image of the area of interest. These lidar systems generally measure the travel time, time between a laser pulse emission and when the reflected return is received, and use it to calculate the range (distance) to the objects encountered by the emitted pulse. By combining a series of these ranges with other information such as platform location, platform attitude and pointing data, a three dimensional (3D) scene of the area of interest is generated. Often this scene is stored as a series of 3D coordinates, (X, Y, Z), per return that is called a point cloud. The example is for lidar on an airborne platform. Many variations of lidar systems have been developed. This annex provides a general overview of the technology and gives the reader enough insight into the technology to understand the physical sensor model described later in this document.

D.2.1.2 System components

Although there are many variants of lidar systems, these systems generally consist of a similar set of core components: a ranging subsystem (laser transmitter, laser receiver), a scanning/pointing subsystem, a position and orientation subsystem, a system controller, and data storage. All of these components are critical to the development of a 3D data set. Additionally, when developing the physical model of the lidar system, many of these components have their own coordinate systems as detailed later in this document. The core components of lidar systems are described in Figure D.1.

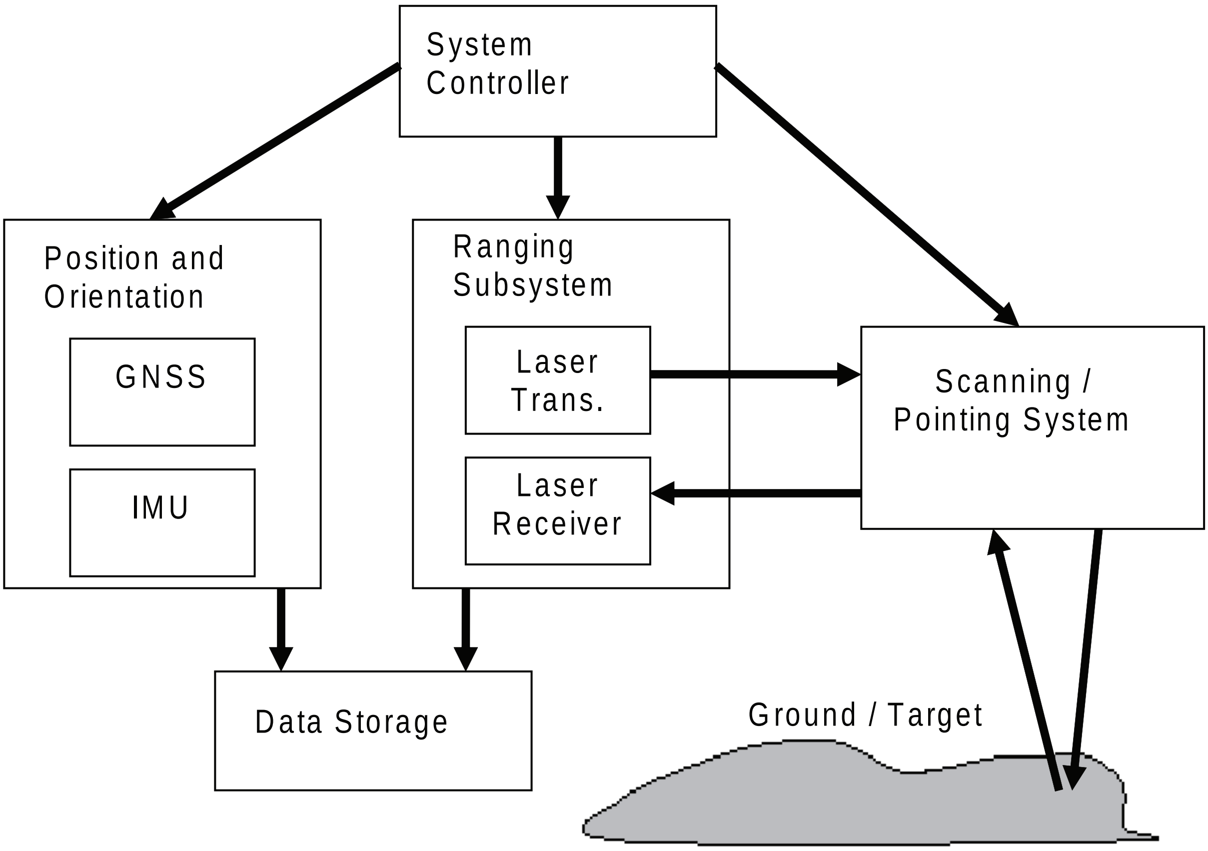

Figure D.1 — Lidar components

D.2.1.3 Ranging subsystem

D.2.1.3.1 Overview

The key component that defines lidar as a unique system is the ranging subsystem. This system consists of a number of subsystems including a laser transmitter and an electro-optical receiver.

The laser transmitter generates the laser beam and emits the laser energy from the system which is then pointed toward the ground by other subsystems. There can be multiple components along the optical path of the laser energy as it is transmitted, including a transmit-to-receive switch, beam expanders, and output telescope optics. Multiple laser types can be used for lidar systems. One common type is neodymium-doped yttrium aluminium garnet. lidar systems are operated at a variety of wavelengths with the most common being 1064 nm (near infrared) for topographic scanners and 532 nm (green) for bathymetric scanners. The selection of the laser wavelength depends upon a variety of factors including: the overall system design, the sensitivity of the detectors being used, eye safety, and the backscattering properties of the target. In addition to the laser wavelength, the laser power is also an important consideration in relation to eye safety.

The electro-optical receiver captures the laser energy that is scattered or reflected from the target and focuses the energy onto a photosensitive detector using the imaging optics. Timestamps from the transmitted and detected light are then used to calculate travel time and therefore range.

Hydrographic lidar systems which typically use green and red lasers for water surface and water bottom detection are not included in this section.

D.2.1.3.2 Ranging techniques

For lidar, one of two ranging principles is usually applied: pulsed ranging or continuous wave.

In pulsed modulated ranging systems, also known as time of flight, the laser emits single pulses of light at high rates of speed (Pulse Repetition Frequency, or PRF). The travel time between the pulse being emitted and then returning to the receiver is measured. This time, along with the speed of light, can be used to calculate the range from the platform to the ground:

$$\text{Range} = R = \frac{1}{2} c \cdot t \tag{D.1}$$

where c is the speed of light and t is the round trip travel time.

In continuous wave systems, the laser transmits a continuous signal. The laser energy is sinusoidally modulated in amplitude and the travel time is directly proportional to the phase difference between the received and the transmitted signal. This travel time is again used with the speed of light to calculate the range from the sensor to the ground.

$$t = \frac{\varphi}{2\pi} \cdot T \tag{D.2}$$

where ϕ is the phase shift and T Is the period of the signal.

Once the travel time (t) is known, the range is calculated as indicated above. To overcome range ambiguities, multiple–tone sinusoidal modulation can be used, where the lowest frequency tone has an ambiguity greater than the maximum range of the system.

An alternative method in continuous wave systems involves modulation in frequency. These chirped systems mix the received signal with the transmitted signal and then use a coherent receiver to demodulate the information encoded in the carrier frequency.

D.2.1.3.3 Detection techniques

Two detection techniques are generally employed in lidar detection systems: direct detection and coherent detection.

In one form of direct detection, referred to as linear mode, the receiver converts the return directly to a voltage or current that is proportional to the incoming optical power. Possible receivers include Avalanche Photo Diodes (APD) and Photo Multiplier Tubes (PMT). lidar detectors (APDs and others) can also be operated in a photon counting mode. When photon counting, the detector is sensitive to very few and possibly individual photons. In a Geiger mode photon counting system, the detector is biased to become sensitive to individual photons. The electronic circuitry associated with the receiver produces a measurement corresponding to the time that a current is generated from an incoming photon, resulting in a direct time of flight measurement.

In coherent detection the received optical signal is mixed with a local oscillator through a heterodyne mixer prior to being focused on the photosensitive element. The mixing operation converts the information to a narrow base band which reduces the noise as compared with the optical filter employed in the direct detection approach. The resultant signal-to noise ratio improvement can be substantial, as in the case with atmospheric turbulence detection systems.

In addition to the methods described above, some systems use alternative detection techniques. One such technique uses the polarization properties of the energy to determine range. As this annex is meant to focus on the lidar geometric sensor model, it will not discuss all possible ranging and detection techniques.

D.2.1.3.4 Flying spot versus array

The sections above describe both ranging techniques and detection techniques that are used in laser scanning. However, these techniques lead to a variety of receiver geometries for collecting the data. In general, most commercial lidar systems operate on a flying spot principle, where for a single outgoing pulse, a small number of ranges (between 1 and 5) are recorded for the returning energy along the same line of sight vector. Receiving and recording more than one range for a given pulse is often referred to as Multiple Returns. The first range measured from a given pulse is often referred to as the “First Return” and the last as the “Last Return.” For the next pulse, the pointing system has changed the line of sight vector, and an additional small number of ranges are recorded. This method (point scanning) is generally associated with linear-mode systems and requires a large return signal to record a return and calculate a range. However, there are other systems (photon counting and others) that spread the outgoing energy to illuminate a larger area on the ground and use a frame array detector to measure a range for each pixel of the array. These systems (frame scanning) require low return signal strength and record hundreds or even thousands of ranges per outgoing pulse. There are pros and cons to both systems, which will not be debated in this document. However, the reader should be aware that both point scanning and frame scanning lidar systems exist. This Annex will address the physical sensor models for both scenarios.

D.2.1.4 Scanning/pointing subsystem

To generate a coverage of a target area, lidar systems must measure range to multiple locations within the area of interest. The coverage of a single instantaneous field of view (IFOV) of the system is not generally adequate to meet this need. Therefore, some combination of platform motion and system pointing is used to develop the ground coverage of a scene. This subclause will describe some of the pointing and scanning concepts that are being employed in current lidar systems.

One of the most common methods for directing the laser energy toward the ground is a scanning mechanism. A popular scanning mechanism is an oscillating mirror which rotates about an axis through a specified angle (the angular field of view) controlling the pointing of the line of sight of the laser energy toward the ground (Figure D.2). The mirror does not rotate completely around the axis, but oscillates back and forth by accelerating and decelerating as it scans from side to side. Oscillating mirrors are generally configured to scan perpendicular to the direction of platform motion, generating a swath width in the cross-track direction and allowing the platform motion to create coverage in the along-track direction. Oscillating mirrors create a sinusoidal scan pattern on the ground.

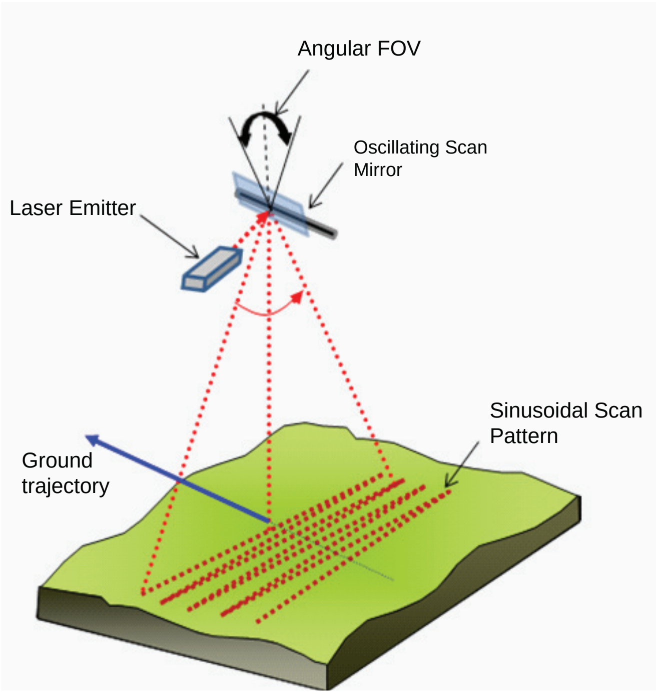

Figure D.2 — Oscillating mirror scanning system

An alternate scanning mechanism is a rotating polygon (Figure D.3). In this system, a multifaceted polygon prism or scan mirror continuously rotates around an axis of rotation. The facets of the polygon combined with its rotation, direct the energy toward the ground. Like the oscillating system, this is generally used to sweep perpendicular to the platform trajectory generating a swath width on the ground and relying on platform motion in the along track direction to generate coverage. However, rather than relying on an oscillating motion requiring accelerations and decelerations, the facet of the polygon controls the pointing of the continuously rotating system. As the laser energy transfers from one polygon facet to the next, there is a discontinuous and sudden jump to the opposite side of the scan resulting in a scan pattern consisting of a series of nearly parallel scan lines.

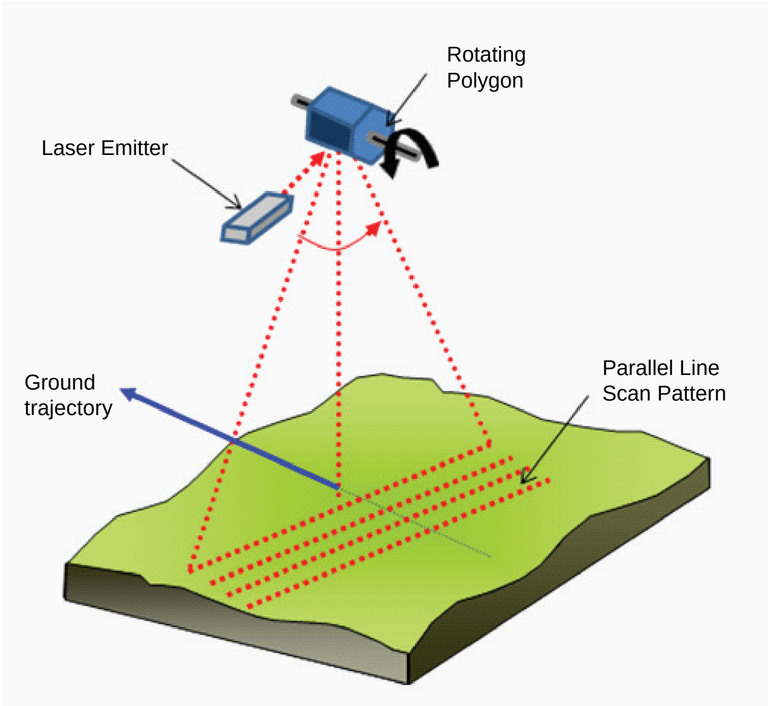

Figure D.3 — Rotating polygon scanning system

Another scanning mechanism uses a nutating mirror which is inclined in reference to the light from the laser emitter (Figure D.4). The rotation of this mirror creates an elliptical scan pattern on the ground and the forward motion of the sensor creates coverage in the along track direction. (A variation on this scanning mechanism employs counter rotating Riesling prisms.)

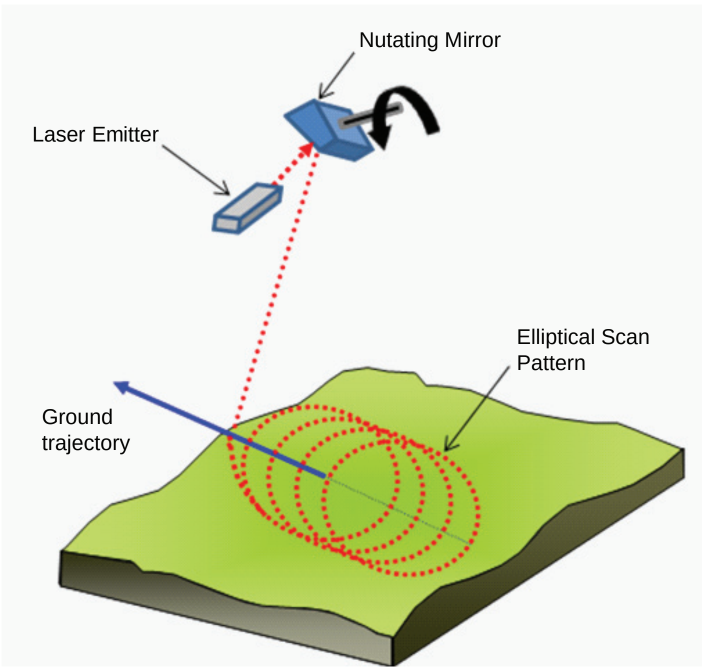

Figure D.4 — Nutating mirror scanning system

As an alternative to using a mechanical scanner, some lidar systems are now using fibre channels to direct the laser energy to the ground (Figure D.5). Their goal is to achieve a more stable scan geometry due to the fixed relationship between the fibre channels and the other lidar components. In this system, the laser light is directed to the ground by a glass fibre bundle and the scan direction for a given pulse depends on the fibre from which it is emitted. A similar system of fibre bundles is then used in the receiving optics.

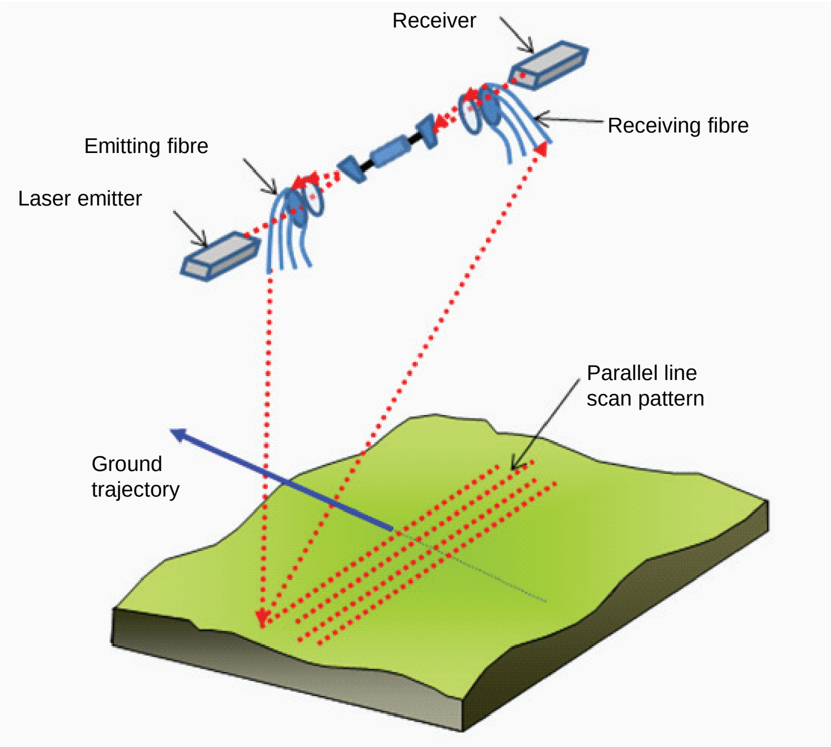

Figure D.5 — Fibre pointing system

D.2.1.4 illustrates several pointing methods, generally using mechanical components that are commonly used on commercial lidar sensors. However, the lidar system could also use a series of gimbals to point the line of sight (Figure D.6). In this case, gimbals are used to rotate the line of sight around various gimbal axes. Multiple gimbal stages (that may or may not be coaxial) are used in series to obtain the desired pointing location. There are many ways that the gimbals could be driven to produce various scan patterns on the ground. The gimbals could be used exclusively to create the desired scan pattern or the gimbals could be used in conjunction with another scanning device. For example, a gimbal could be used to point the entire sensor off nadir, and another scanning system (e.g. oscillating mirror) could then be used to complete the scan pattern and control area coverage (Figure D.7).

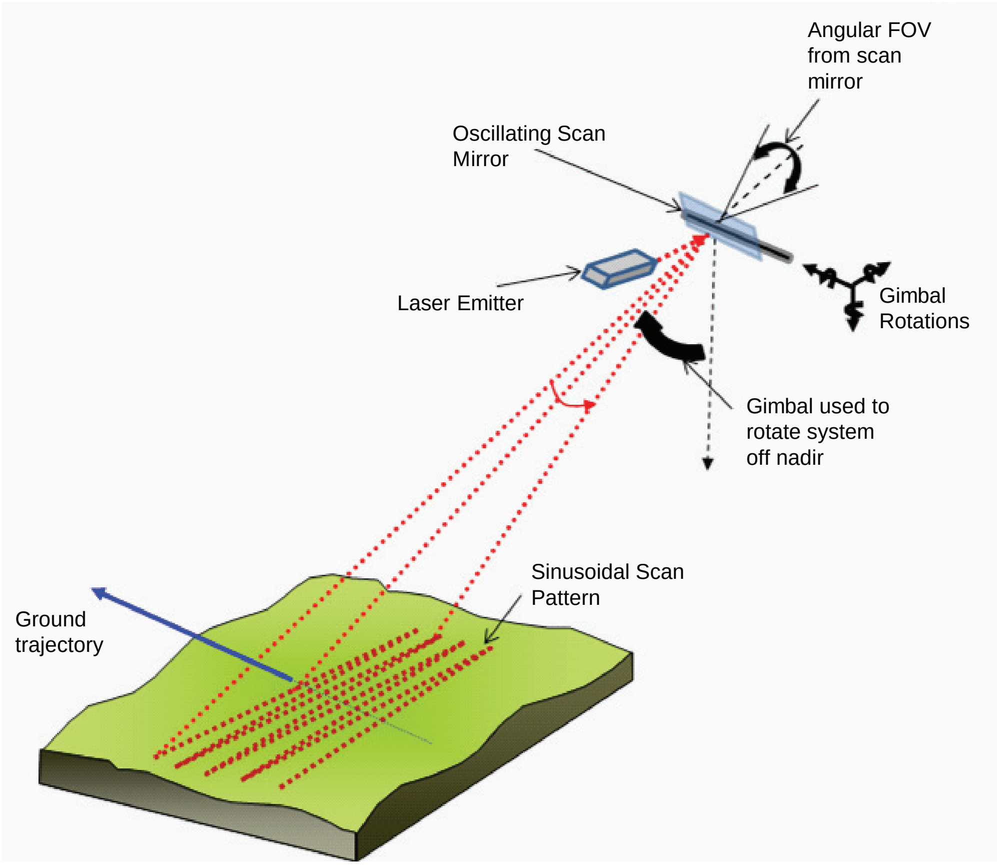

Figure D.6 — Gimbal rotations used in conjunction with oscillating mirror scanning system

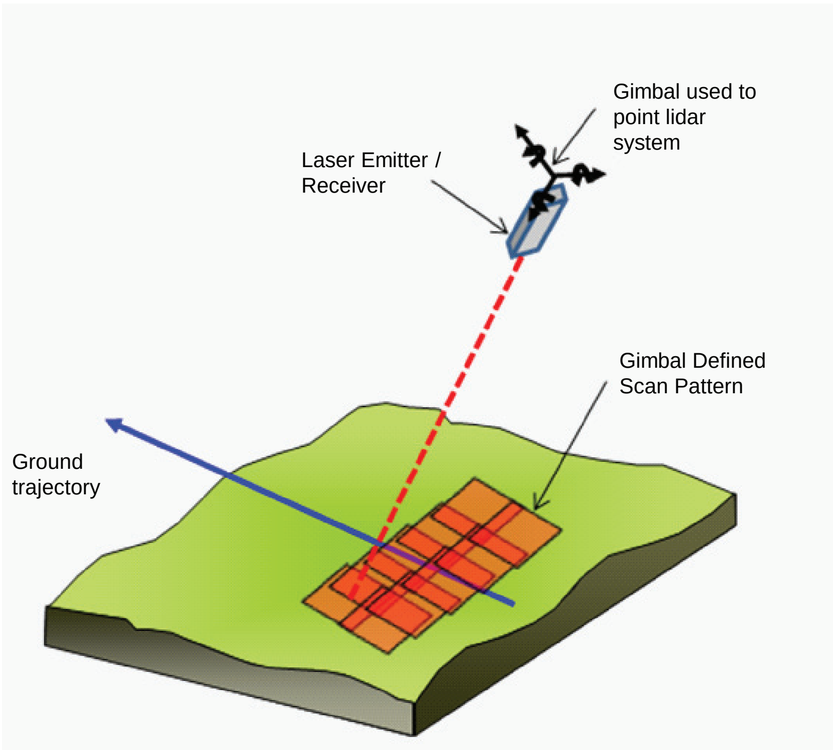

Figure D.7 — Gimbal rotations used to point lidar system

Systems can also be designed with multiple returns for one pulse, for example for a tree canopy. No illustration is given here.

D.2.1.5 Position and orientation subsystem

In the sections above, the hardware used to measure the precise ranges and the techniques used to point and record data off of various locations on the ground were described. However, the information from these systems alone is not enough to generate a three-dimensional point cloud or range image. In addition to knowing how far away the object is (range) and the sensor pointing angles (in relationship to itself), one must also know where the platform carrying the sensor was located and how it was oriented for each incoming pulse. This information is measured and recorded by the position and orientation system. Platform orientation is also applicable for ground moving terrestrial lidar systems.

The position and orientation system consists of two primary subsystems, the GNSS and the inertial measurement unit (IMU). The GNSS is used to record the platform positions at a specified time interval. While there are many methods to develop GNSS coordinates, the accuracies associated with lidar generally require a precise method such as differential post-processing with a static base station or the use of real-time differential updates. For the most accurate data sets, strict constraints are placed on the GNSS base station location and on the allowable baseline separation between the GNSS base station and the kinematic receiver on the platform.

The orientation of the platform is measured by an IMU, which uses gyros and accelerometers to measure the orientation of the platform over time. Both the GNSS and the IMU data are generally recorded during flight. The GNSS and IMU solution will be combined (generally in a post-processing step) to generate the trajectory and attitude of the platform during the data collection.

D.2.1.6 System controller

As shown above, a lidar system consists of many sub-components that must work together to generate a data set. The quality and density of the output product depends on the operation and settings of the subsystems. As the name implies, the system controller provides the user an interface to the system components and coordinates their operation. It allows the operator to specify sensor settings and to monitor the operation of the subsystems.

D.2.1.7 Data storage

Raw lidar data includes files from the GNSS, the IMU, the ranging unit, and possibly other system components. Even in its raw state, lidar systems can generate massive quantities of data. Due to the quantities of data, the data sets are often stored with the system and downloaded after collection. The Data Storage Unit is used to store the data from all of the system components.

D.2.2 Lidar data processing levels

D.2.2.1 Introduction

Several processing steps are necessary to create a useable “end product” from raw lidar data. However, the resultant form of the data at intermediate processing steps may be of use to different groups within the community. In order to classify the degree of lidar processing applied to a given data set, the lidar community has initiated defining multiple lidar data processing levels. Each level describes the *processing state* of the data. Following are definitions of the levels (L0 through L5), along with basic descriptions of the processing involved between levels and the types of users to which each level would apply.

D.2.2.2 Level 0 – Raw data and metadata

Level 0 (L0) data consists of the raw data in the form in which it is stored in as collected from the mapping platform. The data set includes, but is not limited to, data from GNSS, Inertial Navigation System (INS), laser measurements (timing, angles) and gimbal(s). Metadata would include items such as the sensor type, date, calibration data, coordinate frame, units and geographic extents of the collection. Other ancillary data would also be included, such as GNSS observations from nearby base stations. Typical users of L0 data would be sensor builders, data providers, and researchers looking into improving the processing of L0 to Level 1 (L1) data.

D.2.2.3 Level 1 – Unfiltered 3D point cloud

L1 data consists of a 3D point data (point cloud) representation of the objects measured by the lidar mapping system. It is the result of applying algorithms (from sensor models, Kalman filters, etc.) in order to project the L0 data into 3 dimensional space. All metadata necessary for further processing is also carried forward at this level. Users would include scientists and others working on algorithms such as filtering or registration for deriving higher-level data sets

D.2.2.4 Level 2 – Noise-filtered 3D point cloud

Level 2 (L2) data differs from L1 in that noisy, spurious data has been removed (filtered) from the data set, intensity values have been determined for each 3D point (if applicable), and relative registration (among scans, stares or swaths) has been performed [11] . The impetus behind separating L1 from L2 is the nature of Geiger-mode lidar data. Derivation of L1 Geiger-mode lidar data produces very noisy point clouds, which require specialized processing (*coincidence processing*) to remove the noise. Coincidence processing algorithms are still in their infancy, so their ongoing development necessitates a natural break in the processing levels. As with L1, all metadata necessary for further processing is carried forward. Typical users include exploitation algorithm developers and scientists developing georegistration techniques.

D.2.2.5 Level 3 – Georegistered 3D point cloud

Level 3 (L3) data sets differ from L2 in that the data has been registered to a known geodetic datum. Registration may be by an adjustment using data-identifiable objects of known geodetic coordinates or by some other method of control extension for improving the absolute accuracy of the data set. The primary users of L3 data would be exploitation algorithm developers.

D.2.2.6 Level 4 – Derived products

Level 4 (L4) data sets represent lidar-derived products to be disseminated to standard users. These products could include DEMs, viewsheds, or other products created in a standard format and using a standard set of tools. These data sets are derived from L1, L2 or L3 data, and are used by the basic user.

D.2.2.7 Level 5 – Intel products

Level 5 (L5) data sets are a type of specialized product for users in the intelligence community, which may require specialized tools and knowledge to generate. The data sets are derived from L1, L2 or L3 data.

D.3 Coordinate reference systems

D.3.1 Introduction

A sensor model uses measurements from various system components to obtain geographic coordinates of the sensed objects. However, the system components are not centred nor aligned with a geographic coordinate system. The reference frame of each component and their interrelationships must be understood to obtain geographic coordinates of a sensed object. The following sections will define these coordinate systems and their interrelationships.

D.3.2 General coordinate reference system considerations

The purpose of a sensor model is to develop a mathematical relationship between the position of an object on the Earth's surface and its data as recorded by a sensor. The spatial positions of the sensor during data collection may be given, at least initially or in its raw form, either in relation to a coordinate system locally defined or relative to an Earth reference. A 3-dimensional datum will be required to define the origin and orientation of the coordinate systems. Likewise, the positions of the objects may be defined with respect to either the same coordinate system, or attached to any number of Earth-based datums (e.g. WGS84). For purposes of this metadata profile, the transformations among the coordinate systems will be accomplished via a sequence of translations and rotations of the sensor's coordinate system origin and axes until it coincides with an Earth-based coordinate system origin and axes. An overall view of some of the coordinate reference systems under consideration is shown in Figure D.8

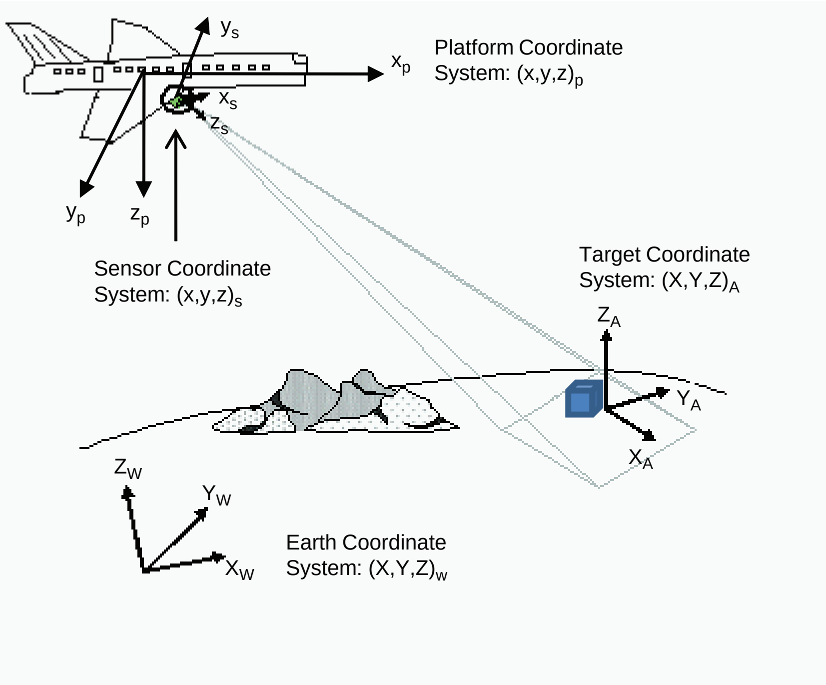

Figure D.8 — Multiple coordinate reference systems

The sensor position may be described in many ways and relative to any number of coordinate systems particularly those of the aerial platform. There may also be one or more gimbals to which the sensor is attached, each with its own coordinate system, in addition to the platform's positional reference to the Global Navigational Satellite System (GNSS) or other onboard INS. Transformations among coordinate systems can be incorporated into the mathematical model of the sensor.

Airborne platforms normally employ GNSS and INS systems to define position and attitude. As illustrated in Figure D.9 the GNSS antenna and the INS gyros and accelerometers typically are not physically embedded with the sensor.

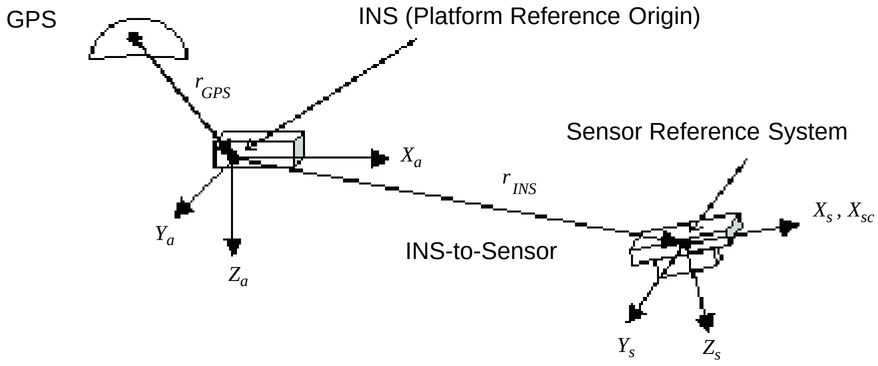

Figure D.9 — Nominal relative GNSS to INS to sensor relationship

For a GNSS receiver, the point to which all observations refer is the phase centre of the antenna. The analogous point for an INS is the intersection of the three sensitivity axes. The physical offset between the two generally is termed a lever arm. Denoting the lever arm vector from the GNSS antenna phase centre to the IMU is the vector r_{GNSS}. An analogous lever arm between the INS and the sensor is labelled r_{INS}. These relationships are illustrated in Figure D.9

D.3.3 Scanner coordinate reference system

This system describes the reference frame of the scanner during a laser pulse firing. The origin of this system is located at the laser firing point. The system axes are defined as follows: z-axis (z_{SC}) positive is aligned with the laser pulse vector; with scan angles set to zero, x-axis (x_{SC}) positive is aligned with the Sensor Reference System x-axis, described below and y-axis (y_{SC}) positive is chosen to complete a right-handed Cartesian system. Non-zero scan angles will cause the x-axis and/or the y-axis to deviate from alignment with the sensor reference system.

D.3.4 Sensor coordinate reference system

This system describes the reference frame of the sensor in which the scanner operates. The scanner reference system rotates within this system as the scan angles change, and is coincident with this system when scan angles are zero. The origin of this system is located at the laser firing point. The system axes (Figure D.9) are defined as follows: z-axis (z_S) positive is nominally aligned with the nadir, although this could depend on the mount configuration; x-axis (x_S) positive is a chosen direction in the scanner plane (orthogonal to the z-axis), which is nominally aligned with the flight direction when no z-rotation is applied to the gimbals, and y-axis (y_S) positive is chosen to complete a right-handed Cartesian system.

D.3.5 Gimbal coordinate reference system

This system describes the reference frame of a gimbal, which houses the sensor and orients it depending on applied gimbal angles. The origin of this system is located at the intersection of the gimbal axes. With gimbal angles set to zero, the gimbal axes are defined as follows: x-axis (x_{GIM}) positive is nominally aligned with the flight direction; y-axis (y_{GIM}) positive is in the horizontal plane, orthogonal to the x-axis pointing to out the right side of the aircraft; and z-axis (z_{GIM}) positive points downward, completing a right-handed Cartesian system. Multiple gimbals or gimbal stages may be used in a system, and the axes may not be coaxial. Therefore multiple gimbal reference systems may be defined.

D.3.6 Platform coordinate reference system

This system describes the reference frame of the aircraft platform to which the gimbal is mounted. The origin is located at the aircraft centre of navigation (i.e. the INS centre of rotation). The axes are defined as follows: x-axis (x_P) positive along the heading of the platform, along the platform roll axis; y-axis (y_P) positive in the direction of the right wing, along the pitch axis; z-axis (z_P) positive down, along the yaw axis. Any rotational differences between the gimbal reference system and the platform reference system describe the rotational boresight (or mounting) angles, which are fixed for a given system installation.

D.3.7 Local-vertical coordinate reference system

This system describes the reference frame with respect to the local vertical. Coordinates in this system are obtained by applying INS measurements to coordinates in the Platform Reference System. The origin is located at the aircraft centre of navigation (i.e. the INS centre of rotation). The axes are defined as follows: z-axis (z_a) positive points downward along the local gravity normal; x-axis (x_a) positive points toward astronomic north; y-axis (y_a) positive points east, completing a right-handed Cartesian system.

The platform reference system is related to the local-vertical reference system with its origin at the centre of navigation. In horizontal flight, the platform z-axis is aligned with the local gravity normal. The platform reference system orientation stated in terms of its physical relationships (rotations) relative to this local-vertical reference (Figure D.10) is as follows:

— Platform heading – horizontal angle from north to the platform system x-axis X_a (positive from north to east).

— Platform pitch – angle from the local-vertical system horizontal plane to the platform positive x-axis X_a (positive when positive x-axis is above the local-vertical system horizontal plane, or nose up).

— Platform roll – rotation angle about the platform x-axis; positive if the platform positive y-axis Y_a lies below the local-vertical system horizontal plane (right wing down).

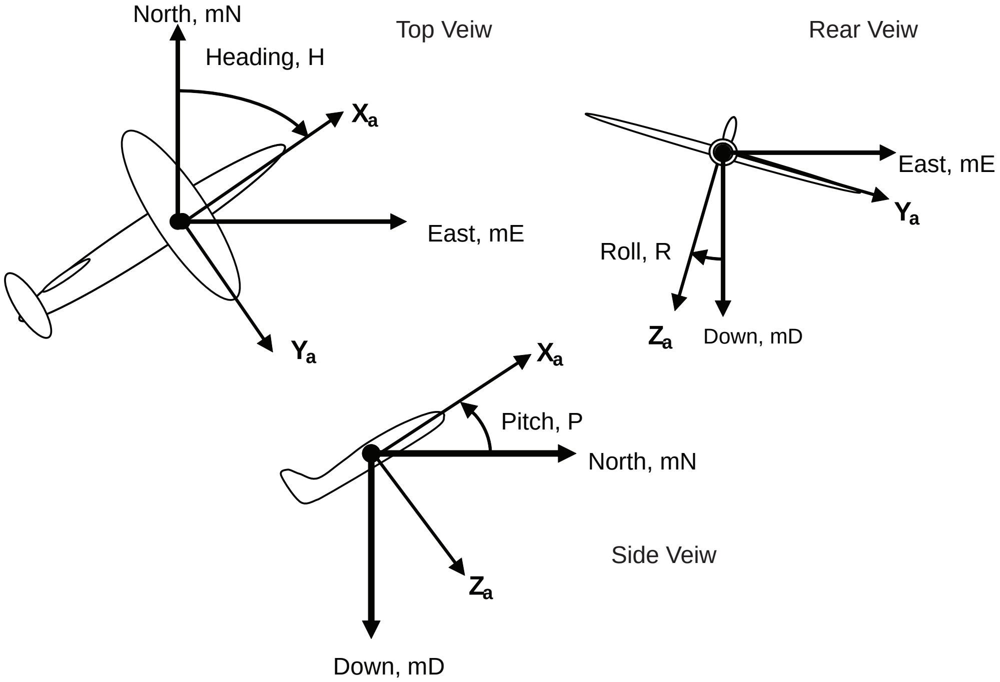

Figure D.10 — Relationship between platform reference system (XaYaZa) and local-vertical system

D.3.8 Ellipsoid-tangential (NED) coordinate reference system

This system describes the North-East-Down (NED) reference frame with the horizontal plane tangent to the geodetic ellipsoid to be referenced (i.e. WGS84). Coordinates in this system are obtained by applying deflection of the vertical (DOV) estimates to coordinates in the Local-vertical Reference System. The origin is located at the phase-centre of the GNSS antenna, fixed to the platform structure. The axes are defined as follows: z-axis positive points downward along the ellipsoidal normal; x-axis positive points toward geodetic north; y-axis positive points east, completing a right-handed Cartesian system.

D.3.9 ECEF coordinate reference system

This system describes the Earth-centred Earth-Fixed (ECEF) reference frame of the geodetic ellipsoid to be referenced (i.e. WGS84). GNSS measurements refer to this system. The origin is located at the origin of the geodetic ellipsoid. The axes are defined as follows: z-axis positive points along Earth's rotational axis toward geodetic north; x-axis positive points toward the 0-degree longitudinal meridian; y-axis positive completes a right-handed Cartesian system. The relationship between the NED reference system and the ECEF reference system is illustrated in Figure D.11

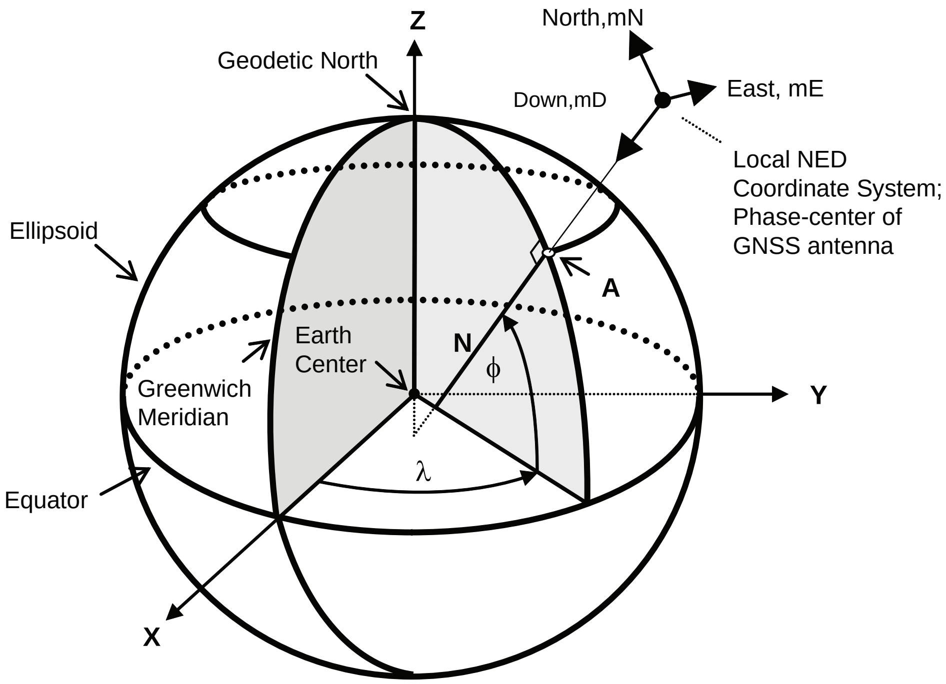

Key

ϕ latitude

λ longitude

Figure D.11 — ECEF and NED coordinate systems

Any point may be described in geocentric (X,Y,Z) coordinates, or alternatively in the equivalent geodetic latitude, longitude and ellipsoid height terms. Also, a point can be described relative to a local reference system with origin on an Earth-related ellipsoidal datum (e.g. WGS84 ellipsoid), specifically in an East-North-Up (ENU) orientation; where North is tangent to the local prime meridian and points North, Up points upward along the ellipsoidal normal, and East completes a right-hand Cartesian coordinate system. Figure D.12 shows an ENU system and its relationship to an ECEF system.

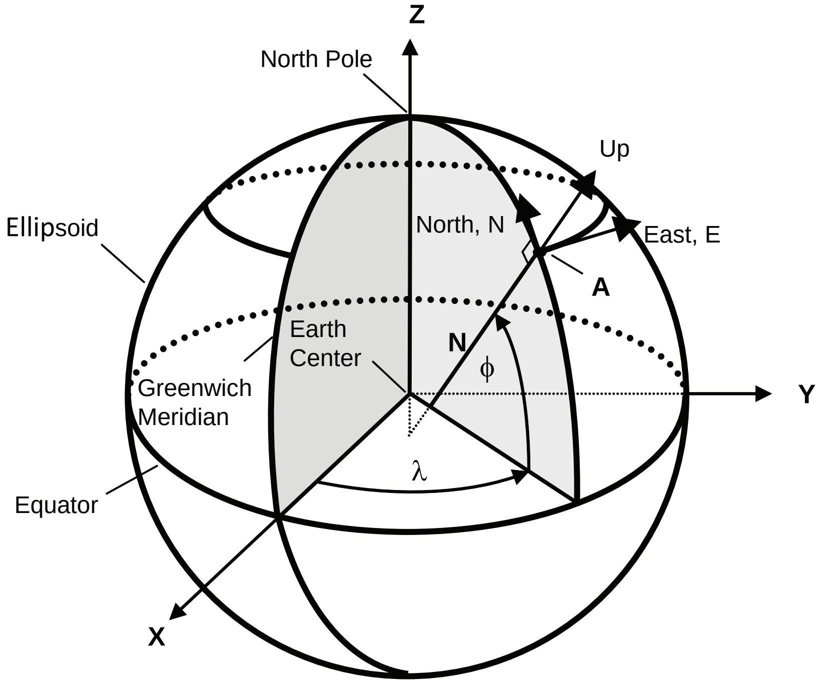

Key

ϕ latitude

λ longitude

Figure D.12 — Earth-centred (ECEF) and local surface (ENU) coordinate systems (MIL-STD-2500C)

D.4 Sensor equations

D.4.1 Introduction

This clause outlines the equations representing the spatial relationships among the various components of a lidar collection system. Equations particular to point-scanning systems are described first, followed by equations particular to frame-scanning systems.

D.4.2 Point-scanning systems

D.4.2.1 General

The relationships among some basic components of a lidar collection system are illustrated in Figure D.13 including the GNSS, INS and sensor. The phase-centre of the GNSS antenna provides the connection to the ECEF reference datum (e.g. WGS84). A series of translations and rotations, obtained from sensor observations and constants, must be applied to a lidar pulse measurement for direct geopositioning of the sensed ground object.

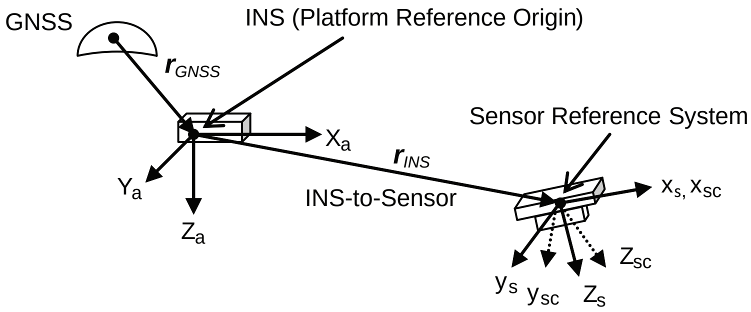

Figure D.13 — Nominal Relative GNSS to INS to sensor to scanner relations

The coordinates of a sensed ground point in a geocentric ECEF coordinate system (e.g. WGS84) are obtained from the following equation:

$$r_{EP} = r_{ECEF} + M_{ECEF} M_{ELL} M_{VER} (M_{PLA} (M_{GIM} M_{SEN} r_{SCA} + r_{GIM}) + r_{INS} + r_{GPS}) \quad \text{(D.3)}$$

The components of Formula (D.3) are described below:

r_{SCA} vector from the scanner to the ground point in the scanner reference frame (range);

r_{GIM} vector from the sensor to the gimbal centre of rotation in the gimbal reference frame;

r_{INS} vector from the INS to the gimbal centre of rotation in the platform reference frame;

r_{GPS} vector from the GNSS antenna phase-centre to the INS in the platform reference frame;

r_{ECEF} vector from the ECEF origin to the GNSS antenna phase-centre in the ECEF reference frame (GNSS observations);

r_{EP} vector from the ECEF origin to the ground point in the ECEF reference frame;

M_{SEN} rotation matrix from scanner reference frame to sensor reference frame (scan angles);

M_{GIM} rotation matrix from the sensor reference frame to the gimbal reference frame (gimbal angles);

M_{PLA} rotation matrix from the gimbal reference frame to the platform reference frame (bore-sight angles);

M_{VER} rotation matrix from the platform reference frame to the local vertical reference frame (INS observations);

M_{ELL} rotation matrix from the local vertical reference frame to the ellipsoid-tangential reference frame;

M_{ECEF} rotation matrix from the ellipsoid-tangential reference frame to the ECEF reference frame.

The components r_{INS}, r_{GPS} and M_{GIM} are constants which are measured at system installation or determined by system calibration.

The vector r_{SCA} does not account for any internal laser propagation within the system, both before the laser is emitted or after it is detected. It is assumed that any such offsets are accounted for by the hardware or processing software in order to provide a measurement strictly from the scanner to the ground point.

Other system component configurations are possible which would alter Formula (D.3). Some systems have the INS mounted on the back of the sensor, which would cause r_{GPS} to vary with the gimbal settings. In this case, the *distance* from the INS to the gimbal rotational centre would be constant, and a vector (constant) from the GNSS antenna to the gimbal rotational centre would be needed.

D.4.2.2 Atmospheric refraction

Light rays passing through media with differing refractive indices are refracted according to Snell's Law. This principle applies to laser beams passing downward through the atmosphere, as the refractive index of the atmosphere changes with altitude. The effect is an angular displacement of the laser beam as described below:

$$\Delta d = K \tan\alpha \tag{D.4}$$

where

Δd is the angular displacement of the laser beam from the expected path;

α is the the angle of the laser beam from vertical;

K is a constant, defined below.

Several models are available to determine the constant K; however, one commonly used approach, is provided below [10]. (Another approach is given in [3]). Using this first model, the constant K is determined as follows:

$$K = \frac{2410H}{H^2 - 6H + 250} - \frac{2410h}{h^2 - 6h250}\left(\frac{h}{H}\right) \tag{D.5}$$

where

H is the flying height (MSL) of the aircraft, in kilometres

h is the height (MSL) of the object the laser intersects, in kilometres.

Applying H and h in kilometres, the resulting units for the constant K are microradians.

Since the angle α is relative to vertical, it can be derived from Formula (D.3) using a chain of rotation matrices $(M_{VER}M_{PLA}M_{GIM}M_{SEN})$. Then the calculation of Δd is applied to M_{VER}, resulting in a new value, M'_{VER}, which is substituted into Formula (D.3).

The above equations are appropriate for most mapping scenarios; however, at very large oblique vertical angles (>60°) a spherically stratified model should be applied (Gyer, 1996). Snell's law for a spherically stratified model is represented by the following:

$$n_s r_s \sin(\alpha_s) = n_g r_g \sin(\alpha_g) = k = \text{constant} \tag{D.6}$$

where

n_s, n_g index of refraction at sensor and ground point, respectively;

r_s, r_g ellipsoid height of sensor and ground point, respectively;

α_s, α_g the angle of the laser beam from vertical at the sensor and ground point, respectively.

The angular displacement Δd is obtained from the following equation:

$$\tan \Delta d = \frac{t\alpha n\alpha\left((r_s / r_g) - \cos\theta\right) - \sin\theta}{t\alpha n\alpha \sin\theta + (r_s / r_g) - \cos\theta} \tag{D.7}$$

where

Δd angular displacement of the laser beam from the expected path;

α angle of the laser beam from vertical;

r_s height of the scanner above centre of sphere (approximating ellipsoid curvature);

r_g height of the illuminated ground point above centre of sphere;

θ angle subtended at the centre of sphere, from the scanner to the ground point.

The value for θ is determined from the integral

$$\theta = \int_{h_g}^{h_s} \frac{k}{r\sqrt{n^2 r^2 - k^2}} dh \tag{D.8}$$

where h_s and h_g are the ellipsoid heights at the sensor and ground point, respectively. The value of θ can be estimated using numerical integration (see Gyer, 1996). The value for n can be computed from

$$n \approx 1 + 0{,}000078831 \frac{P}{T} \tag{D.9}$$

where T (temperature) and P (pressure) are in degrees Kelvin and millibars, respectively. Finally, if local measurements are not available, the values of T and P can be calculated from the following:

$$T = 59 - 0{,}00356h \tag{D.10}$$

$$P = 2116[(T + 459{,}7) / 518{,}6]^{5{,}256} \tag{D.11}$$

where T is in degrees Fahrenheit, P is in lbs/sq ft and h (altitude) is in feet.

D.4.3 Frame-scanning systems

D.4.3.1 General

Frame-scanning lidar systems use the same basic system components as point-scanning systems (Figure D.13); however, the receiver consists of an array of detector elements (similar to an imaging system) rather than a single detector. This different receiver geometry is described by its own coordinate system and has inherent geometric and optical effects which must be accounted for. Following is a description of the frame coordinate system, the corrections necessary for a frame system, and the resulting sensor modeling equations. Much of the information in this clause was obtained from Annex D of ISO/TS 19130.

D.4.3.2 Frame coordinate system

D.4.3.2.1 Frame Imagery

A frame sensor is a digital collection array consisting of a matrix of detectors, or elements, at the focal plane (Figure D.14). The focal plane array (FPA) origin is located at the intersection of the sensor optical axis and image plane.

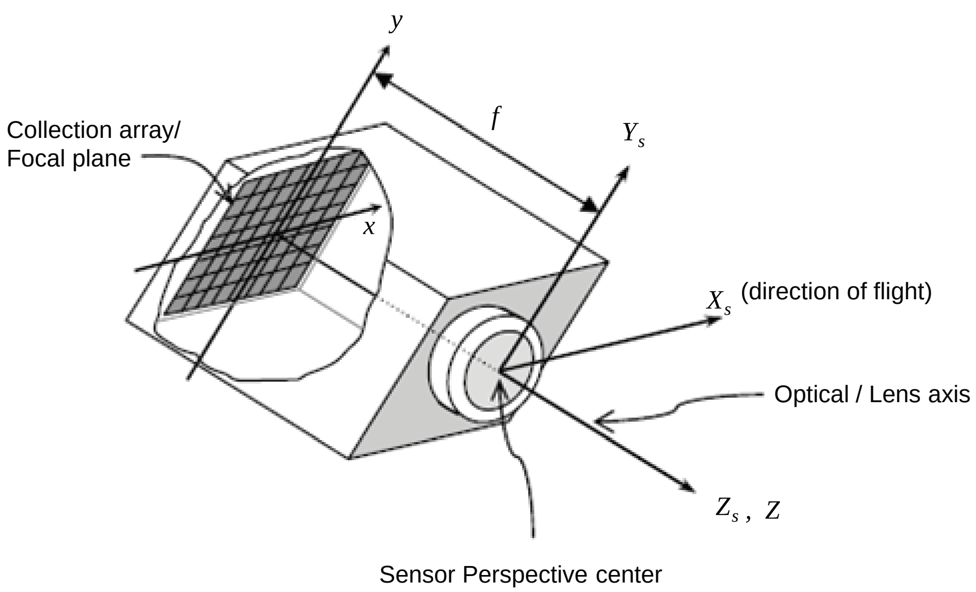

Figure D.14 — Sensor and focal plane coordinate systems

Typical of common imagery formats, and in particular ISO/IEC 12087-5, pixels are indexed according to their placement within a “Common Coordinate System” (CCS), a two-dimensional array of rows and columns, as illustrated in the array examples in Figure D.15. There are three commonly referred to coordinate systems associated with digital and digitized imagery: row, column (r, c), line, sample (ℓ,s), and x,y. The units used in the first two systems are pixels, while the x, y are linear measures such as millimetres. The origin of the CCS (and the line/sample system), as shown in Figure D.15, is the upper left corner of the first (or 0,0) pixel, which in turn is the upper left of the array. Because the CCS origin is the pixel corner, and the row/column associated with a designated pixel refers to its centre, the coordinates of the various pixels, (0.5, 0.5), (0.5, 1.5), etc., are not whole integers.

D.4.3.2.2 Row-Column to Line-Sample coordinate transformation

Typical frame processing uses the geometric centre of the image as the origin. As shown in Figure D.15, the origin of the row-column system is located in the upper-left corner of the array, and the origin of the line-sample system is in the centre of the array. The positive axes of the systems are parallel and point in the same direction, so conversion between the two systems is attained by applying simple translation offsets:

$$\ell = r - C_\ell \tag{D.12}$$

$$s = c - C_s \tag{D.13}$$

where C_ℓ and C_s are each half the array size, in pixels, in the row and column directions, respectively.

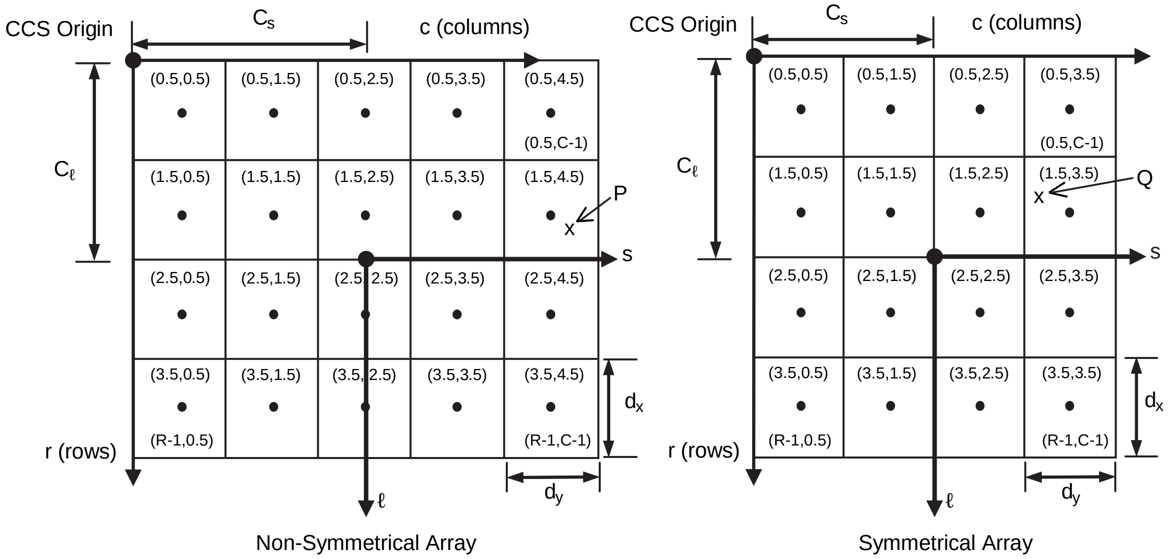

Figure D.15 — Coordinate systems for non-symmetrical and symmetrical arrays

D.4.3.3 Frame corrections

D.4.3.3.1 Kinds of corrections

Corrections to the interior of the frame system, including array distortions, principal point offsets and lens distortions, and exterior corrections such as atmospheric refraction, are described in the following sections.

D.4.3.3.2 Array distortions

Distortions in the array are accounted for by the following equations:

$$x = a_1\ell + b_1 s + c_1 \tag{D.14}$$

$$y = a_2\ell + b_2 s + c_2 \tag{D.15}$$

This transformation accounts for two scales, a rotation, skew, and two translations. The resulting x and y values are typically in millimetre units. The six parameters (a_1, b_1, c_1, a_2, b_2, c_2) are usually estimated on the basis of (calibrated) reference points, such as corner pixels for digital arrays. The (x,y) image coordinate system, as shown in Figure D.16, is used in the further construction of the mathematical model.

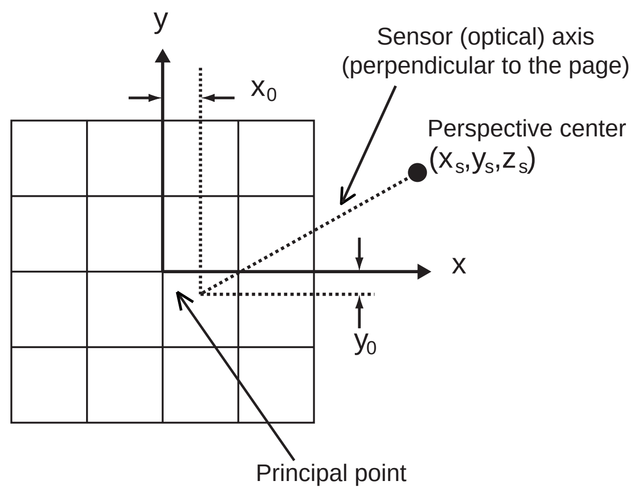

Figure D.16 — (x,y) Image coordinate system and principal point offsets

D.4.3.3.3 Principal point offsets

Ideally the sensor (lens) axis would intersect the collection array at its centre coordinates (x = 0,y = 0). However, this is not always the case due to lens flaws, imperfections, or design, and is accounted for by offsets x_0 and y_0, as shown in Figure D.16. The ground coordinates x_0 and y_0 are in the same linear measure units (e.g. mm) as the image coordinates (x, y) and the focal length, *f*. For most practical situations, the offsets are very small, and as such there will be no attempt made to account for any covariance considerations for these offset terms.

D.4.3.3.4 Lens distortions

Radial lens distortion is the radial displacement of an imaged point from its expected position. Figure D.17 illustrates this distortion and its *x* and *y* image coordinate components. Calibration procedures are employed to determine radial lens distortion, and it is typically modelled as a polynomial function of the radial distance from the principal point, as provided below:

$$\delta r = k_1 r^3 + k_2 r^5 + k_3 r^7 \delta r = k_1 r^3 + k_2 r^5 + k_2 r^7 \tag{D.16}$$

where

$$r = \sqrt{\bar{x}^2 + \bar{y}^2} \qquad \bar{x} = x - x_0 \qquad \bar{y} = y - y_0 \tag{D.17}$$

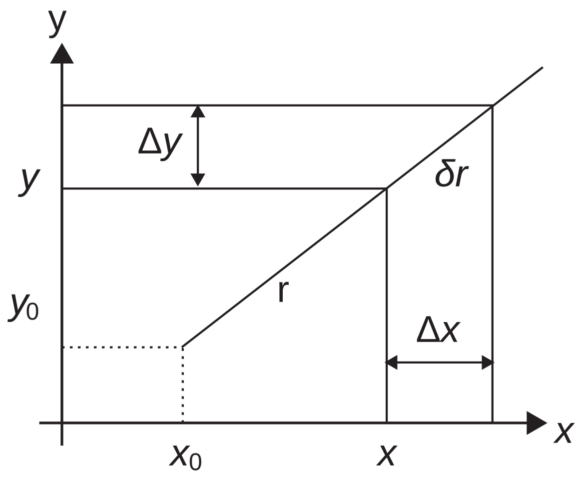

Figure D.17 — Radial lens distortion image coordinate components

The effect of radial lens distortion on the x and y image coordinate components is:

$$\Delta x_{radial} = \bar{x}\frac{\delta r}{r} = \bar{x}\frac{k_1 r^3 + k_2 r^5 + k_3 r^7}{r} = \bar{x}(k_1 r^2 + k_2 r^4 + k_3 r^6) \quad \text{(D.18)}$$

$$\Delta y_{radial} = \bar{y}\frac{\delta r}{r} = \bar{y}\frac{k_1 r^3 + k_2 r^5 + k_3 r^7}{r} = \bar{y}(k_1 r^2 + k_2 r^4 + k_2 r^6) \quad \text{(D.19)}$$

Another lens correction is decentring (or tangential lens distortion), which is caused by errors in the assembly of the lens components and affects its rotational symmetry (Mikhail et al.). This correction is typically insignificant, although it can be more prominent in variable focus or zoom lenses. The *x* and *y* image coordinate components of decentring are commonly modelled by the following equations:

$$\Delta x_{dec} = p_1(2\bar{x}^2 + r^2) + p_2(2\overline{xy}) \quad \text{(D.20)}$$

$$\Delta y_{dec} = p_1(2\overline{xy}) + p_2(2y^2 + r^2) \quad \text{(D.21)}$$

where p_1 and p_2 are decentring coefficients derived from calibration. Combining lens corrections to image coordinates from radial lens distortion [Formulae (D.18) and (D.19)], and decentring [Formulae (D.20) and (D.21)], results in the following:

$$\Delta x_{lens} = \Delta x_{radial} + \Delta x_{dec} = \bar{x}(k_1 r^2 + k_2 r^4 + k_3 r^6) + p_1(2\bar{x}^2 + r^2) + p_2(2\overline{xy}) \quad \text{(D.22)}$$

$$\Delta y_{lens} = \Delta y_{radial} + \Delta y_{dec} = \bar{y}(k_1 r^2 + k_2 r^4 + k_3 r^6) + p_1(2\overline{xy}) + p_2(2\bar{y}^2 + r^{2)} \quad \text{(D.23)}$$

D.4.3.3.5 Atmospheric refraction

The principle of atmospheric refraction for a frame-scanning system is the same as that given by Formula (D.4) and Formula (D.5) for the point-scanning system. However, the frame receiver geometry causes the application of the correction to be similar to that for radial lens distortion. Given Formulae (D.2) and (D.3), the corrected *x* and *y* image coordinates are shown below:

$$x'_{atm} = \bar{x}\frac{r'_{atm}}{r} \quad \text{(D.24)}$$

$$y'_{atm} = \bar{y}\frac{r'_{atm}}{r} \quad \text{(D.25)}$$

where

$$r = \sqrt{\bar{x}^2 + \bar{y}^2} \quad \text{(D.26)}$$

$$\bar{x} = x - x_0 \quad \text{(D.27)}$$

$$\bar{y} = y - y_0 \quad \text{(D.28)}$$

and

$$r'_{atm} = f\tan(\alpha + \Delta d) \quad \text{(D.29)}$$

Therefore the image coordinate corrections are:

$$\Delta x_{atm} = x'_{atm} - \bar{x} = \bar{x}\left(\frac{r'_{atm}}{r} - 1\right) \quad \text{(D.30)}$$

$$\Delta y_{atm} = y'_{atm} - \bar{y} = \bar{y}\left(\frac{r'_{atm}}{r} - 1\right) \quad \text{(D.31)}$$

A spherically stratified model [Formula (D.7)] is needed for highly oblique (>60°) vertical angles. For this formulation, first the image coordinates of the nadir point are calculated using

$$x_n = -f\frac{m_{13}}{m_{33}}$$

$$y_n = -f\frac{m_{13}}{m_{33}}$$

where m_{13}, m_{23} and m_{33} are the rotation matrix components of

$$M = \begin{bmatrix} M_{11} & M_{12} & M_{13} \\ M_{21} & M_{22} & M_{23} \\ M_{31} & M_{32} & M_{33} \end{bmatrix}$$

Formula (D.44) from the sensor to ECEF reference frames. The distance from the image nadir coordinates to the imaged object coordinates $\bar{x}$, $\bar{y}$ is calculated from the following:

$$a=\sqrt{(x_n-\bar{x})^2+(y_n-\bar{y})^2}$$

and the component of that distance attributed to the atmospheric refraction is estimated by

$$\delta\alpha \approx \alpha\left(cot\alpha - cot(\beta+\alpha)\right)\Delta d$$

where α is the angle of the laser beam from vertical and Δ*d* is obtained using (4.4). The value of *β* is obtained using

$$\beta = cos^{-1}\left(\frac{x_n(x_n-\bar{x})+y_n(y_n-\bar{y})}{\sqrt{x_n^2+y_n^2+f^2}\sqrt{(x_n-\bar{x})^2+(y_n-\bar{y})^2}}\right)$$

The resulting image coordinate corrections are:

$$\Delta x_{atm} = -\frac{x_n - x}{\alpha}\delta\alpha$$

$$\Delta y_{atm} = -\frac{y_n - y}{\alpha}\delta\alpha$$

Combining the above atmospheric refraction corrections with the lens corrections (4.14, 4.15) results in the following corrected values (x', y') for the image coordinates:

$$x' = \bar{x} + \Delta x_{lens} + \Delta x_{atm} \tag{D.32}$$

$$y' = \bar{y} + \Delta y_{lens} + \Delta y_{atm} \tag{D.33}$$

Taking into account all the image coordinate corrections needed for a frame-scanning system, if given pixel coordinates (r,c), corrected image coordinates would be calculated using Formula (D.45), Formula (D.46), Formula (D.47), Formula (D.48), Formula (D.41) and Formula (D.42).

D.4.3.4 Frame-scanner sensor equation

The frame-scanner sensor equation takes on a similar form to Formula (D.3) for the point-scanner sensor. However, the value of r_{SCA} (the range vector) must be adjusted to account for the frame geometry. The value will be a function of the corrected image coordinates (x', y'), the focal length and the measured range from the ground point to the receiver focal plane.

Consider the example shown in Figure D.18, a lidar frame-scanning measurement of the ground point A produces an imaged point a at the receiver focal plane, with coordinates (x', y'). This results in a measured range represented by *R*, while *f* is the focal length and L is the location of the lens front nodal point. The value *r* is defined as follows:

$$r=\sqrt{(x')^2+(y')^2} \tag{D.34}$$

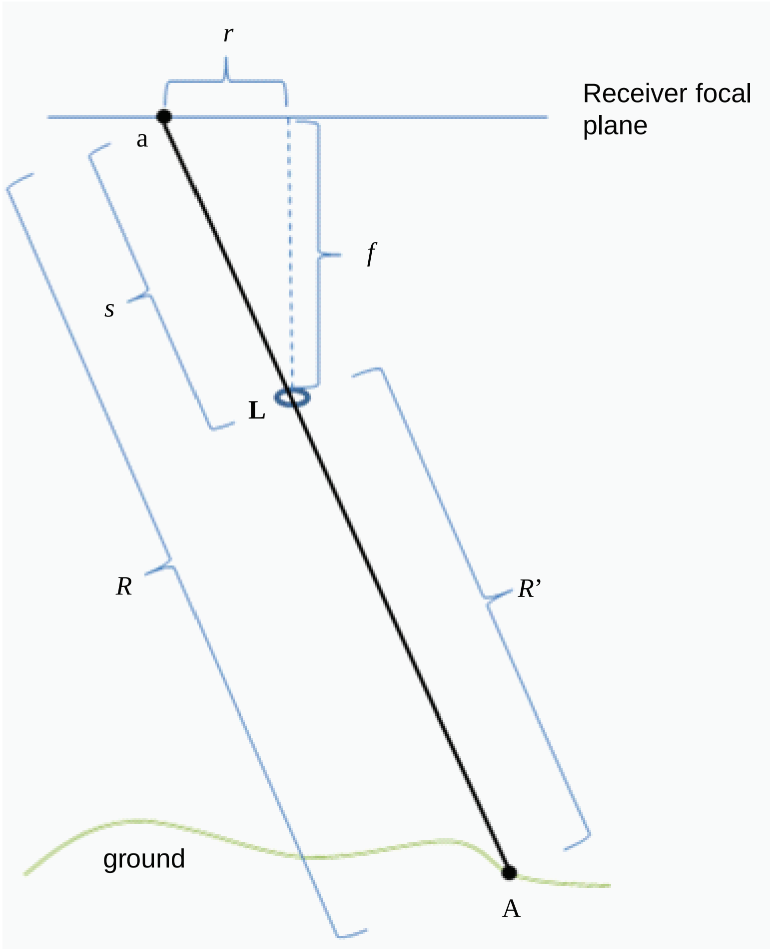

Figure D.18 — Frame receiver to ground geometry

It is necessary to transform the range measurement into the scanner coordinate system, which has its origin at the front nodal point of the lens and has its z-axis aligned with the lens optical axis (see Figure D.19). Two adjustments are necessary: subtracting *s* (the portion of the range measurement from the imaged point to the lens) from the range measurement *R* (resulting in *R'*); and correcting for the angular displacement of the range vector from the lens optical axis. The second correction is directly related to the image coordinates (*x'*, *y'*), as shown by the equations below:

$$\theta = \arctan\frac{x'}{f} \quad \text{(D.35)}$$

$$\phi = \arctan\frac{y'}{f} \quad \text{(D.36)}$$

where θ and φ are the x- and y-components of the angular displacement of the range vector from the lens optical axis. Corrections to the range measurement use the following equations:

$$s = \sqrt{f^2 + r^2} \quad \text{(D.37)}$$

$$R' = R - s \tag{D.38}$$

A rotation matrix **M** can then be constructed from θ and φ and the corrected value for r_{SCA} would then be

$$r_{SCA} = MR' \tag{D.39}$$

Formula (D.3) could then be applied to calculate the geocentric ECEF coordinates of ground point *A*, imaged at image coordinates (x', y'), using the value of r_{SCA} located above.

D.4.4 Collinearity equations

The equations described in D.4.2.3 are applied to obtain 3D ground coordinates of lidar points from a frame-scanner. However, depending on the application, it may be desirable to operate in image space (using *l*, *s* or x', y') rather than ground space (X, Y, Z). Therefore it becomes necessary to describe the relationship between image coordinates and ground coordinates, which is well described by the collinearity equations.

Deriving the relationship between image coordinates and the ground coordinates of the corresponding point on the Earth's surface requires a common coordinate system, a process accomplished by translation and rotation from one coordinate system to the other. Extracting the object **A** from Figure D.18, the geometry is reduced to that shown in Figure D.19

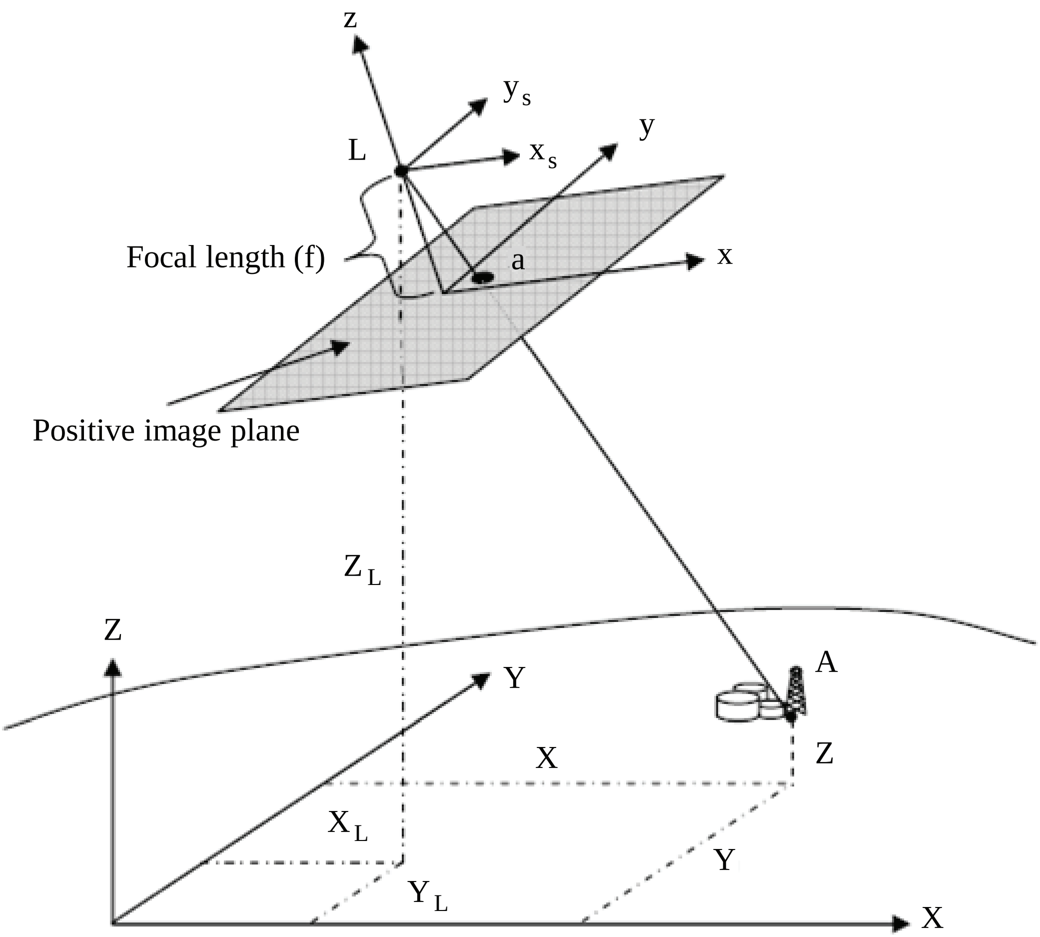

Figure D.19 — Collinearity of image point and corresponding ground point

Geometrically, the sensor perspective centre L, the "ideal" image point **a**, and the corresponding object point **A** are collinear. The "ideal" image point is represented by image coordinates *after* having been corrected for all systematic effects (lens distortions, atmospheric refraction, etc.), as given in the preceding sections.

For two vectors to be collinear, one must be a scalar multiple of the other. Therefore, vectors from the perspective centre L to the image point and object point, **a** and **A** respectively, are directly proportional. Further, in order to associate their components, these vector components must be defined with respect to the same coordinate system. Therefore, we define this association using the following equation:

$$a = k\mathrm{MA} \tag{D.40}$$

where k is a scalar multiplier and **M** is the orientation matrix that accounts for the rotations (roll, pitch, and yaw) required to place the Earth coordinate system parallel to the sensor coordinate system. Therefore, the collinearity conditions represented in the figure become:

$$\left[\begin{pmatrix} x \\ y \\ 0 \end{pmatrix} - \begin{pmatrix} 0 \\ 0 \\ f \end{pmatrix}\right] = k\mathbf{M}\left[\begin{pmatrix} X \\ Y \\ Z \end{pmatrix} - \begin{pmatrix} X \\ Y \\ Z \end{pmatrix}_L\right] \tag{D.41}$$

The orientation matrix **M** is the result of three sequence-dependent rotations:

$$\mathbf{M} = M_K M_\phi M_\omega = \begin{bmatrix} \cos K & \sin K & 0 \\ -\sin K & \cos K & 0 \\ 0 & 0 & 1 \end{bmatrix} \begin{bmatrix} \cos\phi & 0 & -\sin\phi \\ 0 & 1 & 0 \\ \sin\phi & 0 & \cos\phi \end{bmatrix} \begin{bmatrix} 1 & 0 & 0 \\ 0 & \cos\omega & \sin\omega \\ 0 & -\sin\omega & \cos\omega \end{bmatrix} \tag{D.42}$$

Where the rotation ω is about the x-axis (roll), φ is about the once rotated y-axis (pitch), and *K* is about the twice rotated Z-axis (yaw), the orientation matrix **M** becomes:

$$\mathbf{M} = \begin{bmatrix} \cos\phi\cos K & \cos\omega\sin K + \sin\omega\sin\phi\cos K & \sin\omega\sin K - \cos\omega\sin\phi\cos K \\ -\cos\phi\sin K & \cos\omega\cos K - \sin\omega\sin\phi\sin K & \sin\omega\cos K + \cos\omega\sin\phi\sin K \\ \sin\phi & -\sin\omega\cos\phi & \cos\omega\cos\phi \end{bmatrix} \tag{D.43}$$

Using subscripts representing row and column for each entry in **M** results in the following representation:

$$\mathbf{M} = \begin{bmatrix} M_{11} & M_{12} & M_{13} \\ M_{21} & M_{22} & M_{23} \\ M_{31} & M_{32} & M_{33} \end{bmatrix} \tag{D.44}$$

Although the earlier derivation expressed coordinates with regard to the image plane ("negative" plane), the image point **a** in Figure D.19 is represented by coordinates (x,y), whose relation is simply a mirror of the image plane. Thus the components of **a** will have opposite signs of their mirror components (x, y) as follows:

$$\bar{x} = -(x - x_0) \tag{D.45}$$

$$\bar{y} = -(y - y_0) \tag{D.46}$$

Formula (D.43) represents three equations across the three rows of the matrices. Substituting Formula (D.44) into Formula (D.43) and dividing the first two equations by the third eliminates the *k* multiplier. Therefore, for any given object, its ECEF ground coordinates (X,Y,Z) are related to its image coordinates (x,y) by the following equations:

$$x = -f\left[\frac{M_{11}(X - X_L) + M_{12}(Y - Y_L) + M_{13}(Z - Z_L)}{M_{31}(X - X_L) + M_{32}(Y - Y_L) + M_{33}(Z - Z_L)}\right] \tag{D.47}$$

$$y = -f\left[\frac{M_{21}(X - X_L) + M_{22}(Y - Y_L)M_{23}(Z - Z_L)}{M_{31}(X - X_L) + M_{32}(Y - Y_L) + M_{33}(Z - Z_L)}\right] \quad \text{(D.48)}$$

The coordinates (x,y) above represent the *corrected* pair, (*x'*,*y'*), from Formula (D.42) and Formula (D.43). Also, the equations above rely upon the position and orientation of the sensor. The orientation is represented by the rotation matrix **M**, providing the rotation angles necessary to align the sensor coordinate system to the ECEF coordinate system (E.3). Therefore **M** is simply the combination of rotation matrices provided in Formula (D.3), specifically

$$\mathbf{M} = M_{ECEF}M_{ELL}M_{VER}M_{PLA} \quad \text{(D.49)}$$

Also, the position of the sensor r_L (X_L, Y_L, Z_L) can be obtained from Formula (D.3) by setting the range vector r_{SCA} to zero, resulting in

$$r_L = r_{ECEF} + M_{ECEF}M_{ELL}M_{VER}(M_{PLA}r_{GIM} + r_{INS} + r_{GPS}) \quad \text{(D.50)}$$

D.5 Application of a sensor model

D.5.1 Lidar models

Formula (D.3) and its ancillary equations in D.4 can, depending on the system receiver geometry, be applied to many aspects of lidar data for analysis. This clause will discuss access to the components of the lidar sensor model and how the components can be used for sensor parameter adjustment.

In order to adjust sensor parameters, it is necessary to access various features of a sensor model. However, particulars of a model can vary from sensor to sensor, and some of the mathematics may be proprietary. The Community Sensor Model (CSM) concept was developed to standardize access to sensor models. For a given class of sensor (e.g. frame imagery), key functions are used for relating sensed objects to sensor parameters. Sensor vendors then write and provide these functions so users can access the sensor model for a particular sensor without needing model information specific to the sensor. Any sensor within the same sensor class could then be accessed using the same key functions established for that class, assuming the key functions have been provided by the associated vendor.

In the case of a lidar sensor model, five key functions, which help the user obtain the necessary information from the sensor model in order to perform tasks such as error propagation or parameter adjustment, will be described. Other CSM-based functions are available to access a lidar sensor model as well, but are not listed here since they are common across sensor classes. The key functions are:

1) ImageToGround()

2) GroundToImage()

3) ComputeSensorPartials()

4) ComputeGroundPartials()

5) ComputeGroundCovariance()

Instantiation of the key functions is associated with a state. A *state* consists of the estimated sensor metadata values for a particular collection epoch. Therefore, when any of the functions are used, the state of the sensor has already been determined for that function call.

The key functions that are available for a given lidar data set will depend on whether the data are represented in image space or ground space. Image space is the native representation format for data collected from a frame scanner. Each frame consists of a raster of pixels (i.e. an image), with each pixel associated with a line/sample coordinate pair and having some type of height or range value. Ground space is the native representation format for data collected from a point scanner. A ground space data set consists of 3D ground coordinates for each data point in some ground-referenced coordinate system.

Data represented in image space may be converted to ground space, since 3D coordinates can be calculated for each pixel in frame space. Therefore, a frame scanner may have its data available in image space or ground space. However, a point scanner can represent its data only in ground space.

Following are descriptions of the key functions, followed by descriptions of how the functions can be used.

D.5.2 Key functions

D.5.2.1 Overview

Table D.1 provides an overview of the key functions, including the inputs and outputs for data sets provided in image space or ground space.

Table D.1 — Overview of Key Functions

Functions	Image Space	Ground Space
ImageToGround()	Input: line, sample Optional: image cov. Output: ground X, Y, Z Optional: ground cov.	N/A
GroundToImage()	Input: ground X, Y, Z Optional: ground cov. Output: line, sample Optional: image cov.	N/A
ComputeSensorPartials()	Input: ground X, Y, Z Optional: line, sample Output: $\partial_{line} / \partial_{parameter}$, $\partial_{sample} / \partial_{parameter}$	Input: ground X, Y, Z Output: $\partial_{XYZ} / \partial_{parameter}$
ComputeGroundPartials()	Input: ground X, Y, Z Output: ∂_l / ∂_X , ∂_l / ∂_Y , ∂_l / ∂_Z $\partial_s / \partial_X, \partial_s / \partial_Y, \partial_s / \partial_Z$	N/A
ComputeGroundCovariance()	N/A	Input: ground X, Y, Z Output: ground cov.

Following are detailed descriptions of the key functions.

D.5.2.2 ImageToGround()

The ImageToGround() function returns the 3D ground coordinates (in the associated XYZ geocentric ECEF coordinate system) for a given line and sample (*l*, *s*) of a lidar data set in image space. This function is not applicable to data in ground space. If an optional image covariance matrix (2x2) is also provided as input, then the associated ground covariance matrix (3x3) for the returned ground point coordinates will be included in the output.

D.5.2.3 GroundToImage()

The GroundToImage() function returns the line and sample (*l, s*) in image space for the given XYZ coordinates of a 3D ground point. This function is not applicable to data expressed only in ground space. If an optional ground covariance matrix (3x3) is provided as input, then the associated image covariance matrix (2x2) for the returned line/sample pair will be included in the output.

D.5.2.4 ComputeSensorPartials()

The ComputeSensorPartials() function returns partial derivatives of image line and sample (image space) or ground XYZ (ground space) with respect to a given sensor parameter. It can be executed in two different ways, depending on whether the partial derivatives are desired for data in image space or ground space. For both cases, the minimal input is XYZ coordinates of a 3D ground point and the index of a sensor parameter of interest. If image space partials are desired, an optional line/sample pair, associated with the ground XYZ coordinates, may also be provided as input (this allows for faster computation, since a call to GroundToImage() would be needed if the associated line/sample pair was not provided). For image space values, the output consists of partial derivatives of line and sample with respect to the input sensor parameter. For ground space values, the output consists of partial derivatives of ground X, Y and Z with respect to the input sensor parameter.

D.5.2.5 ComputeGroundPartials()

The ComputeGroundPartials() function applies only to image space data. It returns partial derivatives of line and sample with respect to ground X, Y and Z values, resulting in a total of six partial derivatives. The input is the XYZ coordinates of a 3D ground point, and the output is the set of six partial derivatives.

D.5.2.6 ComputeGroundCovariance()

The ComputeGroundCovariance() function applies only to ground space data. It returns a 3x3 ground covariance matrix for a given input of XYZ coordinates for a ground point.

D.5.3 Application

One of the primary uses for a lidar sensor model is parameter adjustment. As an example, if provided multiple overlapping frames of lidar data, one may want to adjust the exterior orientation parameters (X_L, Y_L, Z_L, ω, φ, *κ*) for each frame, as well as the ground coordinates of common points, obtaining the best fit for the data sets in a least-squares sense. This is analogous to a bundle adjustment in photogrammetry, which uses the following equation:

$$v_{ij} + \dot{B}_{ij}\dot{\Delta}_i + \ddot{B}_{ij}\ddot{\Delta}_j = f_{ij} \quad \text{(D.51)}$$

The components of Formula (D.51) are described below:

$\dot{\Delta}_i$ unknown corrections to the sensor parameters;

$\ddot{\Delta}_j$ unknown corrections to the ground coordinates;

$\dot{B}_{ij}$ coefficients of the unknown corrections to the sensor parameters;

$\ddot{B}_{ij}$ coefficients of the unknown corrections to the ground coordinates;

v_{ij} residuals of the frame coordinates:

i index of frames

j index of points.

Values within $\dot{B}_{ij}$ and $\ddot{B}_{ij}$ contain partial derivatives with respect to sensor parameters and ground coordinates, respectively. Calls to ComputeSensorPartials() and ComputeGroundPartials() would be used to derive these values.

The solution for $v_{ij} + \dot{B}_{ij}\dot{\Delta}_i + \ddot{B}_{ij}\ddot{\Delta}_j = f_{ij}$ [Formula (D.51)] would involve construction of weight matrices of ground coordinates and frame coordinates, which could be derived from the optional covariance matrices using functions ImageToGround() and GroundToImage().

Annex E
(informative)

Sonar sensor model metadata profile supporting precise geopositioning

E.1 Introduction

The purpose of this annex is to show how to use metadata defined in this Technical Specification and ISO/TS 19130:2010 to accomplish precise geopositioning of images from sonar imagery systems. This annex is intended to give an example for using the common terminology and a common frame of reference established in this Technical Specification and ISO/TS 19130:2010 to perform precise geopositioning using a physical sonar sensor model.

E.2 Classification of sonar system

E.2.1 Introduction

The word *sonar* is from the acronym for "SOund, Navigation And Ranging." In the simplest terms, an electrical impulse from a transducer is converted into a sound wave by the transmitter and sent into the water. When this wave strikes an object, it rebounds. This echo strikes a receiver (hydrophone) in the transducer, which converts it back into an electric signal. This signal is then amplified by the receiver and sent to the sonar processing system. The sonar processing system interpolates depth positions from the ships GNSS position, applying antenna offset parameters and information on the ship's attitude. The sonar system determines the distance to the bottom from the time lapse between the transmitted signal and the received echo. This process repeats itself many times per second. The time lapse between the transmitted signal and the received echo can be measured and the slant distance to the object is determined in relation to the speed of sound through the medium.

A sonar system applies adjustments to the slant range from the ship's attitude and sound velocity profiles to determine the vertical depth. Depth calibration corrections also may be applied from barchecks and patch tests.

sonar systems may also use different frequencies to find out different things about the seafloor. Scientists typically use sonars that transmit sound at 12–200 kHz to determine how far down the seafloor lies. However, they also use a lower frequency (3,5 kHz) sound, which penetrates the accumulated layers of sediments below it.

E.2.2 Active and passive sonar

There are two general classification of sonar, passive and active. A passive sonar system only receives sound waves from external sources; it does not transmit any sound waves. This is an advantage in military applications, where silence is vital to avoid detection by the enemy. Unlike passive sonar systems, active sonar systems transmit and receive. When transmitting, an acoustical signal is sent into the water; the signal will bounce off any object in the path of the signal and return by the way of an "echo". The signal strength or time of the received "echo" can then be measured and the range and orientation of the object can be determined.

E.2.3 Types of sonar systems

E.2.3.1 Single beam sonar system

Single beam sonar produces one narrow sonar beam directly beneath the transducer/receiver and receives a return from the closest object at which it intersects (Figure E.1). This single beam sonar has been the typical method for collecting hydrographic survey data for Hydrographic Surveys.

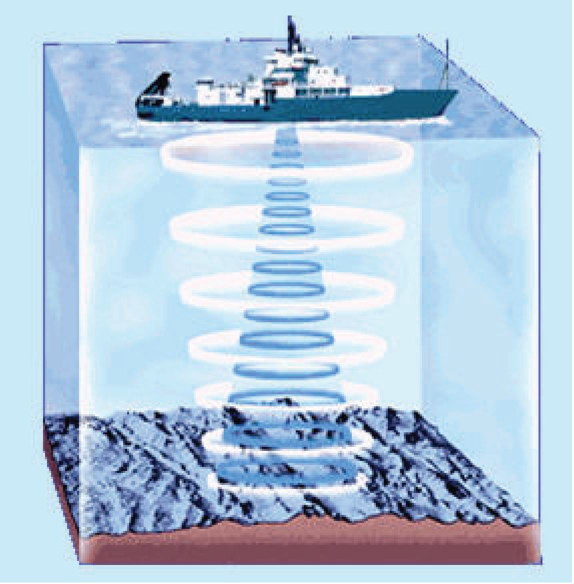

Figure E.1 — Single beam sonar system

The transducer/receiver is customarily mounted on a vessel hull, and although the vessel may be equipped with a heave sensor, there is normally no way to measure the orientation of the transducer during operation. Sonars aboard ships have components called transceivers that both transmit and receive sound waves. Transducers send a cone of sound down to the seafloor, which reflects back to the receivers. Like a flashlight beam, the cone of sound will focus on a relatively small area in places where the ocean is shallow, or spread out to hundreds of metres when water depths reach 3,000 m. The returned echo is received by the receiver, amplified electronically, and displayed on graphic displays and recorded in digital files. The time taken for the sound to travel through the ocean and back is then used to calculate water depths. The sooner the sound waves return, the less the water depth and the higher the elevation of the displayed seafloor. Sonars repeatedly “ping” the seafloor as the ship moves along the track, producing a continuous line showing ocean depths directly beneath the ship.

E.2.3.2 Sweep sonar system

A sweep system is characterized by several single beam transducer/receivers mounted on a boom, which is then operated parallel to the water’s surface and orthogonal to the vessel’s direction of travel. The transducers are equally spaced, to yield sonar bottom coverage of a constant width independent of water depth. These systems are generally used in shallow water where full or close to full coverage is required. See Figure E.2.

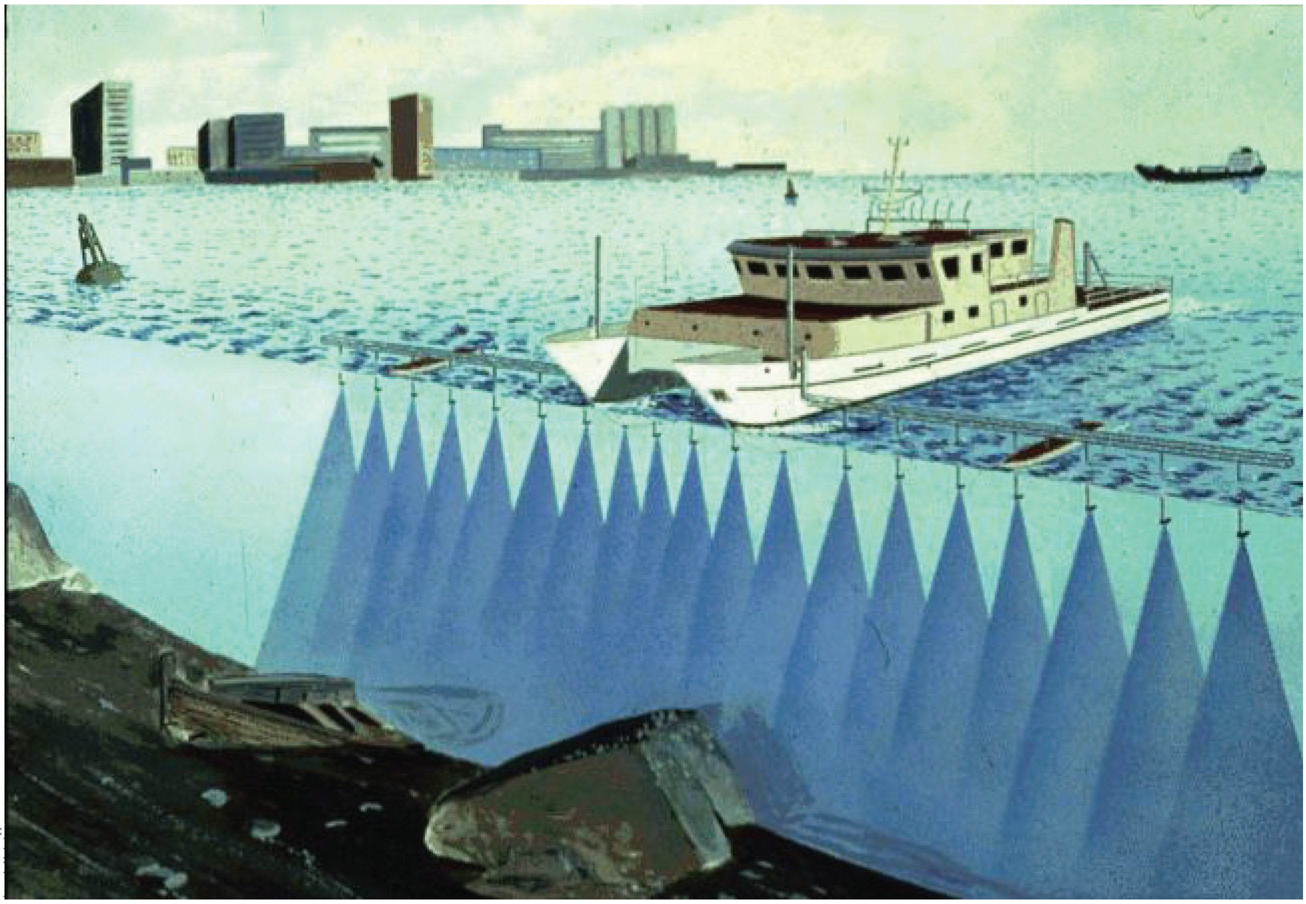

Figure E.2 — Multitransducer vertical sweep system

E.2.3.3 Multibeam sonar system

Multibeam sonar systems have single or multiple transducers that continually transmit numerous sonar beams in a swath or fan-shaped signal pattern. They also can use single or multiple frequencies. They are ideal systems for mapping large areas rapidly, with essentially 100 percent bottom coverage.

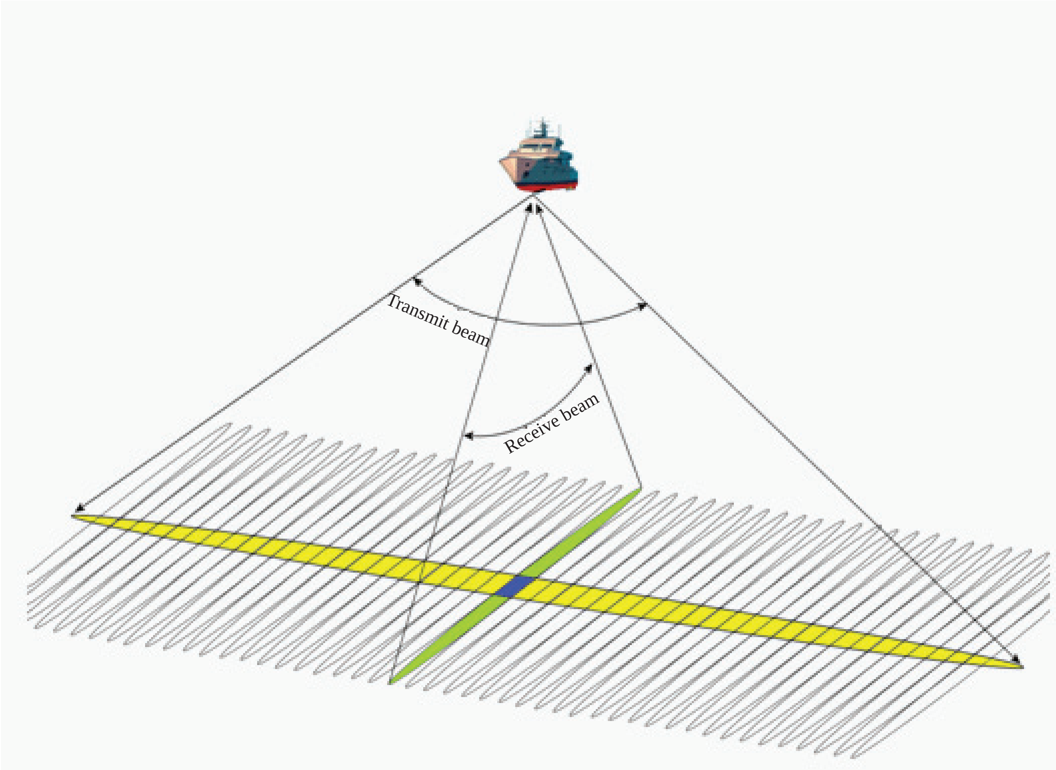

Figure E.3 — Multibeam sonar system

Figure E.3 shows the multibeam sonar footprint below the ship. The transmitted acoustic beam is narrow along track and wide across track, highlighted in yellow. There are many received beams but each one is long along track and narrow across track. One receive beam is highlighted in green. The intersection of the transmit beam area and the individual receive beam area provides the footprint for that beam, shown in blue. The depth is the average depth within the intersection area.

Multibeam, or swath, sonar systems provide fan-shaped coverage of the seafloor (similar to sidescan sonar), but the output data are different. Instead of continuously recording the strength of the return echo, the multibeam system measures and records the time for the acoustic signal to travel from the transducer to the seafloor and back.

The measurement of sound speed profiles for a multibeam survey is required to correct for the sound speed propagation and ray path variability through the water column. This results in a vertical and across-track correction. Sound speed profiles are measured at a sufficient frequency to ensure that the horizontal and depth accuracies for the order of the survey are met. If a continuous profiling system is available, sound speed profiles are measured at the maximum rate that logistics and vessel traffic allows.

E.2.3.4 Sidescan sonar

Sidescan sonar is used for imaging bottom features and targets at a wide variety of water depths (Figure E.4). The sound energy, however, is transmitted from the sides of a towfish, creating a fanlike beam on either side that sweeps between the sea floor and the ship. The return signal is continuously recorded, creating a “picture” of the seafloor and any other objects.

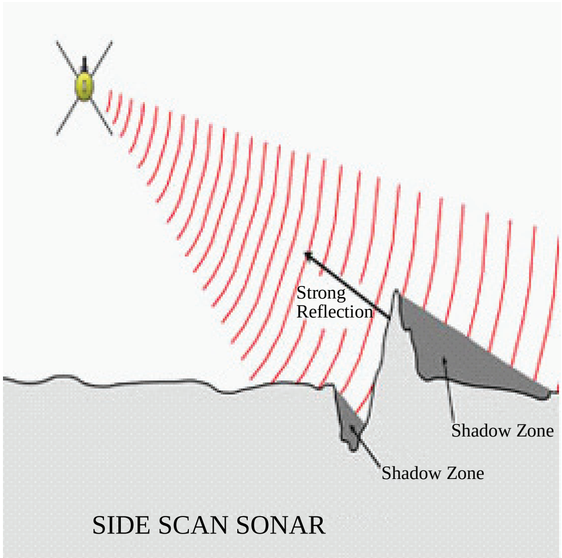

Figure E.4 — Operation of sidescan sonar

Conventional sidescan sonar systems use a single sonar beam on each side to generate an image of the sea floor. Sidescan sonar is very useful for locating sea-floor features and possible obstructions. However, while the contours of the seafloor and objects on it can be imaged quite well, most sidescan sonar systems do not provide accurate bathymetric data.

E.2.4 Sonar calibration processes

E.2.4.1 Introduction

Calibrating components of the sonar system is essential. This requires the measurement and positioning of the individual components, for example establishing the position of the GNSS antennas and each transducer/receivers. It is necessary to allow for the dynamic draft variation of the transducer/receivers due to fuel and water consumption.

sonar systems consist of a transducer, motion sensor, gyrocompass, and navigation system. Reliable data can be acquired only after proper calibration has been performed on the system as a whole. These calibration procedures for multibeam sonar are commonly referred to as a “Patch Test” and involve creating a log of data while the survey vessel is run over specific lines over different types of bathymetric relief at differing speeds, reciprocal directions, and offset to identifiable targets.

The “Patch Test” calibration process is an essential procedure which consists of determining the composite offset angles (roll, pitch and azimuth) for both transducer and motion sensor and the latency from the positioning system. These values are used to correct the initial alignment and calibrate the sonar system. The field procedures necessary for proper calibration are the alignment of each sensor and the patch test.

E.2.4.2 Alignment measurements and static offsets

E.2.4.2.1 Overview

This calibration begins with the alignment and static offsets of the sensors relative to the centreline of the vessel and the transducer. The alignment will reduce the static corrections for each sensor and can be performed with either GNSS receivers (e.g. GNSS) or a total station geodetic instrument. To establish a ground truth area to validate the system and compare results is recommended.

The offsets used for the physical alignment of the vessel platform, transducers, gyrocompass, and HPRH (Heave, Pitch, Roll, Heading) sensor is referred to as static offsets (Figure E.5). The process of determining these offsets should ideally take place in a stable environment in order to obtain exact measurements. This stability minimizes errors in the positioning of the sensors and, with the proper offsets applied, the static corrections are determined. The sensors are measured from a reference point in the vessel that is typically the centre of gravity or the intersection of the pitch and roll axes. The centre of gravity changes with varying load conditions of the vessel and thus must be chosen to represent the typical conditions expected while surveying.

The sensor offsets are measured distances from the reference point to the centre of the sensor. The centre of the sensor can be found in the manufacturer's schematic of the sensor or can be accurately measured with a survey tape. The magnitude and direction of the measurement are verified and recorded.

The order in which these biases are determined may affect the accurate calibration of the sonar system. The biases are determined in the following order: navigation timing error, pitch, roll and heading. The aim of the patch test is to determine any residual time offset, pitch angle, roll angle and azimuth angle of the sonar system. The patch test is conducted at the start and end of a survey to confirm that the system has not changed during the course of the survey. A patch test is also conducted whenever there is a change in significant mechanical, hardware, or software components of the system.

The Heave Pitch Roll Heading (HPRH) sensor is usually placed on the centreline of the vessel as close as possible to the centre of gravity or the intersection of the pitch and roll axes of the vessel, with the same mount angles as for the transducer. The x-axis of the HPRH should match the x-axis of the transducer (the x-axis is defined as the bow-stern axis of the vessel while the y-axis is the beam axis of the vessel). Azimuthal misalignment of the HPRH sensor will result in an error in the depth measurements proportional to the water depth. On deployable/mobile systems the HPRD sensor may be positioned directly on the mounting, for example, an over-the-side mount, or an AUV (Autonomous Underwater Vehicle).

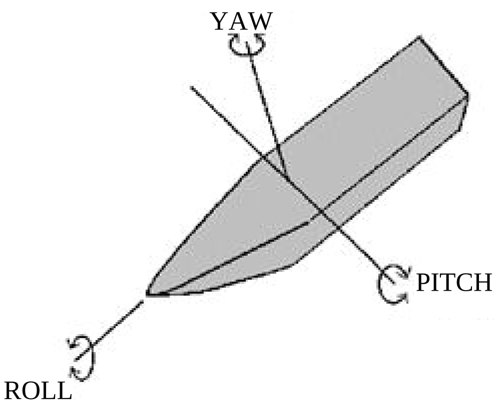

Figure E.5 — Roll, pitch and yaw of a vessel

E.2.4.2.2 Sources of error

Several sources of error and biases exist in surveying using sonar systems. These errors and biases may have more impact with certain types of systems. These sources of error become more important in multi beam surveying.

- *Static offsets of the sensors* are the distances between the sensors and the reference point of the vessel or the positioning antenna.
- *Transducer draft* is the depth of the transducer head below the waterline of the vessel, which may vary depending on the speed of the vessel and depth below keel (settlement/squat).

— *Time delay between the positioning system, sonar measurement, and HPR sensor* is the delay or latency that must be accurately known and compensated for in the processing of the hydrographic data.

— *The error* associated in the ray path model, including sound velocity measurement in the water column that must be accurately known so the correct depth can be measured.[8] *Acceleration and translation measurements* of the HPRH (Heave Pitch Roll Heading) are critical for adjustment of the vessel's attitude

— *Vertical datum* and tide variations, as well as uncertainty in defining the vessel position and orientation on the surface[8].

E.2.4.2.3 Transceivers

Most transceivers consist of integrated transducers and receivers into a single unit. If possible, most transceivers are installed as near as possible to the centreline of the vessel and level about the roll axis (Figure E.6). They should be aligned with the azimuth of the vessel. This alignment is critical when there is no beam steering systems. There is, however, beam steering about the y-axis with some transceivers. Most of the multibeam transceivers are hull mounted; however, on certain vessels transducers are towed or are mounted over-the-side on a shaft and boom device. With this type of mount, the azimuthal alignment between the transducer and keel must be as accurate as possible. This alignment can be accomplished in a stable environment using standard surveying and levelling techniques.

The boom-mounted technique allows for raising the transducer at the end of each day of operations and lowering it at the start of the next day's survey; therefore, this type of mount should be periodically checked for correct alignment. The frequency with which it is checked will depend on what type of surveying is being performed and under what conditions (e.g. different accuracy requirements, weather conditions, vessel draft). Hull mounted transceivers are generally fixed in place and will not need to be checked as frequently. The angle of the transceiver unit mount must be determined and recorded. Since most vessels underway will be lower in the stern, the transceiver will generally need to be rotated aft along the centreline axis to compensate for the angle of the transceiver unit mount. The patch test is used to check the transducer angle for the pitch offset. After alignment, the resulting beam should then project normal to the sea floor while conducting surveying operations

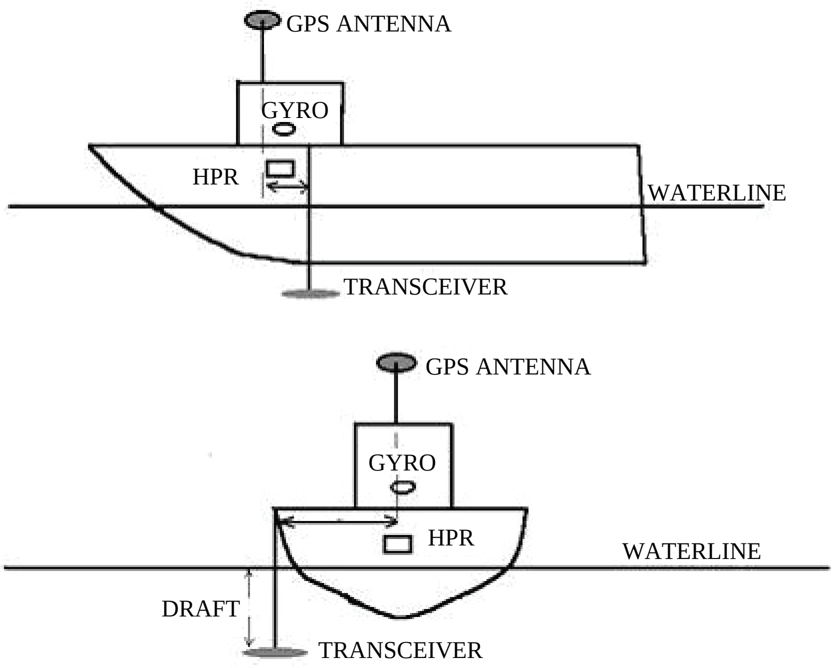

Figure E.6 — The location of transceiver

E.2.4.2.4 Gyro heading

The gyro should be aligned with the x-axis of the vessel using a survey instrument (e.g. theodolite total station) and geodetic control points. This alignment can be done with the vessel on a trailer or secured tightly against a pier where there is minimal wave action. The gyro should be warmed up and, if necessary, the proper corrections for latitude applied. By locating two (2) points on the centreline of the vessel and placing a target on each, the two targets can be observed with the total station, which enables synchronization of the readings with the gyro readings. Several readings are needed for redundancy. The vessel's azimuth is computed and compared with the gyro readings. Following analysis of the mean and standard deviation, if the offset is more than 1 degree at the 95 percent confidence level, the gyro must be realigned with the centreline and the observations repeated. If it is less than 1 degree, the correction is within the specified tolerance and can be applied to the gyro output. This procedure also can be performed using three GNSS receivers instead of the total station, however, the data processing may take longer than using the total station.

E.2.4.3 Patch test

E.2.4.3.1 Introduction

After the static offsets have been determined, a patch test is performed (Figure E.7). This calibration test is designed to reveal the following residual biases: (1) pitch offset, (2) roll offset, (3) positioning time delay, and (4) azimuthal offset. The test consists of a small survey ("patch test") of several lines that are evaluated for inconsistencies and then corrected using software usually designed for multibeam surveys. However the tests could also be applied to single beam surveys. There are several mathematical equations developed for analysing these biases that are incorporated into the processing software for the patch test. The performance test is the final check of the offsets and biases to verify whether the data meet accuracy requirements for the survey. This test is a series of parallel and cross lines with significant overlap to give redundant data.

The patch test or calibration survey is a small survey of several lines that are run in order to check and correct the following potential biases:

a) Residual pitch offset

b) Residual roll offset

c) Residual positioning time delay

d) Residual azimuthal offset

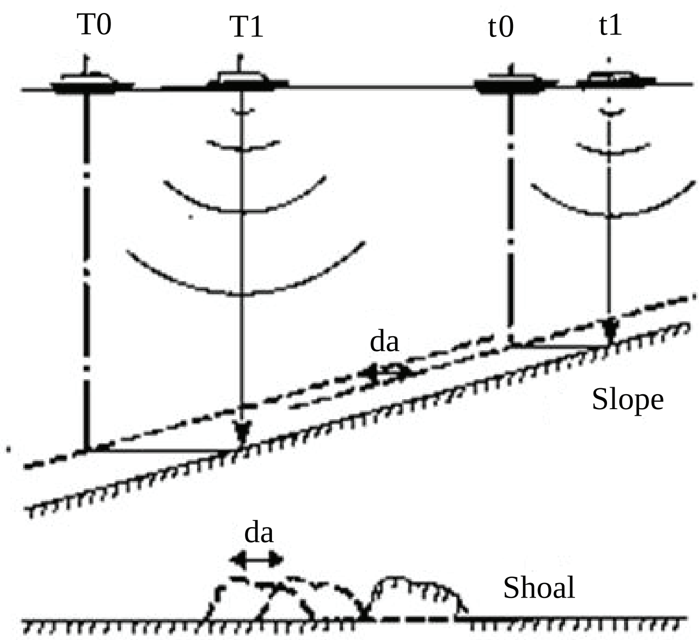

Figure E.7 — Patch tests

Patch tests are generally performed whenever there is a significant change in the survey area or the characteristics of the vessel. Usually, the tests are performed at the start of each new survey or when a significant change in the water mass (usually temperature or salinity) has occurred. The values for the correction parameters should be verified and entered into the sonar processing system. In addition, it is assumed that the positioning instruments used will be Differential Global Navigational Satellite System (DGNSS) with survey quality receivers on the vessel and the shore stations. The weather should be calm to ensure good bottom detection and minimal vessel motion. Since most of the lines to be run will be reciprocal lines, it is important to have capable vessel steering and handling. The lines should be run in water depths comparable to the typical survey areas encountered and will generally be less than 20 m. The order in which the lines are run is not important although it is recommended that at least two sets of reciprocal lines are run for redundancy. Although the outer beams of multibeam sonar are subject to a larger grazing angle, these beams should provide good data if the appropriate corrections are applied from the patch test.

Patch tests are repeated whenever changes (e.g. sensor failure, replacement, re-installations, re-configurations, or upgrade; software changes which could potentially affect data quality) are made to the system's baseline configuration, or whenever assessment of the data indicates that system accuracies do not meet the requirements.

E.2.4.3.2 Settlement measurement

The settlement of the vessel is the increase in the draught resulting from its momentum through the water. It should be measured at several speeds and a corresponding look-up table produced to correct the transducer draught for these speeds. This measurement is essential since the HPR does not measure the low frequency change in elevation. The sensor records a sudden change in elevation, but the measured heave drifts back to zero. The elevation differences at various speeds are recorded and the interpolated settlement values are used as the draft correction while surveying. Application of the correct sign must be ensured when entering the correction value into the software. This correction is generally performed once for each survey area. The settlement measurement can be done by shore based transits or GNSS receivers on the vessel.

E.2.4.3.3 Time delay

Time delay in the attitude sensor will result in roll errors, which greatly affect the orientation of the outer beams of multi-beam systems. Horizontal accelerations in cornering affect the HPR measurements, which result in errors in the depth measurements. Basically, the principle for detecting roll errors is to observe the changes in the across track slope of the seafloor when surveying flat and smooth areas.

Time delays in the positioning system are the time lags between when the time positioning data are first received by the system and the time the computed position reaches the logging module. This difference results in a negative along-track displacement of the depth measurements. In general, the processing time for the position varies with the number of observations used in the final GNSS solution. If the time tag embedded in the GNSS message is used, then the correct synchronization between this time and the transducer or signal processing clock must be ensured.

E.2.4.3.4 Positioning Time Delay and Pitch Bias Lines

Lines should be run in an area with a slope of 10 degrees to 20 degrees. At least two pairs of reciprocal lines should be run up and down slope. If possible, a conspicuous bathymetric feature should be surveyed to assess the time delay as long as it is covered by the beam at nadir. The slope should be at least 200 m long in order to obtain good samples. The lines should be run at two different speeds to assess the time delay. See Figure E.8.

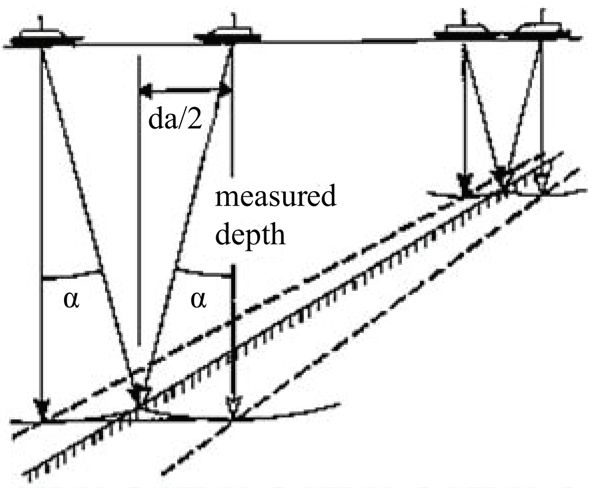

Figure E.8 — Positioning time delay and pitch bias lines

E.2.4.3.5 Roll Bias Lines

In flat areas, at least one pair of lines should be run for testing the roll bias. Figure E.9 shows a schematic of a vessel with a roll to port of 5 degrees, an exaggerated roll bias. If possible, these lines should be run in deep water where it is easier to test for roll errors with the outer beams. Depending on the type of sonar system, these lines should be run at a speed to ensure significant overlap of the beam footprint.

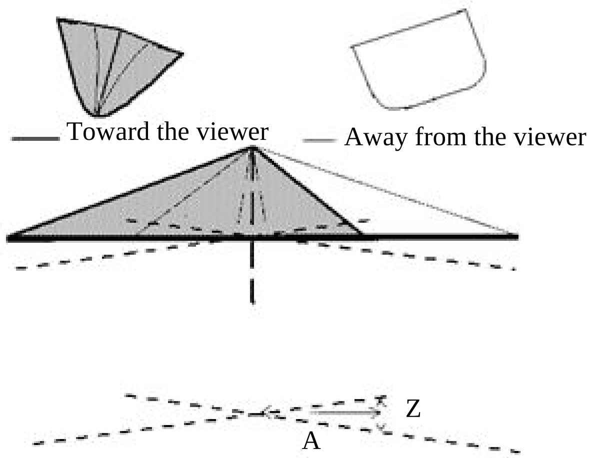

Figure E.9 — Testing for the roll bias

E.2.4.4 Sound velocity corrections

E.2.4.4.1 Bar check

For single beam and sweep systems, a calibration process termed "bar check" was formerly used on one or more transducers in order to determine sound velocity adjustments to allow for sound speed variation in the surveyed area.

Single beam transducers were calibrated with a bar check coupled with a velocity cast. With the bar lowered to a given depth, the depth recorder signal output can be adjusted to match the known bar depth. The velocity cast gives the speed of sound in the water column, and the proper speed can be applied to the echo sounder.

The "Bar Check" was the field procedure for sonar calibration involving a metal cone or plate device lowered to a maximum depth, recording the true depth versus the measured depth and compiling a depth correction table that would be used later to correct the measured depths. The bar check was used to determine the correct draft entry if the size and shape of the vessel permitted. This methodology was used at least once a day and possibly at the end of the day to ensure that no problems occurred during the day.

E.2.4.4.2 Sound velocity profiles

In current modern surveys, sound velocity profiles are generally used to determine the sound velocity adjustments to allow for sound speed changes in the sonar processing system.

The measurement of sound speed profiles for the use of a single beam survey is desired to correct for the sound speed propagation differences caused by changes in sound speed through the water column. This results in a vertical correction only. Sound speed profiles are to be taken at an interval dictated by the variability of conditions in the survey area.

The sound velocity observations must be taken with sufficient frequency, density, and accuracy to ensure that the specified overall depth measurement accuracy criteria are met. The accuracy of the speed of sound correction is determined is a function of the accuracy with which salinity, temperature, and depth, or alternately, sound speed and depth, can be measured.

The sound speed profile in the survey areas must be measured and monitored at sufficient frequency and to an appropriate depth to ensure that the bathymetric data provided meets the required depth accuracy specification. The sound speed profile is determined with a calibrated system capable of measuring the speed of sound with errors no greater than 2 m/sec (at the 95 % confidence level).

Regardless of the sound velocity determination system employed, an independent sound velocity measurement system must be used to establish a confidence check. Confidence checks are conducted at every profile measurement. A comparison between the profile measurements at the depth of the online sound speed sensor may be used as a confidence check.

E.3 Multibeam-system supported swath data formats

Each swath mapping sonar system outputs a data stream that includes some values or parameters unique to that system. In general, a number of different data formats have come into use for data from each of the sonar systems; many of these formats include only a subset of the original data stream. Internally, MBIO recognizes which sonar system each data format is associated with and uses a data structure including the complete data stream for that sonar. At present, formats associated with the following sonars are supported:

— Sea Beam “classic” multibeam sonar

— Hydrosweep DS multibeam sonar

— Hydrosweep DS2 multibeam sonar

— Hydrosweep MD multibeam sonar

— Sea Beam 2000 multibeam sonar

— Sea Beam 2112 and 2136 multibeam sonars

— Sea Beam 2120 multibeam sonars

— Simrad EM12, EM121, EM950, and EM1000 multibeam sonars

— Simrad EM120, EM300, and EM3000 multibeam sonars

— Simrad EM122, EM302, EM710, and EM3002 multibeam sonars

— Simrad Mesotech SM2000 multibeam sonar

— Hawaii MR-1 shallow tow interferometric sonar

— ELAC Bottomchart and Bottomchart MkII shallow water multibeam sonars

— Reson Seabat multibeam sonars (e.g. 9001, 8081, 7125)

— WHOI DSL AMS-120 deep tow interferometric sonar

— Sea Scan sidescan sonar

— Furuno HS-1 multibeam sonar

— Edgetech sidescan and sub-bottom profiler sonars

— Imagenex DeltaT multibeam sonars

— Odom ES3 multibeam sonar

The following swath mapping sonar data formats are currently supported by MB-System (open source software package for the processing and the display of bathymetric and back scatter imagery):

— MBIO Data Format ID: 11

  — Format name: MBF_SBSIOMRG

    - Informal Description: Scripps-Howard Institute of Oceanography (SIO) of multi-beam systems. merge Sea Beam
    - Attributes: Sea Beam, bathymetry, 16 beams, binary, uncentred, SIO.
- MBIO Data Format ID: 12
    - Format name: MBF_SBSIOCEN
    - Informal Description: SIO centred Sea Beam
    - Attributes: Sea Beam, bathymetry, 19 beams, binary, centred, SIO.
- MBIO Data Format ID: 13
    - Format name: MBF_SBSIOLSI
    - Informal Description: SIO LSI Sea Beam
    - Attributes: Sea Beam, bathymetry, 19 beams, binary, centred, obsolete, SIO.
- MBIO Data Format ID: 14
    - Format name: MBF_SBURICEN
    - Informal Description: URI Sea Beam
    - Attributes: Sea Beam, bathymetry, 19 beams, binary, centred, URI.
- MBIO Data Format ID: 15
    - Format name: MBF_SBURIVAX
    - Informal Description: URI Sea Beam from VAX
    - Attributes: Sea Beam, bathymetry, 19 beams, binary, centred, VAX byte order, URI.
- MBIO Data Format ID: 16
    - Format name: MBF_SBSIOSWB
    - Informal Description: SIO Swath-bathy SeaBeam
    - Attributes: Sea Beam, bathymetry, 19 beams, binary, centred, SIO.
- MBIO Data Format ID: 17
    - Format name: MBF_SBIFREMR
    - Informal Description: IFREMER Archive SeaBeam
    - Attributes: Sea Beam, bathymetry, 19 beams, ascii, centred, IFREMER.
- MBIO Data Format ID: 21
    - Format name: MBF_HSATLRAW
    - Informal Description: Raw Hydrosweep
    - Attributes: Hydrosweep DS, bathymetry and amplitude, 59 beams, ascii, Atlas Electronik.
- MBIO Data Format ID: 22
    - Format name: MBF_HSLDEDMB
    - Informal Description: EDMB Hydrosweep

  - Attributes: Hydrosweep DS, bathymetry, 59 beams, binary, NRL.
- MBIO Data Format ID: 23
  - Format name: MBF_HSURICEN
  - Informal Description: URI Hydrosweep
  - Attributes: Hydrosweep DS, 59 beams, bathymetry, binary, URI.
- MBIO Data Format ID: 24
  - Format name: MBF_HSLDEOIH
  - Informal Description: Lamont-Doherty Earth Observatory (L-DEO) in-house binary Hydrosweep
  - Attributes: Hydrosweep DS, 59 beams, bathymetry and amplitude, binary, centred, L-DEO.
- MBIO Data Format ID: 25
  - Format name: MBF_HSURIVAX
  - Informal Description: URI Hydrosweep from VAX
  - Attributes: Hydrosweep DS, 59 beams, bathymetry, binary, VAX byte order, URI.
- MBIO Data Format ID: 26
  - Format name: MBF_HSUNKNWN
  - Informal Description: Unknown Hydrosweep
  - Attributes: Hydrosweep DS, bathymetry, 59 beams, ascii, unknown origin, South Pacific Applied Geoscience Commission (SOPAC).
- MBIO Data Format ID: 32
  - Format name: MBF_SB2000SB
  - Informal Description: SIO Swath-bathy SeaBeam 2000 format
  - Attributes: SeaBeam 2000, bathymetry, 121 beams, binary, SIO.
- MBIO Data Format ID: 33
  - Format name: MBF_SB2000SS
  - Informal Description: SIO Swath-bathy SeaBeam 2000 format
  - Attributes: SeaBeam 2000, sidescan, 1000 pixels for 4-bit sidescan, 2000 pixels for 12+-bit side scan, binary, SIO.
- MBIO Data Format ID: 41
  - Format name: MBF_SB2100RW
  - Informal Description: SeaBeam 2100 series vender format
  - Attributes: SeaBeam 2100, bathymetry, amplitude and side scan, 151 beams and 2000 pixels, ascii with binary side scan, SeaBeam Instruments.
- MBIO Data Format ID: 42
  - Format name: MBF_SB2100B1

  - Informal Description: SeaBeam 2100 series vendor format
  - Attributes: SeaBeam 2100, bathymetry, amplitude and sidescan, 151 beams bathymetry, 2000 pixels sidescan, binary, SeaBeam Instruments and L-DEO.
- MBIO Data Format ID: 43
  - Format name: MBF_SB2100B2
  - Informal Description: SeaBeam 2100 series vendor format
  - Attributes: SeaBeam 2100, bathymetry and amplitude, 151 beams bathymetry, binary, SeaBeam Instruments and L-DEO.
- MBIO Data Format ID: 51
  - Format name: MBF_EMOLDRAW
  - Informal Description: Old Simrad vendor multibeam format
  - Attributes: Simrad EM1000, EM12S, EM12D, and EM121 multibeam sonars, bathymetry, amplitude, and sidescan, 60 beams for EM1000, 81 beams for EM12S/D, 121 beams for EM121, variable pixels, ascii + binary, Simrad.
- MBIO Data Format ID: 53
  - Format name: MBF_EM12IFRM
  - Informal Description: IFREMER TRISMUS format for Simrad EM12
  - Attributes: Simrad EM12S and EM12D, bathymetry, amplitude, and side scan 81 beams, variable pixels, binary, read-only, IFREMER.
- MBIO Data Format ID: 54
  - Format name: MBF_EM12DARW
  - Informal Description: Simrad EM12S RRS Darwin processed format
  - Attributes: Simrad EM12S, bathymetry and amplitude, 81 beams, binary, Oxford University.
- MBIO Data Format ID: 56
  - Format name: MBF_EM300RAW
  - Informal Description: Simrad current multibeam vendor format
  - Attributes: Simrad EM120, EM300, EM1002, EM3000, bathymetry, amplitude, and sidescan, up to 254 beams, variable pixels, ascii + binary, Simrad.
- MBIO Data Format ID: 57
  - Format name: MBF_EM300MBA
  - Informal Description: Simrad multibeam processing format
  - Attributes: Old and new Simrad multibeams, EM12S, EM12D, EM121, EM120, EM300, EM100, EM1000, EM950, EM1002, EM3000, bathymetry, amplitude, and sidescan, up to 254 beams, variable pixels, ascii + binary, MBARI.
- MBIO Data Format ID: 58
  - Format name: MBF_EM710RAW
  - Informal Description: Simrad current multibeam vendor format

    - Attributes: Simrad EM710, bathymetry, amplitude, and sidescan, up to 400 beams, variable pixels, binary, Simrad.
- MBIO Data Format ID: 59
    - Format name: MBF_EM710MBA
    - Informal Description: Simrad current multibeam vendor format
    - Attributes: Simrad EM710, bathymetry, amplitude, and sidescan, up to 400 beams, variable pixels, binary, Simrad.
- MBIO Data Format ID: 61
    - Format name: MBF_MR1PRHIG
    - Informal Description: Obsolete Hawaii Mapping Research Group - School of Ocean and Earth Science and Technology (SOEST)
    - MR1 post processed format
    - Attributes: SOEST MR1, bathymetry and sidescan, variable beams and pixels, xdr binary, SOEST, University of Hawaii.
- MBIO Data Format ID: 62
    - Format name: MBF_MR1ALDEO
    - Informal Description: L-DEO MR1 post processed format with travel times
    - Attributes: L-DEO MR1, bathymetry and sidescan, variable beams and pixels, xdr binary, L-DEO.
- MBIO Data Format ID: 63
    - Format name: MBF_MR1BLDEO
    - Informal Description: L-DEO small MR1 post processed format with travel times
    - Attributes: L-DEO MR1, bathymetry and side scan, variable beams and pixels, xdr binary, L-DEO.
- MBIO Data Format ID: 64
    - Format name: MBF_MR1PRVR2
    - Informal Description: SOEST MR1 post processed format
    - Attributes: SOEST MR1, bathymetry and side scan, variable beams and pixels, xdr binary, SOEST, University of Hawaii.
- MBIO Data Format ID: 71
    - Format name: MBF_MBLDEOIH
    - Informal Description: L-DEO in-house generic multibeam
    - Attributes: Data from all sonar systems, bathymetry, amplitude and sidescan, variable beams and pixels, binary, centred, L-DEO.
- MBIO Data Format ID: 75
    - Format name: MBF_MBNETCDF
    - Informal Description: CARAIBES CDF multibeam

  - Attributes: Data from all sonar systems, bathymetry only, variable beams, Network Common Data Form (netCDF), IFREMER.
- MBIO Data Format ID: 76
  - Format name: MBF_MBNCDFXT
  - Informal Description: CARAIBES CDF multibeam extended
  - Attributes: Superset of MBF_MBNETCDF, includes (at least SIMRAD EM12) amplitude, variable beams, netCDF, IFREMER.
- MBIO Data Format ID: 81
  - Format name: MBF_CBAT9001
  - Informal Description: Reson SeaBat 9001 shallow water multibeam
  - Attributes: 60 beam bathymetry and amplitude, binary, University of New Brunswick.
- MBIO Data Format ID: 82
  - Format name: MBF_CBAT8101
  - Informal Description: Reson SeaBat 8101 shallow water multibeam
  - Attributes: 101 beam bathymetry and amplitude, binary, SeaBeam Instruments.
- MBIO Data Format ID: 83
  - Format name: MBF_HYPC8101
  - Informal Description: Reson SeaBat 8101 shallow water multibeam
  - Attributes: 101 beam bathymetry, ASCII, read-only, Coastal Oceanographics.
- MBIO Data Format ID: 84
  - Format name: MBF_XTFR8101
  - Informal Description: XTF format Reson SeaBat 81XX
  - Attributes: 240 beam bathymetry and amplitude, 1024 pixel sidescan binary, read-only, Triton-Elics.
- MBIO Data Format ID: 88
  - Format name: MBF_RESON7KR
  - Informal Description: Reson 7K multibeam vendor format
  - Attributes: Reson 7K series multibeam sonars, bathymetry, amplitude, three channels sidescan, and sub-bottom up to 254 beams, variable pixels, binary, Reson.
- MBIO Data Format ID: 91
  - Format name: MBF_BCHRTUNB
  - Informal Description: Elac BottomChart shallow water multibeam
  - Attributes: 56-beam bathymetry and amplitude, binary, University of New Brunswick.
- MBIO Data Format ID: 92
  - Format name: MBF_ELMK2UNB

  - Informal Description: Elac BottomChart MkII shallow water multibeam
  - Attributes: 126-beam bathymetry and amplitude, binary, University of New Brunswick.
- MBIO Data Format ID: 93
  - Format name: MBF_BCHRXUNB
  - Informal Description: Elac BottomChart shallow water multibeam
  - Attributes: 56-beam bathymetry and amplitude, binary, University of New Brunswick.
- MBIO Data Format ID: 94
  - Format name: MBF_L3XSERAW
  - Informal Description: ELAC/SeaBeam XSE vendor format
  - Attributes: Bottomchart MkII 50 kHz and 180 kHz multibeam, SeaBeam 2120 20 KHz multibeam, bathymetry, amplitude and sidescan, variable beams and pixels, binary, L3 Communications (Elac Nautik and SeaBeam Instruments).
- MBIO Data Format ID: 101
  - Format name: MBF_HSMDARAW
  - Informal Description: Atlas HSMD medium depth multibeam raw format
  - Attributes: 40 beam bathymetry, 160 pixel sidescan, XDR (binary), STN Atlas Elektronik.
- MBIO Data Format ID: 102
  - Format name: MBF_HSMDLDIH
  - Informal Description: Atlas HSMD medium depth multibeam processed format
  - Attributes: 40 beam bathymetry, 160 pixel sidescan, XDR (binary), L-DEO.
- MBIO Data Format ID: 111
  - Format name: MBF_DSL120PF
  - Informal Description: WHOI DSL AMS-120 processed format
  - Attributes: 2048 beam bathymetry, 8192 pixel sidescan, binary, parallel bathymetry and amplitude files, WHOI DSL.
- MBIO Data Format ID: 112
  - Format name: MBF_DSL120SF
  - Informal Description: WHOI DSL AMS-120 processed format
  - Attributes: 2048 beam bathymetry, 8192 pixel sidescan, binary, single files, WHOI DSL.
- MBIO Data Format ID: 121
  - Format name: MBF_GSFGENMB
  - Informal Description: Science Applications International Corporation (SAIC Generic Sensor Format (GSF)

  - Attributes: variable beams, bathymetry and amplitude, binary, single files, SAIC.
- MBIO Data Format ID: 131
  - Format name: MBF_MSTIFFSS
  - Informal Description: MSTIFF sidescan format
  - Attributes: variable pixels, sidescan, binary TIFF variant, single files, Sea Scan.
- MBIO Data Format ID: 132
  - Format name: MBF_EDGJSTAR
  - Informal Description: Edgetech Jstar format
  - Attributes: variable pixels, dual frequency sidescan and sub-bottom, binary SEGY variant, single files, low frequency sidescan returned as survey data, Edgetech.
- MBIO Data Format ID: 133
  - Format name: MBF_EDGJSTR2
  - Informal Description: Edgetech Jstar format
  - Attributes: variable pixels, dual frequency sidescan and sub-bottom, binary SEGY variant, single files, high frequency sidescan returned as survey data, Edgetech.
- MBIO Data Format ID: 141
  - Format name: MBF_OICGEODA
  - Informal Description: OIC swath sonar format
  - Attributes: variable beam bathymetry and amplitude, variable pixel sidescan, binary, Oceanic Imaging Consultants
- MBIO Data Format ID: 142
  - Format name: MBF_OICMBARI
  - Informal Description: OIC-style extended swath sonar format
  - Attributes: variable beam bathymetry and amplitude, variable pixel sidescan, binary, Monterey Bay Aquarium Research Institute (MBARI)
- MBIO Data Format ID: 151
  - Format name: MBF_OMGHDCSJ
  - Informal Description: University of New Brunswick (UNB) OMG HDCS format (the John Hughes Clarke format)
  - Attributes: variable beam bathymetry and amplitude, variable pixel sidescan, binary, UNB
- MBIO Data Format ID: 160
  - Format name: MBF_SEGYSEGY
  - Informal Description: SEGY seismic data format

    - Attributes: seismic or sub-bottom trace data, single beam bathymetry, nav, binary, SEG (SIOSEIS variant)
- MBIO Data Format ID: 161
    - Format name: MBF_MGD77DAT
    - Informal Description: National Geophysical Data Center (NGDC) MGD77 underway geophysics format
    - Attributes: single beam bathymetry, nav, magnetics, gravity, ascii, NOAA NGDC
- MBIO Data Format ID: 162
    - Format name: MBF_ASCIIXYZ
    - Informal Description: Generic XYZ sounding format
    - Attributes: XYZ (lon lat depth) ASCII soundings, generic
- MBIO Data Format ID: 163
    - Format name: MBF_ASCIIYXZ
    - Informal Description: Generic YXZ sounding format
    - Attributes: YXZ (lat lon depth) ASCII soundings, generic
- MBIO Data Format ID: 164
    - Format name: MBF_HYDROB93
    - Informal Description: NGDC binary hydrographic sounding format
    - Attributes: XYZ (lon lat depth) binary soundings
- MBIO Data Format ID: 165
    - Format name: MBF_MBARIROV
    - Informal Description: MBARI Remotely Operated Vehicle (ROV) navigation format
    - Attributes: ROV navigation, MBARI
- MBIO Data Format ID: 166
    - Format name: MBF_MBPRONAV
    - Informal Description: MB-System simple navigation format
    - Attributes: navigation, MBARI
- MBIO Data Format ID: 167
    - Format name: MBF_NVNETCDF
    - Informal Description: CARAIBES CDF navigation
    - Attributes: netCDF, IFREMER.
- MBIO Data Format ID: 168
    - Format name: MBF_ASCIIXYT
    - Informal Description: Generic XYT sounding format

  - Attributes: XYT (lon lat topography) ASCII soundings, generic
- MBIO Data Format ID: 169
  - Format name: MBF_ASCIIYXT
  - Informal Description: Generic YXT sounding format
  - Attributes: YXT (lat lon topography) ASCII soundings, generic
- MBIO Data Format ID: 170
  - Format name: MBF_MBARROV2
  - Informal Description: MBARI ROV navigation format
  - Attributes: ROV navigation, MBARI
- MBIO Data Format ID: 171
  - Format name: MBF_HS10JAMS
  - Informal Description: Furuno HS-10 multibeam format,
  - Attributes: 45 beams bathymetry and amplitude, ascii, JAMSTEC
- MBIO Data Format ID: 181
  - Format name: MBF_SAMESURF
  - Informal Description: SAM Electronics SURF format.
  - Attributes: variable beams, bathymetry, amplitude, and sidescan, binary, single files, SAM Electronics (formerly Krupp-Atlas Electronik).
- MBIO Data Format ID: 182
  - Format name: MBF_HSDS2RAW
  - Informal Description: STN Atlas raw multibeam format
  - Attributes: STN Atlas multibeam sonars, Hydrosweep DS2, Hydrosweep MD, Fansweep 10, Fansweep 20, bathymetry, amplitude, and sidescan, up to 1440 beams and 4096 pixels, XDR binary, STN Atlas.
- MBIO Data Format ID: 183
  - Format name: MBF_HSDS2LAM
  - Informal Description: L-DEO HSDS2 processing format
  - Attributes: STN Atlas multibeam sonars, Hydrosweep DS2, Hydrosweep MD, Fansweep 10, Fansweep 20, bathymetry, amplitude, and sidescan, up to 1440 beams and 4096 pixels, XDR binary, L-DEO.
- MBIO Data Format ID: 191
  - Format name: MBF_IMAGE83P
  - Informal Description: Imagenex DeltaT Multibeam

  - Attributes: Multibeam, bathymetry, 480 beams, ascii + binary, Imagenex.
- MBIO Data Format ID: 192
  - Format name: MBF_IMAGEMBA
  - Informal Description: MBARI DeltaT Multibeam
  - Attributes: Multibeam, bathymetry, 480 beams, ascii + binary, MBARI.

Bibliography

[1] *Admiralty Chart Availability List*. The United Kingdom Hydrographic Office, Available at <http://www.ukho.gov.uk/PRODUCTSANDSERVICES/Pages/ChartAvailabilityList.aspx>

[2] ASTM E2544-11a, *Standard Terminology for Three-Dimensional (3-D) Imaging Systems*. ASTM International, Available at <http://www.astm.org/Standards/E2544.htm>

[3] *Atmospheric Refraction Error and its Compensation for Passive Optical Sensors*, Lincoln Laboratory, Massachusetts, Institute of Technology, Lexington, Massachusetts, Technical Report 686 1984

[4] Aull B., Loomis A., Young D., Heinrichs R., Felton B., Daniels P. et al. *Geiger-Mode Avalanche Photodiodes for Three-Dimensional Imaging*. Lincoln Laboratory Journal, 13(2):335-350, 2002. Available at <http://www.ll.mit.edu/publications/journal/pdf/vol13_no2/13_2geigermode3d.pdf>

[5] *Hydrographic Dictionary, S-32*, Fifth Edition, International Hydrographic Organization, Monaco, 1994. Available at < http://www.iho.int/iho_pubs/IHO_Download.htm>

[6] *IHO Standards for Hydrographic Surveys*, 5th Edition, International Hydrographic Organization, February 2008. Available at <http://www.iho.int/iho_pubs/IHO_Download.htm>

[7] *Implementation Specification — a Draught Information System for the St. Lawrence Seaway*, St. Lawrence Seaway Management Corporation, 2011. Available at <http://greatlakes-seaway.ca/en/pdf/Draught_Info_Sys_En.pdf>

[8] *Manual of Hydrography*, C-13, International Hydrographic Organization, 2012. Available at <http://www.iho.int/iho_pubs/IHO_Download.htm>

[9] McGlone J.C. *Manual of Photogrammetry*, American Society for Photogrammetry and Remote Sensing, Available at <http://www.asprs.org/Publications-Other/Bookstore.html>

[10] Minzner R., & Chanpion K.S.W. *The ARDC Model Atmosphere*, Airforce Cambridge Research Centre (US), Geophysics Research Directorate, Bedford, Massachusetts, (ARDC) US Airforce, 1959

[11] *NGA Standardization Document, Light Detection and Ranging (LIDAR) Model, Supporting Precise Geopositioning*, NGA.SIG.004_1.1, National Geospatial-Intelligence Agency, 2011. Available at <http://www.gwg.nga.mil/focus_groups/csmwg/LIDAR_Formulation_Paper_Version_1.1_110801.pdf>

[12] NISTIR 7117*, Performance Analysis of Next-Generation LADAR for Manufacturing, Construction, and Mobility. Building and Fire Research Laboratory*, Manufacturing Engineering Laboratory, National Institute of Standards and Technology, United States Department of Commerce. Available at http://www.stoneaerospace.com/about-us/NISTIR_7117_Final_Complete2.pdf

[13] Rosen P., Hensley S., Joughin I., Li F., Madsen S., Rodríguez E. et al. Synthetic Aperture Radar Interferometry. *Proc. IEEE*. 2000, **88** (3) pp. 333–338

ICS 35.240.70

Price based on 151 pages